Exploring the neogene sedimentation of the eastern South Atlantic with reflection seismic data

Untersuchung der neogenen Sedimentation im östlichen Südatlantik aus reflexionsseismischen Daten

Etienne Wildeboer Schut

Ber. Polarforsch. Meeresforsch. 518 (2005)
ISSN 1618 - 3193

Etienne Wildeboer Schut

Alfred-Wegener-Institut für Polar- und Meeresforschung
Am Alten Hafen 26, D-27568 Bremerhaven

Die vorliegende Arbeit ist die inhaltlich unveränderte Fassung einer Dissertation, die 2003 dem Fachbereich Geowissenschaften der Universität Bremen vorgelegt wurde.

Eine elektronische Version dieser Dissertation kann unter
http://www.awi-bremerhaven.de/GPH/dissertationen.html
bezogen werden.

CONTENTS

ABSTRACT

Ocean currents play an important role in shaping the climate of the earth. Studying sediments deposited by ocean currents help us understand the development of these currents and their influence on palaeoclimate.

The South Atlantic Ocean is a place where dominant water masses as the Antarctic Bottom Water and the North Atlantic Deep water meet. Seismic data over the Agulhas Ridge, collected by the Alfred Wegener Institute, and sediment core data from Sites 1088, 1089 and 1090 of the Ocean Drilling Program Leg 177 are connected to understand the palaeo-oceanographic history of the south Atlantic ocean after the Gondwana break-up.

The physical properties measured on the sediment cores are used to create a link between structures observed in reflection seismic data to layers and hiatuses in corresponding sediment bodies. This way, an extrapolation of the observations at the drilling locations over a wider area is made possible.

An hiatus present in the early Oligocene section of the cored sediments at ODP Site 1090 can be traced over a wide area in the seismic data of the Cape Basin. This hiatus corresponds to a change in sedimentation in the early Oligocene, from rapidly accumulating sediment sheets to the build-up of distinct drift structures. Large scale drift structures are observed in the seismic data parallel to the Agulhas Ridge.

There is still a controversy about the timing of the opening of Drake Passage as a gateway for deep water masses in the Oligocene, and its role as a critical gateway in the development of the Antarctic Circumpolar Current as a prerequisite for the formation of deep water near Antarctica. The data from the Cape Basin adds additional insights in this debate, as it shows that deep water influx from the Antarctic region into this area has existed since the early Oligocene.

The accumulation of contourite sediment structures found in the Cape Basin indicate a sustained influx of sediment particles by a deep water current, interrupted by periods of erosion or non-deposition in the middle Miocene and early Pliocene.

The south-westward direction of the bottom current transporting the sediments, following the bathymetric contours of the Agulhas Ridge in the Cape Basin, is inferred from the geometry of the layers within the contourite drifts. This direction is similar to the presently active bottom current consisting of Circumpolar Deep Water.

1. INTRODUCTION

The earth's climate has gone through a significant change since the end of the Eocene from a warm 'Greenhouse' state with ice-free polar regions , to the present 'Icehouse' state. This transition is intimately connected to the opening of the South Atlantic Ocean after the Gondwana breakup during the Cretaceous. During this period, South America and Africa drifted apart along the Falkland-Agulhas Fracture Zone, a transform fault which extends from the east coast of South Africa to the southern tip of the American continent (LaBrecque and Hayes, 1979; Marks and Stock, 2001). The glaciation of the now separated Antarctic continent started around the Eocene/Oligocene boundary with the opening of the Tasmanian gateway and the Drake Passage (Barker and Burrell, 1977; Lawver and Gahagan, 1998), although it is not yet clear when this happened exactly. The opening of these gateways enabled the formation of the Antarctic Circumpolar Current (ACC) (Kennett, 1977; Lawver et al., 1992) around Antarctica as a ring of water that brought a thermal isolation to the continent and led to the establishment of the East Antarctic Ice sheet. Studies on sea-level curves (Haq et al., 1987) and oxygen isotope curves (Zachos et al., 2001) indicate that, after an initial cooling during the Oligocene, temperature rose again during the early and middle Miocene. In the late Miocene, a gradual cooling set in, which led to further glaciation of the Antarctic continent with the formation of the West Antarctic Ice Sheet (Kennett, 1977; Kennett and Barker, 1990).

As a result of the reorganisation of the continents, the onset of a global thermohaline circulation was made possible. In the Southern Atlantic ocean this leads to the exchange and mixing of water masses which have their origin around Antarctica with water masses coming from the northern hemisphere. The waxing and waning influx of North Atlantic Deep Water (NADW) (Berger and Wefer, 1996) leads to variations in the relative amounts of these water masses, which is reflected in the sediments in the South Atlantic. The Agulhas Ridge (du Plessis and Simpson, 1974), sometime also named Cape Rise, along the Falkland-Agulhas Fracture Zone on the southern border of the Cape Basin, restricts the north-south flow of bottom currents due to its pronounced topography. The sediments in this area form an excellent climate archive because variations in the sedimentation in this area mainly reflect the response of bottom current variations to different climatological conditions.

Up until recently only limited data sets existed in the Agulhas Ridge area. The only previously existing seismic data consisted of single channel seismic data (Tucholke and Embley, 1984). For establishing a seismic stratigraphy more data and a deeper penetration was needed, and a seismic survey was planned to cover the area with multichannel reflection seismic data, which were then collected on a 1997 cruise with the R/V Petr Kottsov.

Simultaneously, a drilling campaign by the Ocean Drilling Project (ODP) was carried out with the Joides Resolution of which three of the seven drilling locations of Leg 177, Sites 1088-1090 (Gersonde, Hodell, Blum et al., 2003), were selected at and near the Agulhas Ridge.

The objective of the work described here is to combine both the seismic and the ODP data sets to obtain new insights into eastern South Atlantic sedimentation by looking from different angles. This involves processing the data in a form to make them comparable, a complicated task which, with very few exceptions (Shipley, 1983; Sun, 2000; Zühlsdorff and Spiess, 2001), is not normally done with ODP data. A second goal is to determine whether it is justified to regard extrapolated results obtained from the ODP data set as representative for the sediments at some distance from the drill holes. The third goal is to determine thickness and structure of sediments by establishing a seismostratigraphy for the Cape Basin. The thickness of seismic units is indicative of variations in the amount of sediment transport and deposition, and also identifies erosion. The shape and internal structure of sediment bodies in the Cape Basin can indicate whether turbidity currents or contour currents control the sedimentation. A well layered structure within the sediment bodies is an indicator for variation of current strength, which has influence on the particle size of deposited sediments.

Chapter 4 on page 21 (Wildeboer Schut and Uenzelmann-Neben, 2003) focuses on the technical aspects of combining seismic data with the information of physical properties measurements of cored sediments. Using data from boreholes is widely applied in the oil exploration industry, but usually in the form of measurements inside the holes with downhole logging equipment, and complemented with additional checkshots. Such methods are difficult to deploy, if possible at all, in a deep-sea setting. For the three drill-sites of Leg 177, which were located on the Agulhas Ridge, downhole logging data was not available and instead measurements were done on board of the Joides Resolution on specific core samples.

The seismic survey crossed the location of the drilling holes. Using the physical properties it is possible to correlate the various geological datasets with the seismic data. This allows for a joint interpretation of both micropalaeontological information of the sediments and the seismic data, and is the topic of chapter 5 on page 41 (Wildeboer Schut et al., 2002).

The final chapter 6 on page 59 (Wildeboer Schut and Uenzelmann-Neben, 2005) discusses the sedimentation patterns which are observed in the seismic data. Variations in bottom current sedimentation reflect the response of oceanic currents to a changing climatic system. Patterns of sedimentation observed in the seismic data are indicative of the bottom current regime at the time of sedimentation. The results from a drilling campaign, by its very nature, are very much tied to the location of the operations, whereas seismic data covers a much wider region. Extrapolating the results from the location of the drilling operations into the nearby Cape Basin establishes control on the age and extent of the various sediment layers as seen in the seismic sections. A stratigraphy based on the seismic profiles gives insight into the extent and timing of sedimentation and thus the influence of climate events on the bottom current conditions in the southern Cape Basin.

2. AN OVERVIEW OF THE SOUTH ATLANTIC

2.1 Geography and oceanography of the South Atlantic

The eastern Atlantic ocean (Fig. 2.1 on the next page) consists of several up to 5 km deep ocean basins separated by ridge systems which rise up to 2 km below sea-level. Near the equator the Guinea Seamounts separate the Angola Basin from the Guinea Abyssal Plain. Further south on this side of the Atlantic we find the Cape Basin, separated from the Angola Basin in the north by the Walvis Ridge, and from the Agulhas Basin in the south by the Agulhas Ridge. The Agulhas Rift, an now extinct spreading axis in the Agulhas Basin, marks the north-eastern tip of the Agulhas Ridge at 41°S, 14°E. The south-western end of the Agulhas Ridge is defined by the Meteor Rise (Fig. 2.2 on page 6) at 45°S, 4°E.

The western South Atlantic ocean consists of two large basins, the Brazil Basin in the north and the Argentine Basin in the south separated by the Rio Grande Rise. Along the South American Coast the Vema Channel enables the transfer of deep water between these two basins. Between the 5 to 7 km deep Argentine Basin and the much shallower Scotia Sea, lies the Falkland Plateau between 50°S and the Scotia Ridge near 55°S.

The South West Indian Ridge and the American-Antarctic Ridge west of it separate the Atlantic Basins, from the Antarctic deep-sea areas of the Enderby Abyssal Plain and the Weddell Sea.

The deep-sea ridge systems and mountain ranges limit the exchange of deep-sea water masses between the ocean basins. Where gaps exist there will be interaction between bottom currents and the sediments of the sea-floor. This has been observed in the Vema Channel in the western Atlantic, off the coast of Brazil (Mézerais et al., 1993; Faugères et al., 1998) where contourite formations have been built up, ie. sediments were deposited along the contours of an elevated topography. The present study shows evidence that a similar scenario takes place in the eastern part of the Atlantic, with water funnelled through a relatively narrow gap between the Agulhas Ridge and the African coast. The current velocity accelerates during the passage of the gap and erosion can occur. When the water masses are unleashed in the ocean basin, the velocity drops and the sediments which were carried along, or were picked up by the bottom current, are deposited. This process often builds up voluminous sediment bodies in the form of sheets, fans or sediment ridges; in the case of the Vema contourite fan it amounts to a 200-400 m thick mud-rich sediment accumulation by a bottom current of Antarctic origin (Faugères et al., 1998).

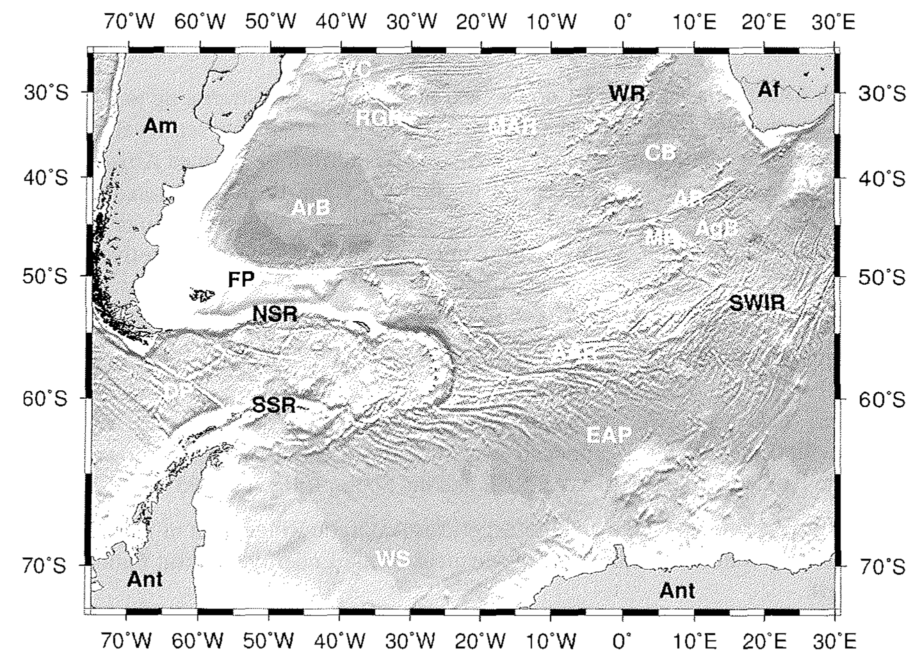

Fig. 2.1: *bathymetric map of the basins and ridge systems in the southern Atlantic ocean; abbreviations: AAR - American-Antarctic Ridge, Af - Africa, Am - South America, Ant - Antarctica, AP - Agulhas Plateau, AP - Agulhas Ridge, AgB - Agulhas Basin, ArB - Argentine Basin, DP - Drake Passage, EAB - Enderby Abyssal Plain, FP - Falkland Plateau, MAR - Mid Atlantic Ridge, MR - Meteor Rise, NSR - North, RGR - Rio Grande Rise, Scotia Ridge, SSR - South Scotia Ridge, SWIR - South West Indian Ridge, WR - Walvis Ridge, WS - Weddell Sea, VC - Vema Channel; bathymetry after Sandwell and Smith (1997).*

2.2 *Tectonic evolution of the Agulhas Ridge*

Mid-oceanic ridge spreading centres are at many places segmented through transform faults along fracture zones. Often, new ridge systems with a considerable topography are formed along such transform faults, and separate ocean basins from one another. The Agulhas Ridge is such a ridge, formed along the Falkland-Agulhas Fracture Zone after the Early Cretaceous break-up of West Gondwanaland. How the ridge was exactly formed is still unclear, Bonatti (1978) speculates that it may have formed by extension and subsequent serpentinite diapirism, others (Hartnady and Le Roux, 1985; Kastens, 1987) consider hotspot magmatism as a source.

The reconstructions of (Marks and Stock, 2001) places the extinction of the Agulhas Rift (Fig. 2.2 on the next page) as part of the Mid Atlantic Ridge at 61.2 Ma. The active spreading centre has since jumped to the west and left an offset of only ~180 km (Barker, 1979) between the segments of the mid-oceanic ridge system at both sides of the fracture zone. This ridge jump involved the creation of the Meteor Rise (LaBrecque and Hayes, 1979) and the transfer of lithosphere from the South American plate to the African plate (Hartnady and Le Roux, 1985) in what is now the Agulhas Basin.

The Agulhas Ridge is clearly separated in two segments divided by the transform fault. This is visible on satellite derived bathymetry maps (Fig. 2.2 on the following page), but especially on a north-south transect of the seismic data collected for this research (Fig. 2.3 on page 7).

Due to the nature of the ocean floor spreading process, lithospheric age differs across the transform fault, and therefore also the sedimentation and erosion history of ridge segments directly opposite of transform faults are different.

The elevated topography at the flanks of transform faults can be explained as a flexural response of the lithosphere. Sandwell (1984) shows that vertical tectonic movement remains along fracture zones even after migration of the active segments. This enables fracture zones ridges to maintain their topography, in spite of erosion and the subsidence that takes places when oceanic lithosphere ages. Long fracture zones, such as the Falkland-Agulhas Fracture Zone, are according to Cande et al. (1988) resistant to a shifting drift direction of the continents, thus largely preserving the original orientation. Combined with the absence of an active spreading since the beginning of the Cenozoic, can the assumption been made that the Agulhas Ridge has largely existed in much the same shape as today, throughout the Neogene.

The exact tectonic history of the Atlantic ocean south of the Falkland-Agulhas Fracture Zone is not yet fully understood. For the Agulhas Basin, some authors suggest that a Malvinas plate was located inside the Agulhas Basin during the Late Cretaceous. LaBrecque and Hayes (1979) proposed the idea of a Malvinas plate which existed from Campanian to Maestrichtian times based on magnetic data, and Marks and Stock (2001) reach a similar conclusion based on gravity field analysis. Others however, do not see indications for such a plate (Livermore and Woolet, 1993).

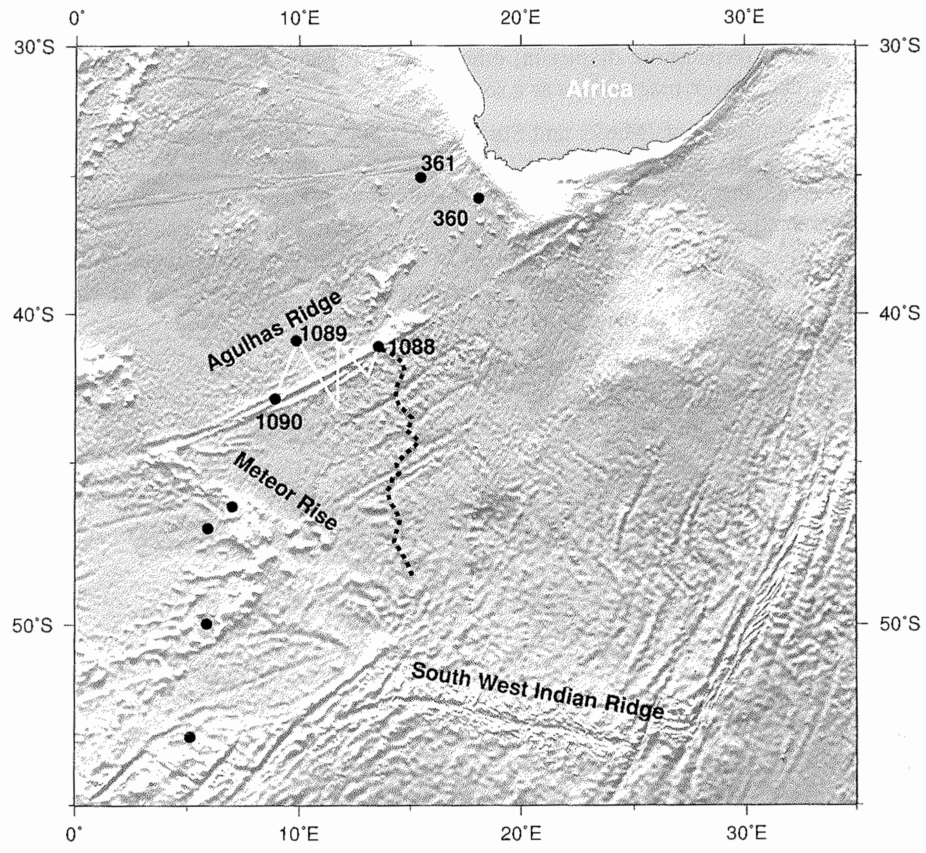

Fig. 2.2: *Bathymetric map of the Agulhas Ridge (Sandwell and Smith, 1997) with the location of the seismic profiles. The dots indicate the location of ODP Leg 177 drill-sites, and Sites 360 and 361 of DSDP Leg 40. The location of an extinct mid-ocean spreading centre is indicated by the dashed line.*

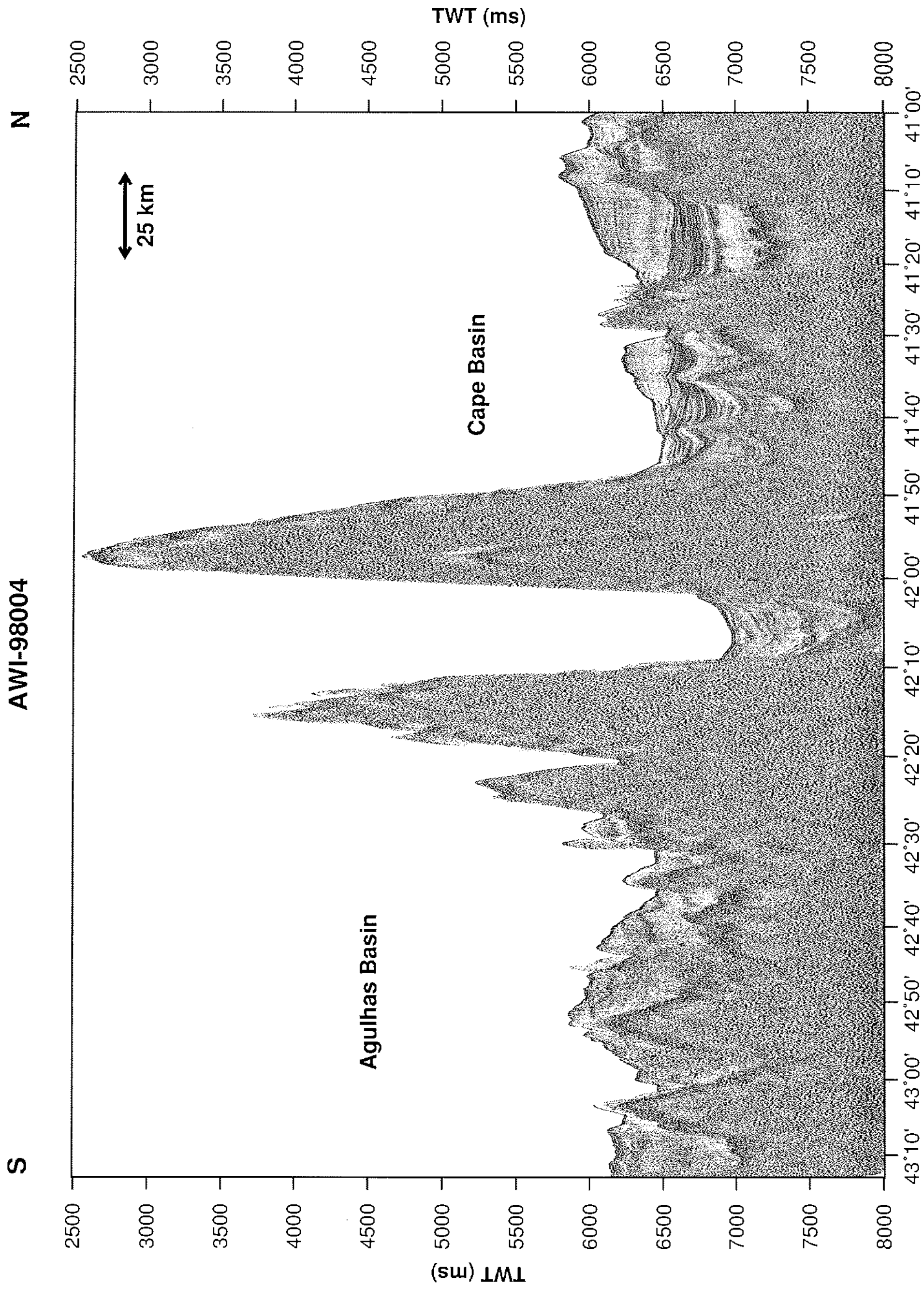

Fig. 2.3: *North-south seismic transect over the Agulhas Ridge.*

2.3 Oceanography

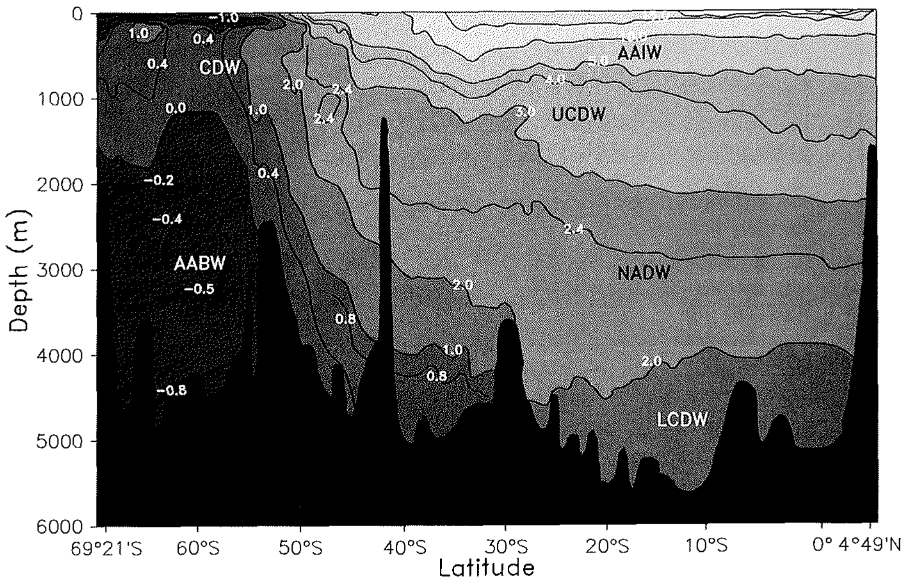

Fig. 2.4: *Potential temperature (°C) of the southern Atlantic ocean in a cross section from Antarctica to 5°N along the Greenwich meridian; from Reid (1989). The peak at 40°S is not the Agulhas Ridge but one of the Discovery Seamounts.*

The present ocean circulation is characterised by the large scale exchange of water masses between the oceans through the global conveyor belt. Since this mechanism connects all the oceans water masses, this means that the climate of the northern and southern hemispheres are coupled to each other as well. The main contribution to this conveyor comes from Atlantic Ocean water (20 Sv) and Pacific Ocean water (15 Sv), with a smaller contribution from the Indian Ocean (5 Sv) (Anisimov et al., 2002). On the other hand, before the reorganisation of continents following the Cretaceous Gondwana breakup, circulation was restricted within regional cells (Droxler et al., 1998). The global circulation was only possible after gateways opened around Antarctica in the Oligocene (Lawver et al., 1992; Lawver and Gahagan, 1998; Latimer and Filipelli, 2002), and others closed, such as the Panama gateway in the late Miocene (Mikolajewicz et al., 1993; Droxler et al., 1998). Presently, the South Atlantic is dominated by water masses originating near Antarctica, by southward flowing North Atlantic water masses, and contributions from the Indian Ocean, entering the Cape Basin in the form of Agulhas Rings (Lutjeharms, 1996; De Ruijter et al., 1999).

The geologic history at Site 361 of DSDP Leg 40, located in the Cape Basin near the African coast (Fig. 2.2 on page 6) shows that sedimentation shifted from a terrigenous to a pelagic input at the Cretaceous-Tertiary boundary (Melguen, 1978). This shows that ocean currents are the major source of sediment supply for the eastern South Atlantic.

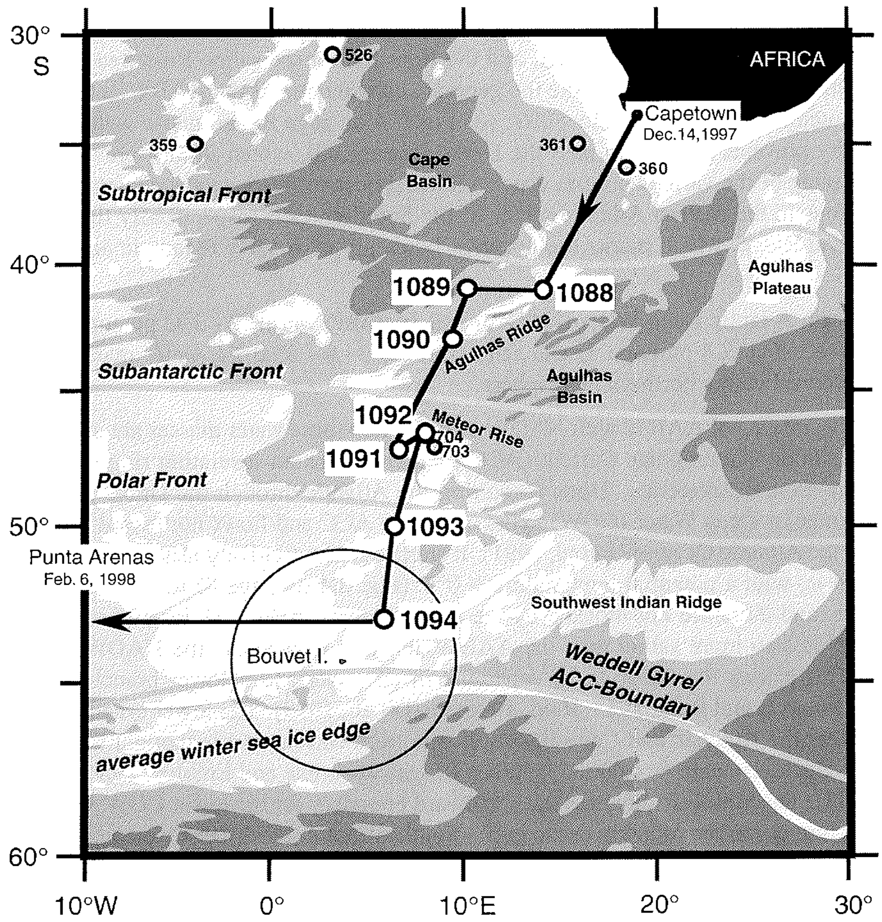

Fig. 2.5: *Location of the frontal zones in the eastern south Atlantic ocean (from Gersonde, Hodell, Blum et al., 1999).*

Water masses originating in the Antarctic region enter the Atlantic Ocean either directly in the case of Antarctic Bottom Water (AABW) from the Weddell Sea, or through the Drake passage, between south America and the Antarctic Peninsula in the case of the Antarctic Circumpolar Current (ACC). ACC water is funnelled through the Scotia Ridge system, which rises up to 1000 m below sea level before it enters into the Atlantic Ocean.

The Antarctic Bottom Water (AABW) is a cold water mass which has two main sources, the Weddell Sea as the very cold (potential temperature < -0.8°C) and fresh (salinity < 34.63 ‰) Weddell Sea Bottom Water, and the Ross Seas more saline Ross Sea Bottom Water (Orsi et al., 1999). Overall the the general characteristic of the AABW is that it is a cold (potential temperature below 0°C, see Fig. 2.4 on page 8) and dense water mass. It's density prevents AABW to pass the Drake Passage sill, which in turn prevents the lateral mixing of the various bottom waters. Several ocean ridge systems constrain deep current flow, in the eastern Atlantic sector of the Southern Ocean specifically the South West Indian Ridge, which marks the northern boundary of AABW (Mantyla and Reid, 1983).

The North Atlantic Deep Water (NADW) is a relatively warm (2 - 3°C potential temperature) (see Fig. 2.4 on page 8) and salty (salinity 34.8 - 35.0 ‰) water mass (Reid, 1989) produced on the northern hemisphere.

Intensive mixing of AABW with NADW occurs when these water masses are absorbed in the Antarctic Circumpolar Current (ACC), which lies as an insulating ring of water circulating around Antarctica. Upon reentering the Atlantic through the Drake passage, the Circumpolar Deep Water (CDW) splits off of the ACC and flows northward into the basins of the Atlantic Ocean (Rintoul, 1991). It starts out as a relatively near-surface water mass, and is, with a potential temperature > 0°C (Fig. 2.4 on page 8) less dense as the AABW is, and therefore not blocked by the ridge systems in the vicinity of Antarctica. The CDW is also more saline than the AABW, but less so than the the NADW (Reid, 1989). This causes the CDW to be separated in an upper and a lower branch by the NADW (Mantyla and Reid, 1983; Reid, 1996; Orsi et al., 1999). The lower branch of the CDW enters the Agulhas and Cape Basins as a bottom current and is thought to follow a counter-clockwise path around the Agulhas Ridge (Tucholke and Embley, 1984; Sykes et al., 1998). The Walvis Ridge is as the northward boundary for the lower CDW, whereas the upper branch can be found over the entire South Atlantic (Reid, 1989).

The Antarctic Intermediate Water (AAIW) overlies the upper branch of CDW. It originates from the surface waters near Antarctica (Turneau and Ledbetter, 1989) and constitutes the major part (63% from the Drake Passage and 16% from the South Indian Ocean) of the intermediate water mass flow in the central South Atlantic crossing the 25°S latitude (You et al., 2003). It is a relatively light and fresh water mass which can be traced from the Sub Antarctic Front (SAF) (Fig. 2.5 on the preceding page) up to the equator (Meredith et al., 1999). The AAIW follows an anti-cyclonic path in the Cape Basin (Shannon and Hunter, 1988).

The band of water involved in the ACC can be subdivided in zones with distinct surface water characteristics (see Fig. 2.5 on the previous page). The Antarctic Polar Front (PF), defined as the northernmost 2°C isotherm (at 200 m depth) shows a sharp drop in surface temperature as the Antarctic surface water sinks below the Sub-Antarctic Water near 50°S (Lutjeharms and Valentine, 1984; Lutjeharms, 1985). This Sub-Antarctic Water in turn sinks below the Sub-Tropical Surface Water at the Subtropical Front (STF) at ~39°S, causing a sharp thermal gradient. The highest thermal gradient in this zone however, exists at the Sub Antarctic Front (SAF) at ~45°S (Lutjeharms and Valentine, 1984; Lutjeharms, 1985). This is where cold, nutrient and oxygen rich Antarctic water separates from the warmer and less nutrient rich Sub-Antarctic waters. Different temperature and salinity conditions of near surface water masses impact on the primary sediment production of foraminifers and diatoms, which are observable in the geologic record in which they can be studied as a proxy for palaeoceanographic conditions. Indeed, there is a change in the lithology from diatom ooze south of the PF to a mixed siliceous-calcareous ooze near the SAF (Gersonde et al., 1999).

Oceanographic models indicate that increased fresh water input in the northern hemisphere leads to reduced NADW production and northern hemisphere cooling. The southern hemisphere reacts with a more vigorous ACC current, which in turn leads to increased cooling and sea-ice growth in the Antarctic, and this again results in increased AABW production (Rind et al., 2001). In this way, the South Atlantic ocean is affected not only by glaciation of the Antarctic, but also by northern hemisphere glaciation. The response to the northern hemispheres glaciation cycles are indeed observable in the ODP Leg 177 sediments (Shipboard Scientific Party, 1999c). Various studies also indicate a correlation of sea-level variations with the size of the Antarctic ice cap (Haq et al., 1987; Abreu and Anderson, 1998; Zachos et al., 2001).

3. AVAILABLE DATA

3.1 Processing of the seismic data

In December 1997, eight profiles of seismic data (Table 3.1 on page 15) were collected over the Agulhas Ridge area (Fig. 2.2 on page 6) on board of R/V Petr Kottsov, the first multichannel seismic data available in this area.

The source of the seismic data were two GI (Generator Injector)-guns™ (45 ci each) which emitted seismic waves with a centre-frequency around 75 Hz (Wildeboer Schut and Uenzelmann-Neben, 2003). The seismic reflections were recorded using a 2400 m long oil filled Syntron™ streamer behind a 50 m long lead-in cable and three 50 m stretch sections. This streamer consisted of 96 hydrophone groups, more conveniently called a channel, at 25 m interval spacing between the group centres. The EG&G Geometrics 2420 instrument digitally recorded 8192 ms of seismic data per shot, at a 1 ms sample interval, on magnetic tapes which were subsequently processed (see the flowchart in fig. 3.2 on page 16) with Paradigms DISCO® processing software on Convex™ C3420 and Silicon Graphics Origin 2000 computing systems.

The first processing step is to transform data from a multiplexed (data from all channels stored consecutively at each time step) SEG-D format into demultiplexed (data ordered per channel) format. A plot of a single channel now gives a first impression of the quality of the data, and helps to select locations for velocity analysis. Rough weather, which is common in the area under study, was responsible for many sections with poor data quality. A manual check of these 74000 shot records for dead traces is too labour intensive, therefore an automatic editing of traces based on both anomalous amplitudes and frequencies was applied. Also, two channels appear to be to weak (i.e. have a signal-to-noise ratio too poor to recover during processing) throughout the survey and were discarded.

The data were, after demultiplexing, sorted within 25 m sub-surface intervals to form common midpoint gathers. Figure 3.3a shows a typical CMP-gather (profile AWI-98003, CMP 4800) before processing. Reflections are already visible, but both very high frequency noise, especially at large offsets, and noise with a period much larger than the reflections obscures the continuation of reflectors. The amplitude spectrum shows (in figure 3.1(a) on page 15) that noise for near offsets is largely restricted to the low frequency range, up to approx. 20 Hz. The signal recorded at far offsets on the other hand is more attenuated, thus the impact of low frequency noise is bigger, and a wider frequency filter stop-band needs to be deployed. Also some high-frequency noise is present in the large offset data, especially a strong 50 Hz electrical noise component. Application of a filter with a pass-band from 10 Hz to 250 Hz and fully open between 25 Hz to 200 Hz for the nearest channels, and 55 Hz to 200 Hz from channel 20 upwards, removes most noise (as can be seen in Fig. 3.1(b) on the facing page).

Now an interactive determination of RMS-velocities can be done, and was carried out on a Sun UltraSparc™ 5 workstation. These velocities are used to compensate for offset dependent differences in the path followed by the seismic waves from source to receiver, the so called Normal Moveout (NMO) correction, which essentially transforms the data so as if it were recorded with source and receiver both directly above the centre of the CMP. Also, this velocity is used in the calculation of the amount of compensation necessary to adjust for diminishing energy with increasing offset, due to spherical expansion of the seismic waves. Figure 3.4a again shows profile AWI-98003, CMP 4800, now with spherical spreading compensation, and NMO correction applied. The reflectors are continuous over the whole offset range, but still the depth of a reflector varies by approximately half a wavelength. This is undesirable if the traces are summed (stacked) to one composite trace per CMP location, as the strength of a reflector gets cancelled out due to summation of traces with an excursion of opposite sign. To counter this effect a technique called residual static correction is applied, which normally is used in the processing of land seismic data. Correlation of all traces at one single shot location, or one single receiver location, are used to line-up the events within a CMP-gather. Although the depth of the hydrophone-group at a certain location is not fixed over time, in contrast to a geophone group in land seismic data, figure 3.4b shows that this procedure has successfully lined up the various reflectors. With the reflectors aligned, there is obviously still a lot of incoherent noise, and a coherency filter is applied to reduce such noise while leaving the the reflection energy unaffected (see Fig. 3.4c). Figure 3.3c shows this record with NMO correction removed to illustrate the effects of coherency filtering compared to a record with only bandpass filtering (Fig. 3.3b). Especially the weak reflections at large (>1500 m) offsets benefit considerably from such a processing step.

A velocity analysis was done every 100th CMP, which translates into an interval of 2.5 km, and at additional locations with varying stratigraphy as identified on the plot of a section of a single channel unprocessed data or when poor quality data prevents an accurate determination of RMS-velocities at certain locations.

The NMO corrected data is then stacked into a single zero-offset trace with a far better signal to noise ratio than the individual traces of a CMP gather because non-coherent noise is suppressed. The resulting stacked section is an image of the sub-seabottom, which, although it represents the stratigraphy, is still difficult to interpret, because the shape of geological structures are not represented correctly yet. Therefore a final step, migration, was carried out on the stacked data, both to increase the definition of seismic reflectors and for being able to accurately determine the shape of structures inside the ocean basin sediments bodies. For migration, it is critical to have a correct velocity model, for it can seriously distort stratigraphic features. If done correctly, then diffraction energy, which is always present in the stacked section because it is a coherent signal, should be contracted to one single point. The ability to suppress diffraction hyperbolas is thus an indicator for the effectiveness of the migration and the correctness of the velocity field that was applied. A finite difference migration yielded superior results, although it is computationally more intensive than other migration methods. The migrated sections were loaded into the Landmark seismic interpretation system SeisWorks™ in which seismic horizons can be tracked across connected profiles, and correlated with the physical properties measured on the core data acquired on ODP Leg 177.

Since the Agulhas Ridge comprises a deep-ocean setting, there are no multiples at locations where it could be disrupting to the interpretation of the data. Therefore multiple suppression techniques like deconvolution have not been applied. A test with application of deconvolution to enhance the signal did not result in improved definition of the reflectors, and thus was not needed, and indeed would even be harmful if it were applied, because it deteriorates the possibility to successfully correlate the seismic data with core log data.

profile	number of shots	start of line		end of line		total length (km)
		northing	easting	northing	easting	
AWI-98001	17955	-41° 8'25"	13°34'15"	-42°55'27"	8°52'45"	435
AWI-98002	9516	-42°55'44"	8°53'44"	-40°54'58"	9°56' 2"	240
AWI-98003	11793	-40°54' 3"	9°55'19"	-43°13' 6"	11°44'57"	298
AWI-98004	9156	-43°12'58"	11°44' 0"	-40°59'59"	11°44' 5"	246
AWI-98005	6441	-40°59'17"	11°43' 8"	-42° 9'55"	13° 7' 7"	175
AWI-98006	6428	-42° 8'54"	13° 6' 2"	-40°34'59"	13°44'18"	182
AWI-98007	3171	-40°35'11"	13°43' 5"	-41° 6'24"	14°31'26"	89
AWI-98008	9540	-41° 7' 1"	14°33'31"	-41° 9' 0"	11°43'39"	237

Tab. 3.1: *location and length of the seismic profiles over the Agulhas Ridge*

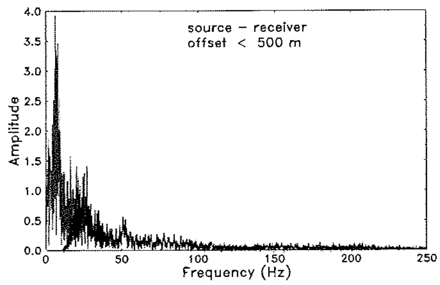

(a) channels 1 trough 19

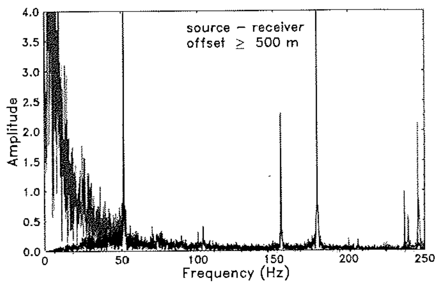

(b) channels 20 trough 96

Fig. 3.1: *The light coloured curve shows the amplitude spectrum of the data (profile AWI-98003, CMP location 4800). Superimposed, using the same scale, in a darker colour is the amplitude spectrum after bandpass filtering.*

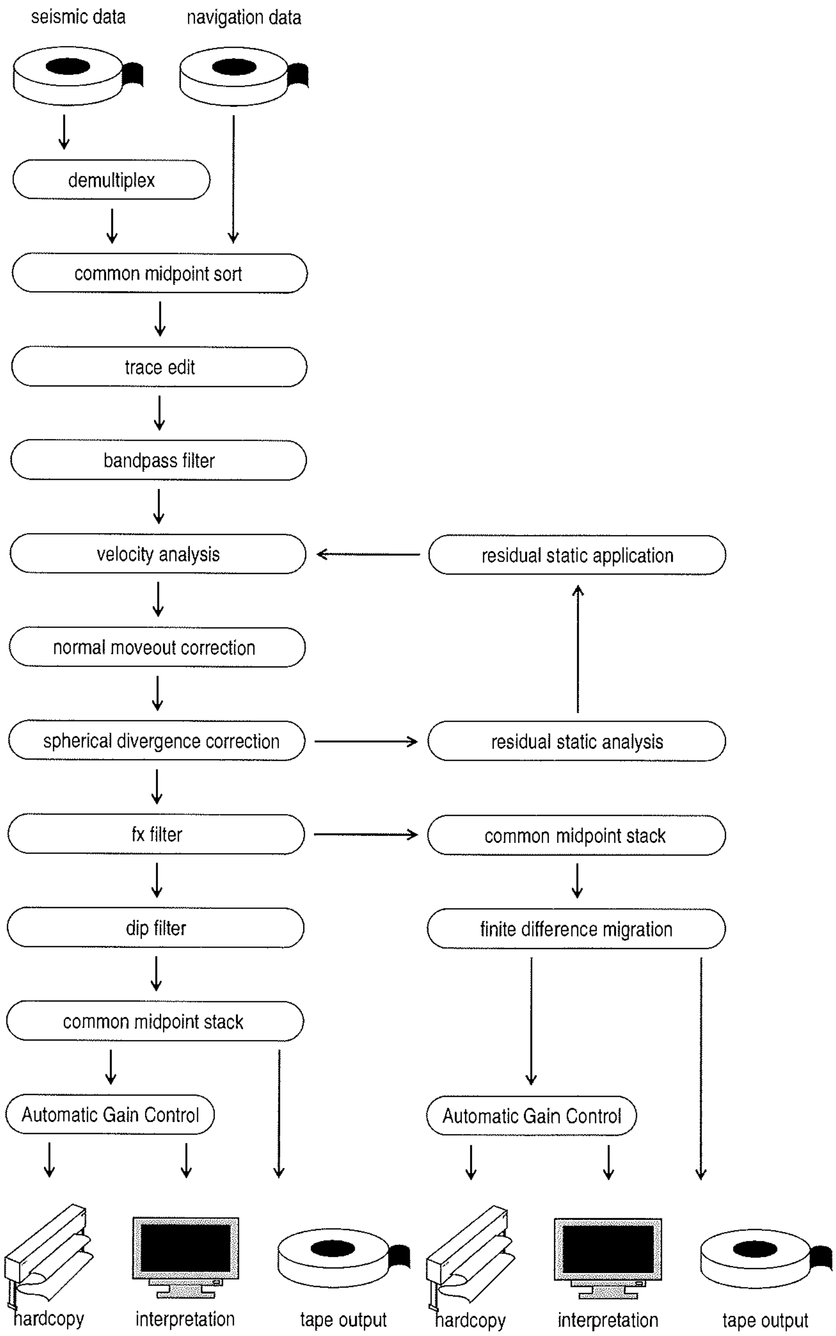

Fig. 3.2: *Flowchart of the processing steps for the seismic data.*

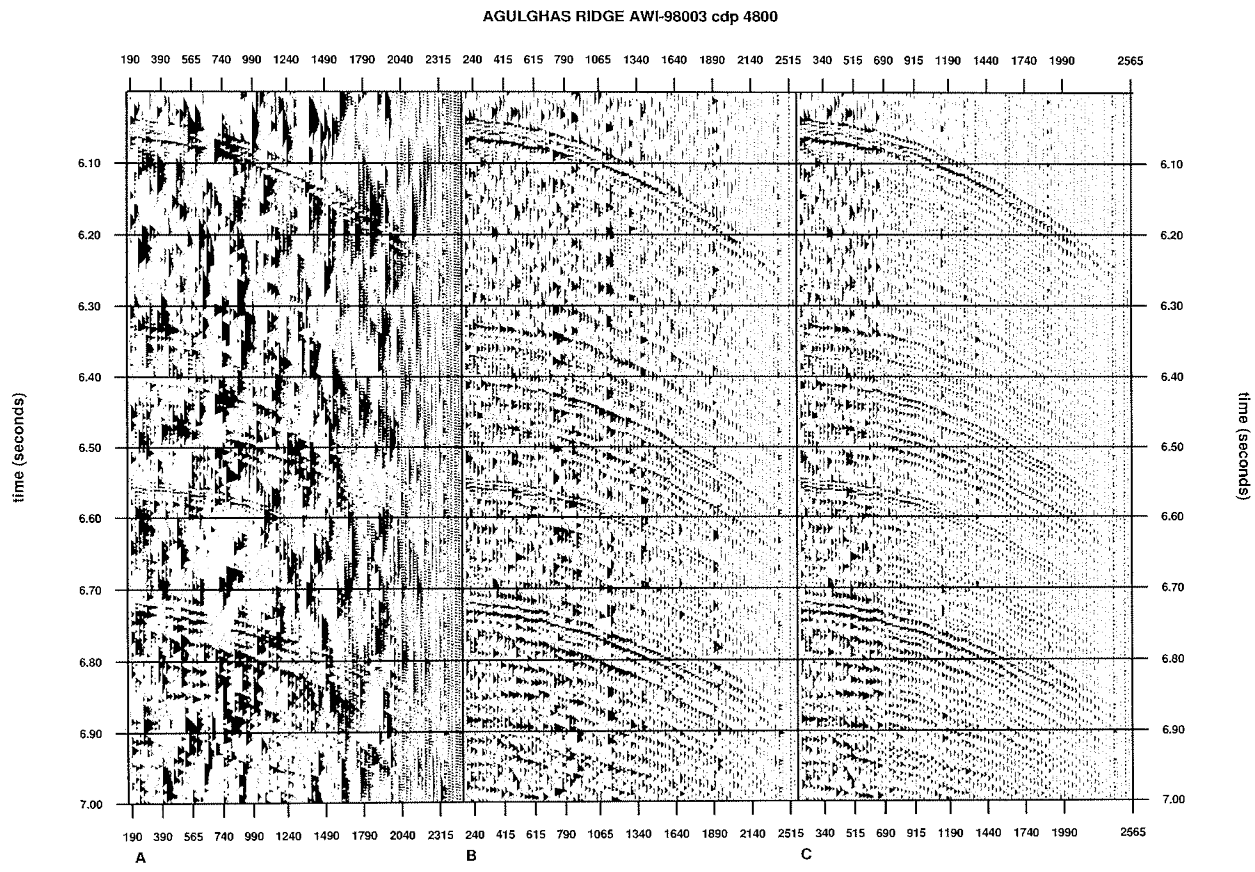

Fig. 3.3: *Seismic data of profile AWI-98003 at CMP location 4800 a) unprocessed data; b) bandpass filtered data; c) bandpass and coherency filtered data; the offsets of the traces are annotated in m*

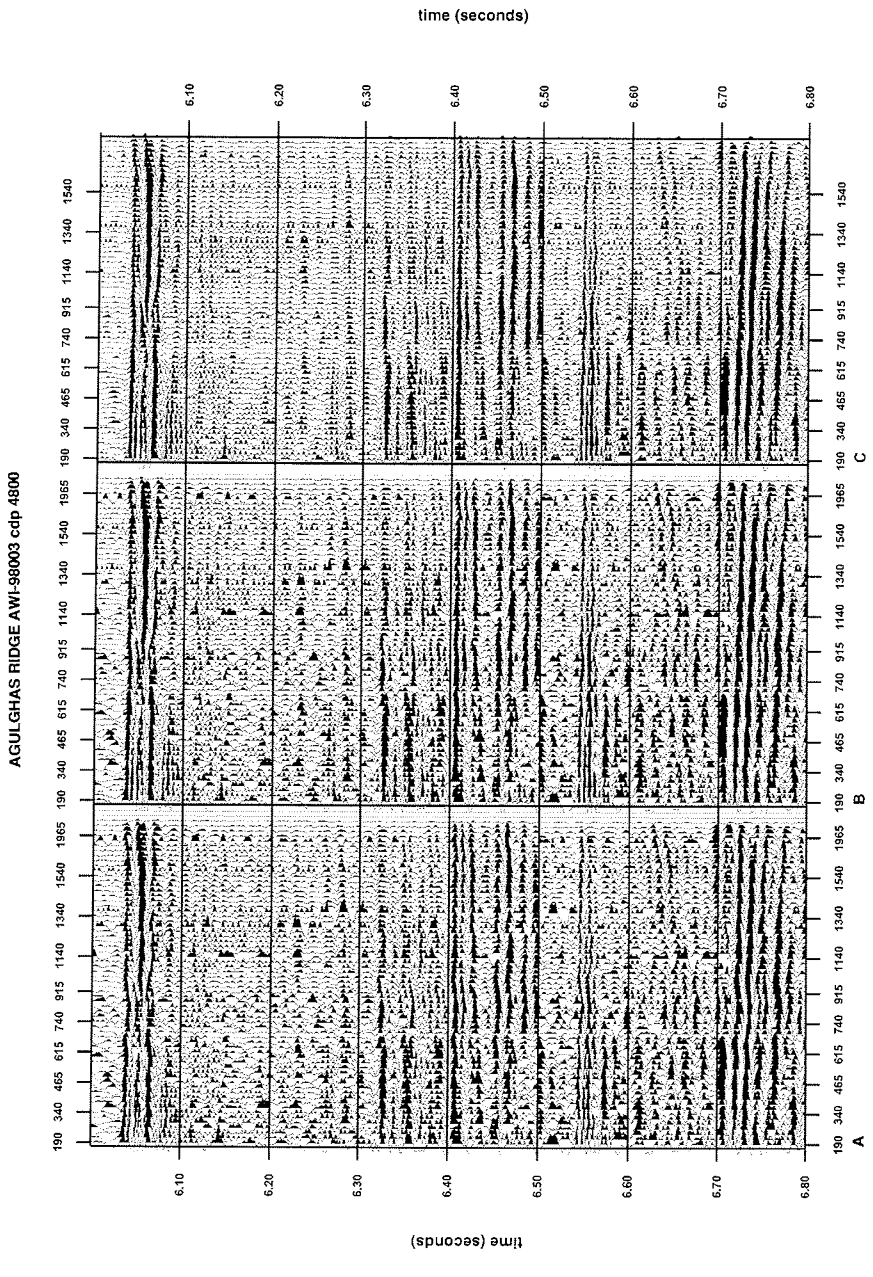

Fig. 3.4: Seismic data of profile AWI-98003 at CMP location 4800 a) bandpass filtered data with NMO correction applied; b) same as a), but with additional residual static correction applied; c) same as b), coherency filtered; the offsets of the traces are annotated in m

3.2 Palaeontological data

The ODP Leg 177 cruise with the Joides Resolution from Cape Town to Punta Arenas in Chile was held from 14 December 1997 until 6 February 1998, concurrently with the Petr Kottsov seismic survey. It was the first Southern Ocean drilling project since the DSDP Leg 71 and ODP Legs 113, 114, 119 and 120 in the 1980's. These data however were inadequate for comprehensive high resolution palaeoclimatic reconstructions, mainly due to recovery losses. The objective of Leg 177 therefore was to collect long, continuous records (Gersonde, Hodell, Blum et al., 1999), that would allow interpretation on a millenial timescale of late Neogene sediments and to add to the biostratigraphic and palaeoceanographic history of the high southern latitudes of the global climate archive, as established through previous drilling by the ODP project.

A total of 7 locations (Gersonde, Hodell, Blum et al., 1999) were drilled between 41°S and 53°S on the Agulhas Ridge, the Meteor Rise and within the circum-Antarctic opal belt (Fig. 2.5 on page 9). These seven sites cover a north-south transect in with Cenozoic sequences from various ocean bottom depths, such that the influence of all the major water masses of the South Atlantic were represented in the cores, with the opporunity to study the mixing behaviour of these water masses.

An important goal is the dating of biostratigraphic markers through calcareous and siliceous microfossils and a correlation with the geomagnetic record and isotope stratigraphy. Several chemical and physical properties were measured on the core samples. Changes in these records result from a change in climatic conditions as well as from variations in oceanographic conditions. The measured physical properties can be correlated with variations in the biostratigraphic record as well as with seismic data, which gives the opportunity to track events in the geological sequence in the seismic data.

4. THE CHALLENGE OF TIEING SEISMIC DATA TO GEOLOGIC INFORMATION: AN EXAMPLE FROM ODP LEG 177, SITES 1088-1090 *

Etienne Wildeboer Schut and Gabriele Uenzelmann-Neben

Abstract

The integration of seismic data with core data provides ground-truth to a structural interpretation of seismic data. The most important difficulty that arises in an integration effort is the correct translation between the different scales of the core data and the seismic data. In the absence of check-shots, detailed knowledge of the velocity structure at the drilling locations is required, either from downhole logging measurements, velocity analysis of the seismic data, or direct measurements on core samples. Three of the seven drill-sites during ODP (Ocean Drilling Program) Leg 177 in the south-eastern Atlantic were located on the Agulhas Ridge and connected through eight seismic profiles. Synthetic seismograms created from velocity and density measurements on selected core samples generally show a good agreement with real seismic data with respect to amplitude and waveform, whereas timing of the events is troublesome. The use of velocity profiles with inaccurate sections along cores, a false depth scale due to recovery problems, and inaccuracies in the positioning during both seismic and coring operations are the main shortcomings of this method. The main reflectors identified on seismic data correspond to hiatuses or periods of reduced sedimentation rates, and correlate well with density variations. In this way the cored data provide a calibration tool for the overall geological interpretation of the seismic sections.

Key words: South Atlantic; Agulhas Ridge; palaeo-reconstruction; seismic; core logs; ODP Leg 177; Site 1088; Site 1089; Site 1090

4.1 Introduction

To obtain a comprehension of the geological history of a study area often requires the integration of data from different disciplines, available in different forms. Petrophysical

* Submitted for publication

4. THE CHALLENGE OF TIEING SEISMIC DATA TO GEOLOGIC INFORMATION: AN EXAMPLE FROM ODP LEG 177, SITES 1088-1090

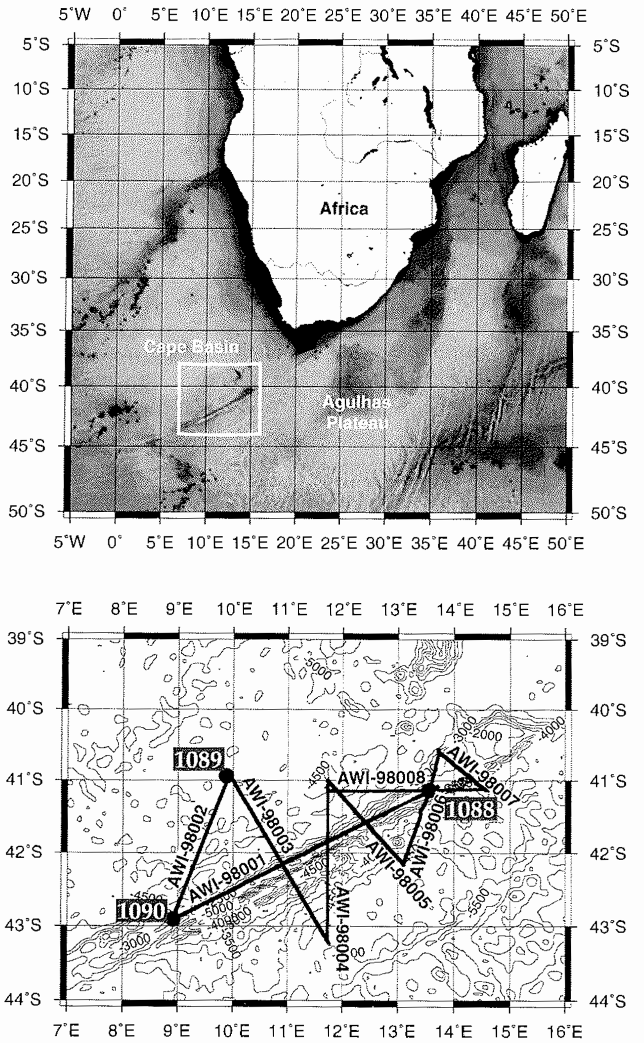

Fig. 4.1: *a) Bathymetry map of the Agulhas Ridge area (after Sandwell and Smith (1997));*
b) with seismic profiles AWI-98001 through AWI-98008 and drilling locations of ODP Leg 177 Sites 1088, 1089 and 1090 (big dots).

information, when available in analogue form by core samples, has to be made comparable with the geophysical data, usually in digital form, such as seismic data. This paper addresses some of the problems that arise in linking these two types of data. Usually, downhole logging data is used to link seismic and well data, supplemented by checkshots, i.e. a geophone is inserted in the well and records the traveltime of the seismic waves generated by a source near the top of the hole, a procedure typically repeated at several marker horizons. In case no such data are available, but core samples do exist, tools like P-Wave Logger (PWL) for P-wave velocity data and Gamma Ray Attenuation Porosity Evaluator (GRAPE) for density, can provide data directly measured on core samples. Unfortunately, this can introduce serious bias, as the *in situ* conditions in the well differ from the conditions in the lab. This is due to decompression of the samples, pore-fluid variations, material loss during drilling operations and temperature variations (Boyce, 1976; Hamilton, 1976). Also the cores are usually sampled at a spatially small interval, and sometimes at irregular intervals, compared with the sampling rate typically applied in a seismic survey. The integrated velocity profile, expressed in a depth scale to tie the depth domain sampled core data with time domain seismic data, could produce inaccurate results with respect to the depth of seismic reflectors.

ODP data from Leg 177, located in the southern Atlantic Ocean (Fig. 4.1a), is shown as an example of core to seismic correlation. The cores of this Leg were collected with the objective to reconstruct the palaeo-oceanographic history of the southern Ocean during the Palaeogene and early Neogene (Gersonde, Hodell, Blum et al., 1999). This is the time frame during which the Antarctic ice sheet developed, associated with major changes in oceanographic currents (Lawver and Gahagan, 1998). The core data was supplemented by seismic data acquired during a seismic cruise by the Alfred Wegener Institute which collected approx. 2000 km of multi-channel reflection seismic data. Correlation of seismic reflectors with cores offers an indication of the coverage and the sediment transport of palaeo-currents and can show how widespread hiatuses are.

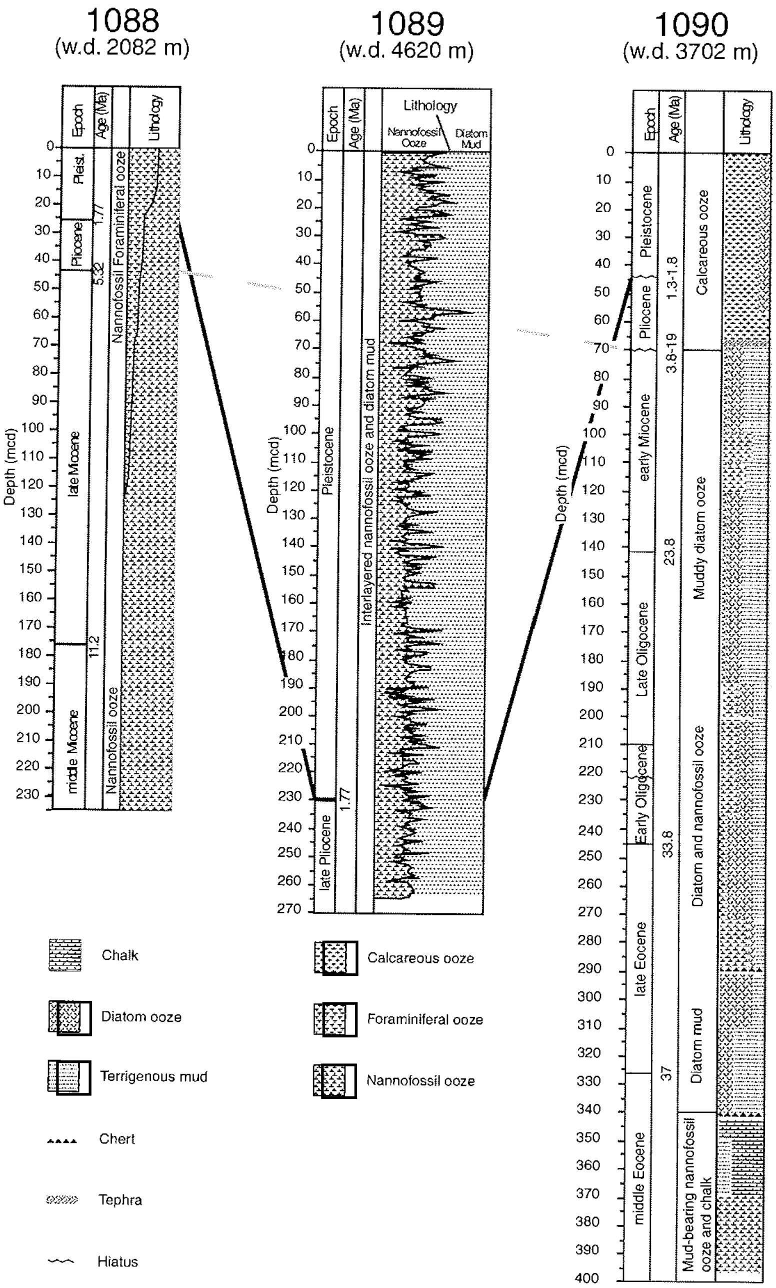

Fig. 4.2: *Summary of lithologies for ODP Leg 177 Sites 1088, 1089 and 1090 after Shipboard Scientific Party (1999a,b,c,d).*
wd = water depth.

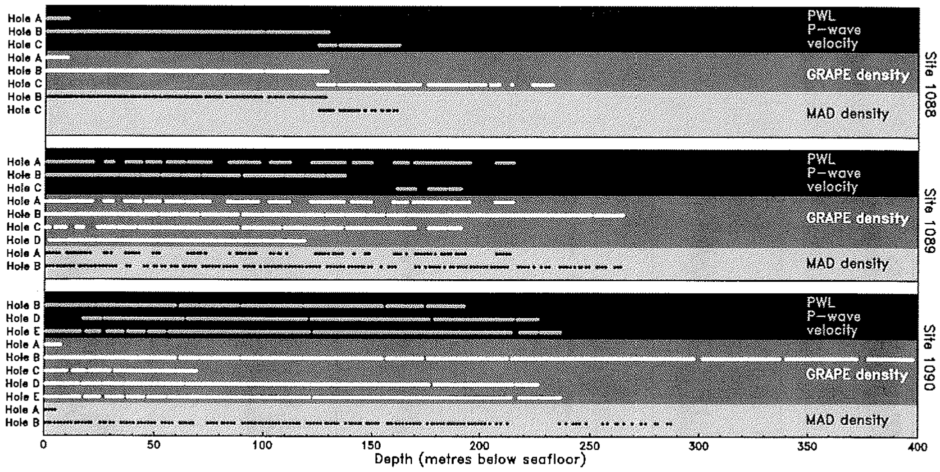

Fig. 4.3: *Indicated are the depth ranges for which physical properties measurements exist of P-wave Logger (PWL) derived seismic P-wave velocity, Gamma Ray Porosity Evaluator (GRAPE) derived densities and Moisture and Density (MAD) density measurements. Not every type of measurement is always available for each hole of Sites 1088, 1089 and 1090.*

4.2 Leg 177 Holes

ODP Leg 177 Sites were situated in the eastern South Atlantic, several hundred km south-west of Cape Town, South-Africa. Three of the sites were located near the Agulhas Ridge, a ridge associated with the Falkland-Agulhas Fracture zone (Fig. 4.1a). The objectives of Leg 177 were to reconstruct the palaeo-oceanographic, bio-geographic and bio-stratigraphic history of the Antarctic region in the Palaeogene and early Neogene (Gersonde, Hodell, Blum et al., 1999) which includes the development of the Antarctic glaciation. A second objective was to obtain high-resolution late Neogene sediment records suitable for correlation and calibration with Antarctic and Greenlandic ice core data (Gersonde, Hodell, Blum et al., 1999). The Agulhas Ridge separates the Cape Basin from the Agulhas Basin by a 2.5 km elevation of the seafloor relative to the adjacent ocean basins (Fig. 4.1b). Up to 400 m of mainly calcareous sediments were cored on the Ridge and in the basins (Fig. 4.2). Site 1088, the northernmost site of Leg 177, is located on the Agulhas Ridge itself (Fig. 4.1b). The core with a length of 233 metres is constituted mainly of calcareous sediments, middle Miocene to present in age, and shows several hiatuses (Shipboard Scientific Party, 1999b). Three holes have been drilled, which could not be spliced accurately into one continuous section due to the lack of depth ranges that were cored in multiple holes. Site 1089 is located in the Cape Basin (Fig. 4.1b) and shows in the 264.9 m cored interval diatom ooze and nannofossil mud of an age mainly younger than Pliocene (Shipboard Scientific Party, 1999c). This short geological time span, in comparison with Sites 1088 and 1090, is characterised by high sedimentation rates, which allows for a high, millennial scale, temporal analysis of the cored data. The

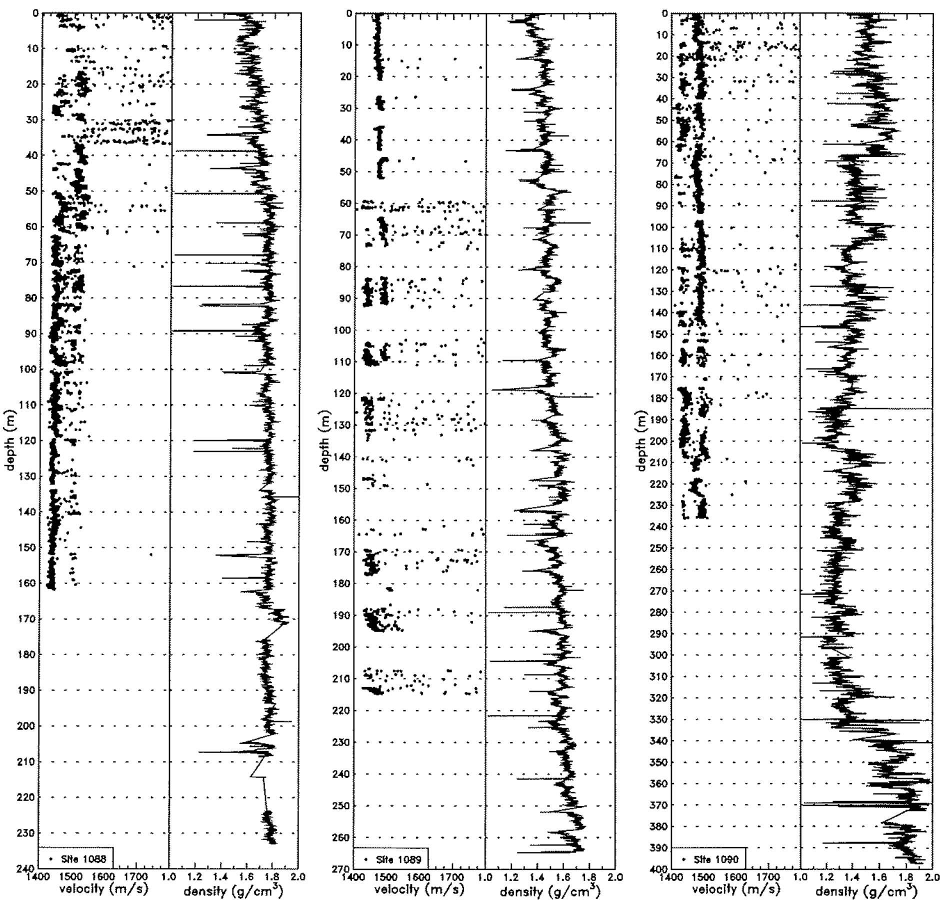

Fig. 4.4: *P-wave velocity from PWL measurements and density from GRAPE measurements for Sites 1088, 1089 and 1090 of Leg 177.*

porosity of the sediments at this site is higher than those of sites 1088 and 1090. Also, it is affected by much more siliceous components. The oldest sediments were recovered at Site 1090, at the south western part of the Agulhas Ridge (Fig. 4.1b). The 406 m cores contain sediments up to late Eocene, predominantly of calcareous composition. Several hiatuses have been found, which are linked to variations in deep water circulation. Between lower Miocene and early Pliocene, an 11.7 My. hiatus was found, possibly related to the emplacement of cold and corrosive bottom water masses (Galeotti et al., 2002). An hiatus between Pliocene and Pleistocene (Shipboard Scientific Party, 1999d) is likely due to variation in the depth and location of the boundary between various deep water masses (Venz and Hodell, 2002).

Because none of the holes of Leg 177 located near the Agulhas Ridge has downhole logging data available, the determination of the density and seismic velocity depends on shipboard measurements on whole-round core sections run through a Multi-sensor Track (MST) and sampled at an interval of either 2 cm or 4 cm for physical properties (Shipboard Scientific Party, 1999a). Fig. 4.3 gives an overview of the depth ranges for which density and P-wave velocity values are available. Numerous intervals though, have no data available for either P-wave velocity or density or both, especially at Site 1089. The limited overlap in the depth range covered by the various holes of Site 1088, reveals why a hole-to-hole correlation was not possible (Shipboard Scientific Party, 1999b). The density of the core samples was obtained by GRAPE measurements (Gamma Ray Attenuation Porosity Evaluator) and additionally weight and volume measurements on selected samples. These Moisture and Density (MAD) density measurements were generally only conducted once or twice per core section and on a few selected other samples, resulting in a very sparsely sampled log (Fig. 4.3). The GRAPE density values generally exist over the whole length of a hole (Fig. 4.3) and yield a series which can be used in the construction of synthetic seismograms after filtering of spurious measurements (Fig. 4.4).

Overall there is a good agreement between MAD an GRAPE densities for all three Sites near the Agulhas Ridge. At Site 1088 a downhole increase of the density can be observed, which coincides with increasing carbonate content (Shipboard Scientific Party, 1999b). The density data of Site 1089 shows an increase downhole as a result of compaction. Site 1089 bulk density data shows a considerable cyclicity with a period of 120 - 140 k.y. (Shipboard Scientific Party, 1999c). As in Site 1088, high density values at Site 1090 correspond to low porosity, carbonate rich sediments. The lower density values correspond to intervals rich in diatom ooze (Shipboard Scientific Party, 1999d). Remarkable is a strong drop in density at 70 m, which coincides with a disconformity, below which biogenic opal content increases and carbonate content decreases.

The P-wave velocity was measured by a P-Wave Logger (PWL) mounted on the MST, however this device suffered from a calibration error in the threshold detection during the sites cored at the Agulhas Ridge area (Shipboard Scientific Party, 1999a). Fig. 4.4 shows that there are clearly two trends for the P-wave velocity in all three sites, one near and above 1500 m/s and one that is lower and therefore unrealistic, as it is below the seismic velocity of water. A second instrument, a P-wave Velocity Sensor 3 (PWS3) has been applied on selected core samples which can be used to reconstruct a PWL curve. PWL data were of poor quality at all three Sites due to high signal attenuation and insufficient contact between the sediment and core liner, combined with a non-optimum threshold setting (Shipboard Scientific Party, 1999b,c,d). As a result, a low signal can cause the auto-picker to pick the second wavelet rather than the first. This artificially lowers the recorded traveltime, and yields apparently slow velocities.

Beside density and velocity measurements there were measurements on natural gamma ray emission, magnetic susceptibility and colour reflectance to aid in the hole-to-hole correlation of the samples.

4.3 Seismic data

During a seismic campaign in December 1997 and January 1998 carried out in the eastern South Atlantic by the Alfred Wegener Institute for Polar and Marine Research, seismic reflection profiles were collected with a total length of approx. 2000 km (Uenzelmann-Neben, 1998). This data covers the Agulhas Ridge and the adjacent parts of the Cape and Agulhas Basins. The profiles connect the three locations of ODP Leg 177 that were located at the Agulhas Ridge. The tie between core data and seismic data provides the potential to extrapolate the findings of the core information over a wider area, as well as the possibility to calibrate the depth of seismic units as determined from processing the seismic data. An energy source of two GI-guns™, 45 cubic inch volume each and operating at a pressure of 150 bar yielded records with a bandwidth of approx. 150 Hz and a frequency-maximum near 75 Hz (Fig. 4.5). This provided the necessary resolution within the imaged sediments and a penetration to reach the basement. The data was recorded with a sample-interval of 1 ms on a Syntron™ 96 channel streamer with 25 m spacing between the channels. The shot-interval of 10 s approximates 25 m between successive shots. Rough weather conditions necessitates extensive editing and filtering of noisy traces, especially for large offsets. A bandpass-filter of 25 Hz to 200 Hz was used for traces with offsets smaller than 700 m. The low-cut frequency has been raised to 55 Hz for larger offsets because low frequency contamination of the data starts dominating the signal. A residual source static correction proved to enhance trace-to-trace coherency significantly, necessary for a proper velocity analysis. Additional processing steps were carried out to further improve the signal-to-noise ratio of the stacked sections by improving lateral coherence within NMO-corrected CMP records such as a pre-stack f-x deconvolution. This step however has the potential to distort the amplitudes which is undesirable since we want to establish a correlation between the seismic data with data extracted from the physical properties measured at core samples. Adding 40 percent of the original data back proved to yield an adequate balance between resolution and preservation of amplitudes.

4.4 Conversion of logs to seismic

In general, log data or data from core measurements is not sampled in a way that is directly comparable to seismic data. A basic problem is that seismic data is measured

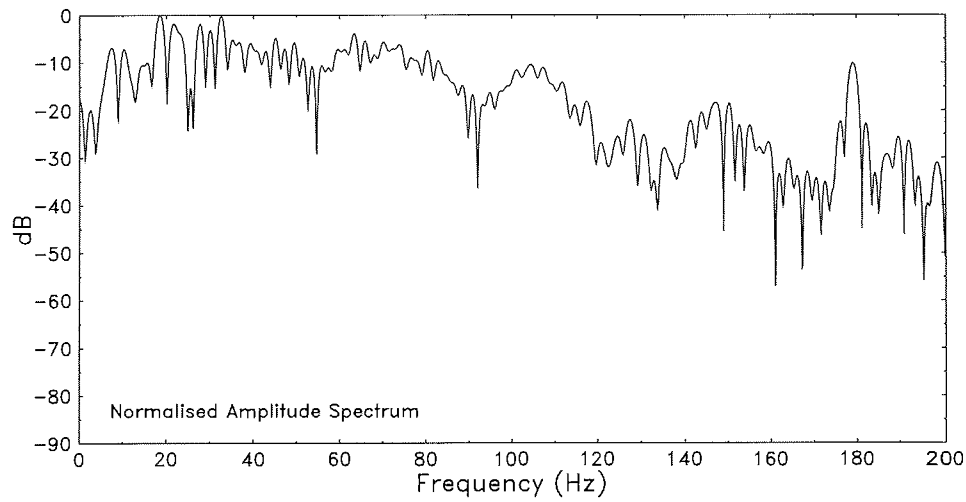

Fig. 4.5: *Frequency spectrum of the seismic data in dB down from the maximum amplitude.*

in time-domain, whereas log and core data are measured on a depth scale. One needs detailed information on the relationship between depth and time to perform a conversion. It is desirable to have data available from a check-shot or VSP survey (where a downhole receiver at regular intervals registers seismic signals from the source above the receiver as well as reflections from below) because of their direct comparability with seismic data, but alternatively, velocity information can be obtained from sonic logs or measured from core samples in case such data is not available (Adcock, 1993). Both core measurements and sonic log data suffer from uncertainty about the depth of the sampled rocks, in the case of log data because of cable stretch and in the case of core data because of incomplete core recovery and expansion of the cores. Particularly, core data is prone to bias for several reasons: usually data recovery is far from complete, leaving blanks in parts of depth range; recovered cores are measured under laboratory conditions, which are different from *in situ* conditions with respect to temperature, pressure and pore-fluid; or sampling might be biased towards specific intervals of interest to the operator. The accuracy of on-board Gamma Ray Attenuation measurements for general sediment-water mixtures is such that an error less than 5% is made (Blum, 1997). Velocities measured on sediment cores originating from depths shallower than a few hundred metres tend to be up to 5% lower than corresponding downhole measurements (Blum, 1997). Data from previous ODP projects suffered from these problems too, as discussed previously by several authors (Shipley, 1983; Edwards, 1998; Sun, 2000; Delius et al., 2001). Another problem is the difference in sampling interval; log and core data is often sampled at a centimeter scale, in the case of the Leg 177 data at a rate of either 2 cm or 4 cm. The seismic data however is insensitive to very small scale layering, depending on its frequency content and sampling rate. The seismic data was sampled at 1 ms interval, which roughly equals a sampling rate of 75 cm to 1 m in the depth-domain for assumed seismic velocities of 1500 m/s

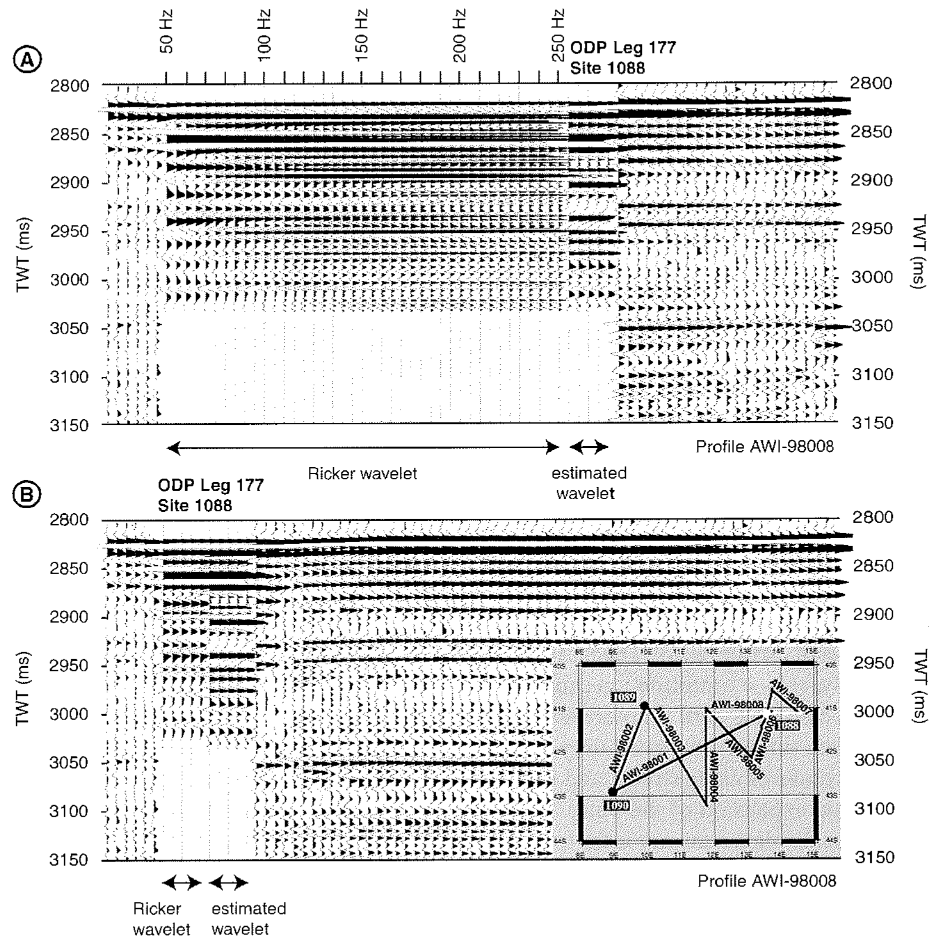

Fig. 4.6: *a) comparison of seismic data with synthetic data constructed with a wavelet extracted from the real seismic data, and a sequence of synthetic traces constructed with Ricker wavelets. The dominant frequency of the Ricker wavelet increases in 10 Hz steps between 50 Hz and 250 Hz. Seismic data from profile AWI-98008 at the location of Site 1088 is shown.;*
b) The same real seismic data as the top figure shows a comparison of synthetic traces constructed with a 75 Hz Ricker wavelet and synthetic traces constructed with a wavelet that was estimated from the seismic data.

to 2000 m/s. Considering that the dominant frequency of the seismic data is below 100 Hz, this means that the resolution is even lower by one order of magnitude, and therefore considerably lower than the ODP data.

Device coupling to the core samples, or the influence of the casing for log data, can also influence the obtained values. This can lead to parts of well measurements that are either missing or of poor quality, and filtering and interpolation for missing data is therefore usually necessary. This is also necessary when seismic P-wave velocity and density are measured at different intervals on core sections. The filtered, interpolated and re-sampled velocity and density information can then be used to calculate a reflectivity series by $R = (v_2\rho_2 - v_1\rho_1)/(v_2\rho_2 + v_1\rho_1)$. This is the seismic trace that would be obtained if a perfect spike source would be used. Median filtering is used to remove spurious values from the data series without affecting strong instantaneous contrasts, i.e. at buried erosional surfaces. A threshold value is used to remove the ambiguity from the velocity data caused by the auto-picking algorithm of the P-wave logger where it erroneously picked the second wavelet and recorded an incorrect P-wave velocity. The reflectivity series is calculated after re-sampling and spline-interpolation to reduce the sensitivity to effects on a smaller scale than the real seismic data warrants and to have a continuous and regularly sampled series of data.

Real, non-deconvolved, seismic data is basically the earth response to a source signal. An additional convolution of the reflectivity series with the source wavelet as used in the seismic survey is therefore necessary to make synthetic and real seismic data comparable. Internal reflections in the sediment layer have been included in the calculation of the synthetic traces, although their influence is very limited due to the small reflection coefficients values. If a measured source signature is not available one has to resort to either a synthetic wavelet or a wavelet estimated from the seismic data. An estimated wavelet has the disadvantage that it itself is not a pure wavelet, but contains geological information as well, and might be affected by attenuation effects and noise which can lead to a rather unsharp signature. An artificial wavelet on the other hand usually produces sharp signals in the synthetic data but has a different characteristic with respect to real data. With the availability of both velocity and density information, as in our case, the construction of a series of reflection coefficients is possible. At the deeper parts of the wells we only have density information available though (Fig. 4.3). If either velocity or density data is not available or if these are of a quality too poor to be used, one could use an empirical relationship to estimate the missing variable such as Gardner's relationship (Gardner et al., 1974; Adcock, 1993).

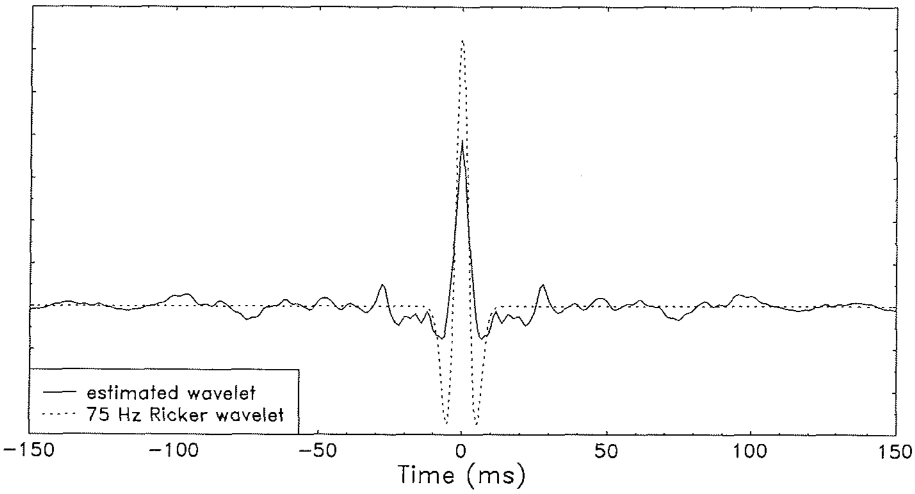

Fig. 4.7: *Comparison of a zero-phase seismic wavelet estimated from the data near Site 1088 and a Ricker wavelet with a maximum amplitude at 75 Hz.*

4.5 Results

The data from the seismic survey has been processed to approximate a zero phase section to facilitate interpretation. Spherical spreading is accounted for, other gain corrections as for attenuation loss have not been applied. Figure 4.6a shows a comparison between synthetic traces obtained using Ricker wavelets (Ricker, 1953) and by using a signature extracted from the seismic data for Site 1088. Ricker wavelets having a maximum amplitude between frequencies of 50 Hz and 250 Hz were applied to the reflectivity series. This shows that synthetic traces constructed with Ricker wavelets of low frequencies exhibit a serious loss of resolution; the reflector at 2900 ms for instance, is not resolved in these traces. On the other hand, higher frequency wavelets introduce seismic reflectors where they are not resolved in the real seismic data such as the series of reflections between 2950 ms and 2975 ms. Although there might be layers in the sediments, which would act as reflectors for high frequency seismic waves and can indeed be resolved by the small sampling interval in core sections, they are not sensitive to the frequencies emitted by the actual seismic source and would obscure rather than aid a correlation of seismic data with the cored sediments. This is especially so when a single strong reflector in the recorded seismic data, e.g. the reflector at 2850 ms, actually consists of several reflectors when higher frequencies are used. A meaningful interpretation requires the bandwidth of the synthetic data to be adapted to the real seismic data to obtain the same resolving power. A best correlation is obtained with a Ricker wavelet of 75 Hz as shown by the comparison with the seismic data of profile AWI-98008 (Fig. 4.6b). Reflectors at 2840 ms and 2900 ms are still represented in the synthetic seismogram whereas lower frequency wavelets cannot resolve these reflectors. On the other hand, the reflector at 2880 ms appears as a single reflector the same as in the real seismic data, but not if higher frequency wavelets are used in the calculation of the synthetics. Figure 4.7 shows the time domain characteristic of both the 75 Hz Ricker wavelet and a zero-phase wavelet, estimated from data near the location of Site 1088. Application of lower frequency wavelets results in detail loss, whereas higher frequency wavelets introduce artifacts in the synthetic data that do not exist in the real data, thereby obscuring important reflectors. The 75 Hz Ricker wavelet also shows a better result than synthetics obtained by application of a wavelet estimated from the seismic data. This is likely due to the fact that it is difficult to accurately estimate such a signature when the sediments directly below the seafloor are not more or less seismically transparent.

Processed seismic data should have seismic reflectors that clearly stand out with respect to the noise, and this usually involves a deconvolution processing step. If we want the seismic data to be comparable to synthetic data then this step cannot be applied. This however, is not a big issue, as Shipley (1983) shows. Comparing different deconvolution models for deep sea seismic sections at Blake Bahama Basin, he did not obtain a much better result for seismic reflectors immediately below the sea-floor.

The step following the computation of the synthetic seismograms is their use in the interpretation of the seismic data. The cored samples have not only been analysed on physical properties, but on micro-palaeontological, sedimentological and petrological properties as well. In this way, a known erosional contact in the cored sequence for instance, can be traced to a unique location in the synthetic seismogram constructed from data on the very same core samples. In this way the seismic sequence can be assigned a petrophysical, or palaeontological stratigraphy as well as a time scale.

For Site 1088 there is a very good correlation between seismic data and synthetic seismograms. The lithology at this site (Fig. 4.2) is quite uniform throughout the section. This means that the seismic reflectors do not represent compositional variations, but rather a jump in density due to different compaction at stratigraphic discontinuities. The reflector at 2950 ms however coincides with an increase of the sedimentation rates from 17 m/m.a. to 30 m/m.a. (Shipboard Scientific Party, 1999c). Indeed, (Fig. 4.8) at profile AWI-98006 shows that the major reflections in both the synthetic data as well as in the real seismic data coincide with a Pliocene hiatus at 2860 ms and the Pliocene/Pleistocene (at 2850 ms) and Miocene/Pliocene (at 2880 ms) boundaries, as marked by geological core analysis. Also the upper/middle Miocene boundary observed in the cored material correlates roughly with the seismic reflector at 3050 ms, although it should be noted that this observation is based on extrapolation of the data since seismic velocity information, and therefore an accurate time scale, is not available up to this depth, only density data. (Fig. 4.3).

Site 1089 is an example of the problems that arise when the velocity information is incomplete (Fig. 4.3 and 4.9). This is especially true for the deeper parts of the well which only exists from Hole 1089A and had a poor recovery rate (Shipboard Scientific Party, 1999c). Unreliable velocity information and missing or spurious density information (Fig. 4.4), even after filtering the density logs, make it difficult to construct an accurate reflectivity series for Site 1089. This results in unrealistically high amplitudes in the synthetic seismic data especially in a seismic transparent zone between 6350 ms and 6440 ms (Fig. 4.9). Correlation of the synthetic data with the seismic section still is adequate for the upper 70 ms (Fig. 4.9), but below 6270 ms the synthetic data seems to be shifted downwards, which indicates that the velocities used in the depth-to-time conversion were too low. It should be noted however that this site is located at a slight offset from the seismic profile AWI-98003 (Fig. 4.1) which might account for some of the misfit.

Fig. 4.10 shows a visual correlation of synthetic and real data at Site 1090. The major reflectors in the seismic data (Fig. 4.11) can be directly linked to geological units, such as the Miocene/Pliocene boundary at 5070 ms, the Oligocene-Miocene boundary at 5170 ms and the early/late Oligocene boundary at 5255 ms. One of the dominant reflectors in the seismic data, and in the synthetic data as well is the hiatus found in the early Oligocene (at 5280 ms in Fig. 4.10). The analysis of the seismic data of Fig. 4.11 shows a clear stratigraphic discontinuity, which however was initially not evident on the basis of geological core analysis alone. Remarkable is the phase shift between the real and synthetic data at 5110 ms, which is associated with a lithologic change from an episode with increased carbonate accumulationand preservation to an episode of relatively strong input of terrigenous matter (Diekmann et al., 2002) (Fig. 4.2). This, and the differences in reflection strength of the reflectors 5220 ms and near the early Oligocene Hiatus at 5280 ms in comparison to the real seismic data are indicators that a Ricker wavelet does not completely describe the source signature as used in the seismic survey in an adequate way. Because Site 1090 is located on the northern flank of the Agulhas Ridge, which has a strong relief, the possibility also exists that part of the phase shifts are indeed in the seismic sections due to oblique incidence of the seismic waves on the tilted layers. The deeper parts of the synthetic data, roughly the lower half, might be slightly displaced in time, due to calibration and coupling problems with the P-wave logger.

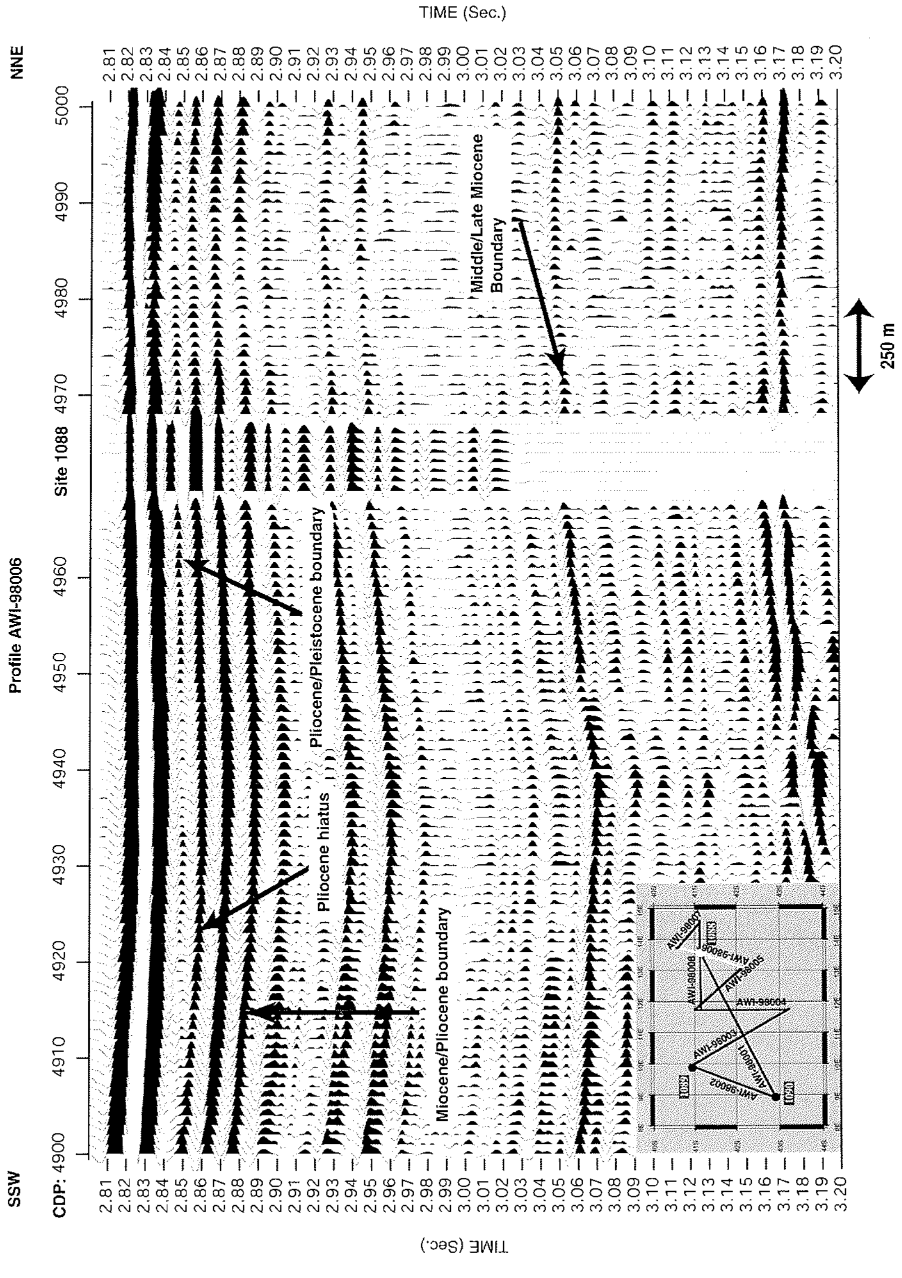

Fig. 4.8: An excellent correlation exist between Site 1088 derived synthetic seismograms with real seismic data of profile AWI-98006. Identification of the origin of the seismic reflectors as hiatuses in the biostratigraphic record (see Fig. 4.2) is made possible through linking physical properties analysis and stratigraphy, both derived from core samples.

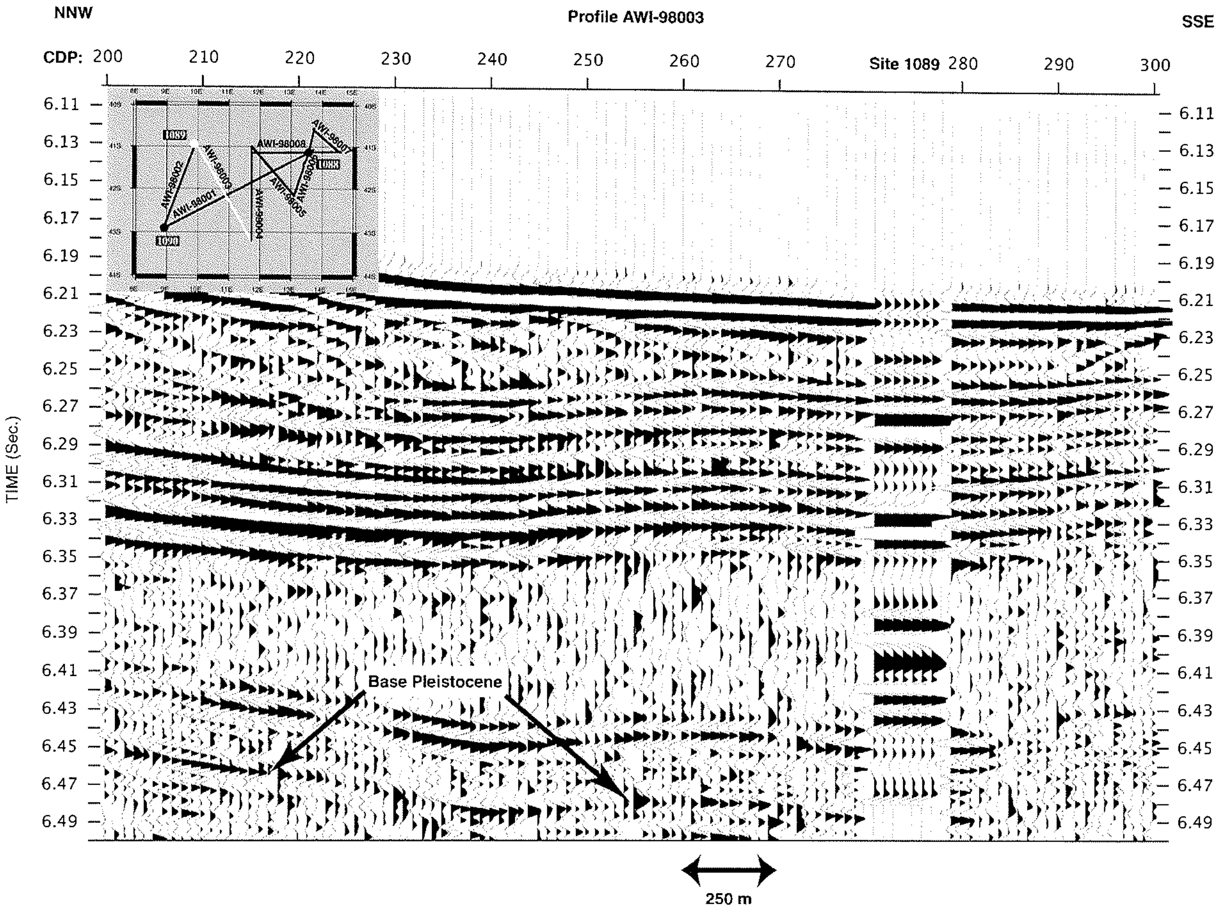

Fig. 4.9: *Profile AWI-98003 shows that lack of a high quality series of core measured velocity data, as measured at Site 1089 results in a poor correlation between real and synthetic seismic data.*

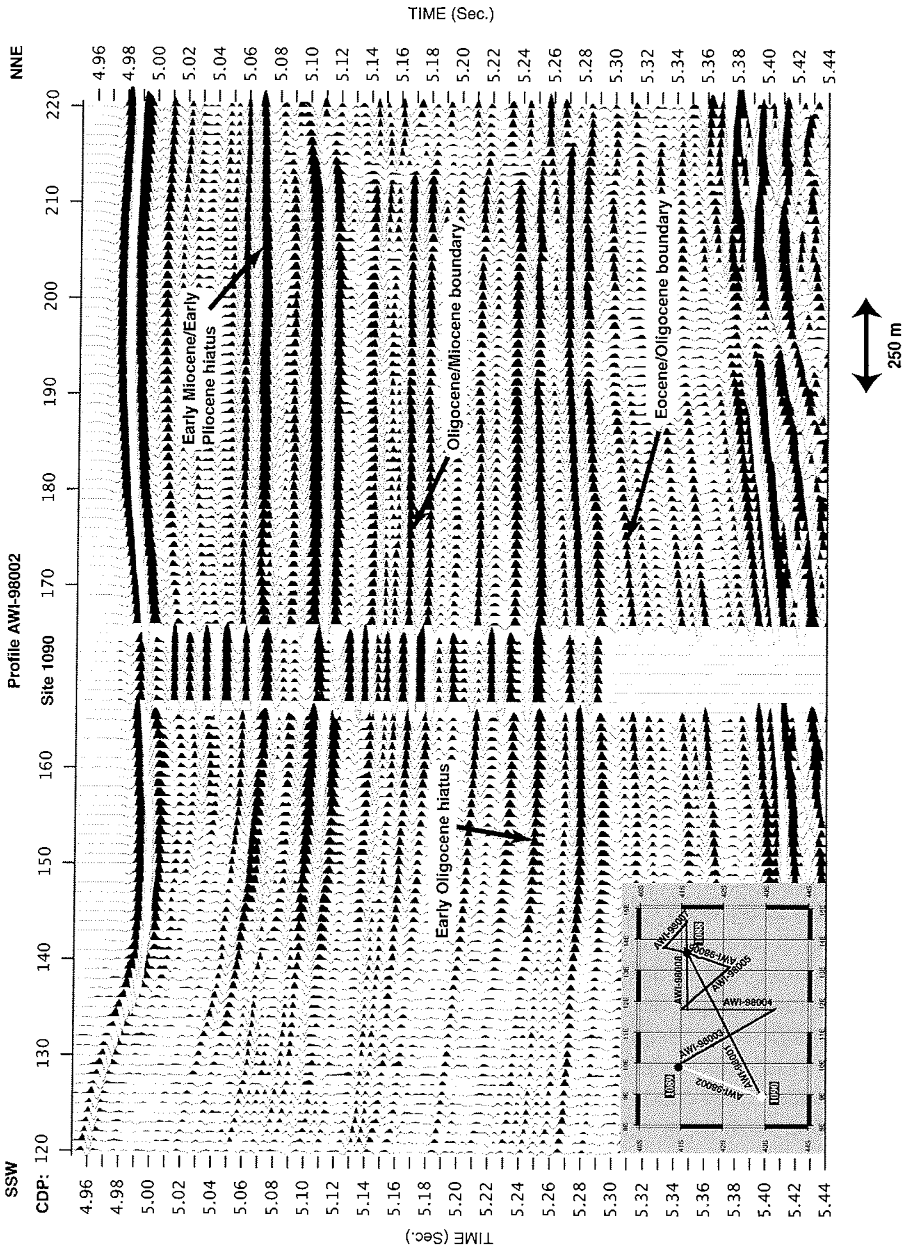

Fig. 4.10: *This section from the south-western end of profile AWI-98002 shows a comparison between real data and synthetic data obtained from convolution of a reflectivity series from core data of Site 1090 with a 75 Hz main frequency Ricker wavelet.*

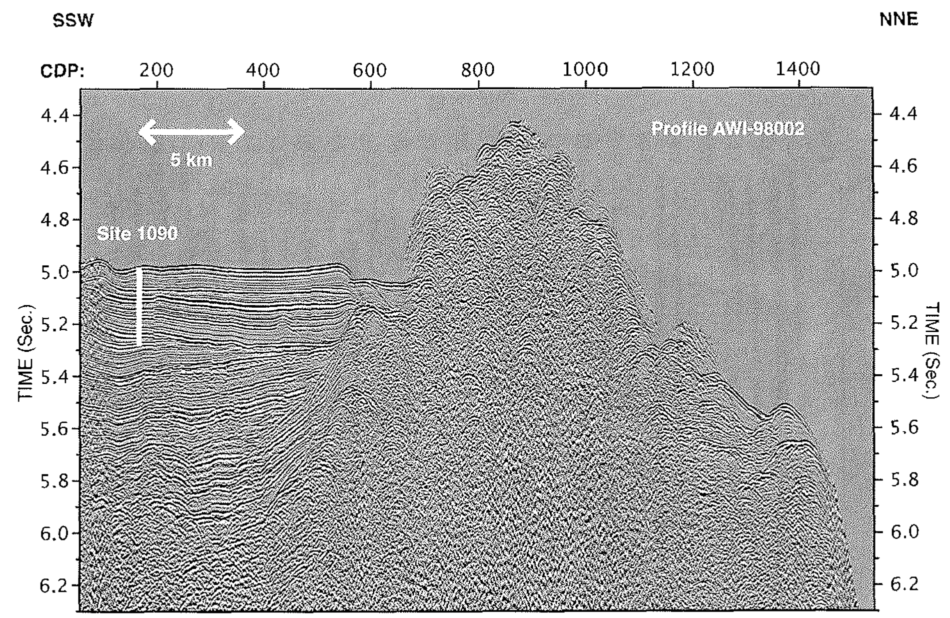

Fig. 4.11: *Seismic data of profile AWI-98002 on the top of the Agulhas Ridge over the location of Site 1090.*

4.6 Conclusions

If downhole logging data and check-shot data do not exist then one can instead use physical properties measured on core samples to establish a correlation between seismic and geological data. ODP Leg 177 data show that the quality of synthetic seismograms mainly depends on the accuracy of measured density information, which appears to be the dominant factor in the deep sea environment of the South Atlantic Ocean. Because seismic data exists in time-domain whereas the core data is sampled in the depth-domain it can be difficult to correlate the constructed synthetic seismograms with seismic data. It can be done either visually or by converting either the synthetic seismograms to time, or by converting the seismic sections to depth. This requires detailed knowledge of the velocity structure which can be derived from velocity measurements on cores, but can be problematic since *in situ* conditions are different from the conditions under which the cores are sampled. Also these velocity logs are far from complete, which introduces a serious bias when applied in the time-depth conversion process. Structural bias from calibration errors of the equipment can also play a role in the construction of synthetic seismograms and the subsequent interpretation of seismic sections. Biased density or velocity values lead to incorrect reflection coefficients, which in turn causes over- or under-estimated amplitudes. A more serious problem is that in the conversion between time and depth every deviation adds up to what can result in conversion errors of up to several tens of metres.

Therefore a visual correlation or adjustment of the synthetic data remains a necessity to identify the geological units of the core data on the seismic sections. Site 1090 of Leg 177 shows that the opposite is possible as well. A prominent reflector in the seismic data could be identified in the geological data as a hiatus in the early Oligocene with the assistance of synthetic seismograms constructed from the cores. This shows that valuable structural information, available through seismic interpretation, can arise from only slight variations in some properties of the sediments which are not always evident considering geological information alone.

Acknowledgements

We are grateful for the support of the captain and crew of R/V Petr Kottsov for their help during the expedition. The expedition was funded by the German Bundesministerium für Bildung, Forschung und Technologie under contract No. 03G0532A, and the work of E. Wildeboer Schut by the German Science Foundation, proposal No. Ue 49/3.
This research used data provided by the Ocean Drilling Program (ODP). The ODP is sponsored by the U.S. National Science Foundation (NSF) and participating countries under management of Joint Oceanographic Institutions (JOI), Inc. Funding for this research was provided by the Deutsche Forschungsgemeinschaft. This is AWI contribution AWI-......

4. THE CHALLENGE OF TIEING SEISMIC DATA TO GEOLOGIC INFORMATION: AN EXAMPLE FROM ODP LEG 177, SITES 1088-1090

5. SEISMIC EVIDENCE FOR BOTTOM CURRENT ACTIVITY AT THE AGULHAS RIDGE *

Etienne Wildeboer Schut, Gabriele Uenzelmann-Neben and Rainer Gersonde

Abstract

In the South Atlantic water masses from the Atlantic and Indian Oceans meet Antarctic water masses. The Agulhas Ridge, a pronounced elevation of the ocean bottom in the eastern South Atlantic, has acted as a barrier for deep oceanic currents since the Cretaceous, such as the North Atlantic Deep Water (NADW) and Antarctic Bottom Water (AABW), or water masses derived from AABW such as Circumpolar Deep Water (CDW). The history of these currents is recorded in the sedimentary sequence in the adjacent Cape and Agulhas Basins. Seismic profiles over the Agulhas Ridge show sediment packages in the Cape Basin which are interpreted as contourite sheets. These consist of thick sequences interrupted by widespread hiatuses, with a predominantly low seismic reflectivity. The seismic data shows prominent reflectors inside contourite drift bodies which, at the location of the drill-sites of ODP Leg 177, can be attributed to hiatuses in the early Oligocene, the middle Miocene, around the Miocene/Pliocene boundary and in the early Pleistocene. In this way ODP Leg 177 cores were used to date an elongate contourite drift in the Cape Basin. This drift shows sediments deposited by a westward current, implying that the bottom current in the Oligocene followed the same trajectory as present-day CDW does.

Key words: South Atlantic; Agulhas Ridge; seismic reflection; palaeo-reconstruction; bottom currents

5.1 Introduction

One of the prime factors controlling regional climate is ocean circulation. The present day inter ocean exchange of water masses is driven by a global thermo-haline convection system, that transports deep water sediments and partly erodes the ocean bottom. Past ocean

* Published in: Wildeboer Schut, Uenzelmann-Neben, and Gersonde (2002), *Global and Planetary Change*, Vol. 34:185–198; An electronic version of the published paper can be obtained from `http://www.elsevier.com/wps/find/journaldescription.cws_home/503335/description`

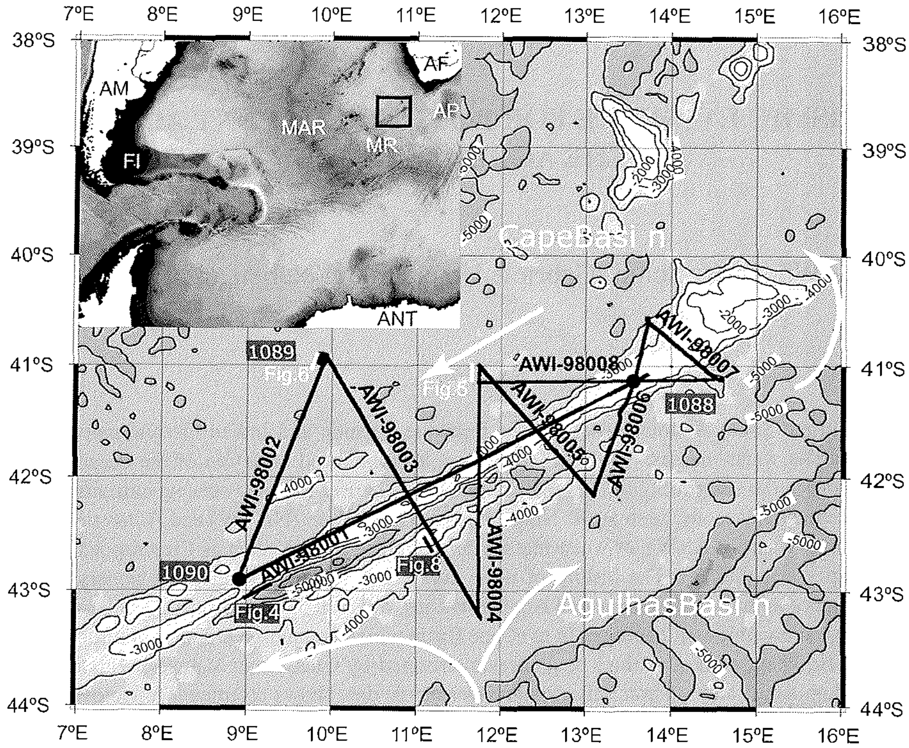

Fig. 5.1: *Bathymetry map of the Agulhas Ridge area after Sandwell and Smith (1997) with seismic profiles AWI-98001 through AWI-98008 and drilling locations of ODP Leg 177 Sites 1088, 1089 and 1089 (big dots); abbr.: AF: Africa, AM: South America, AP: Agulhas Plateau, ANT: Antarctica, FI: Falkland Islands, MAR: Mid Atlantic Ridge; arrows denote flow of the bottom water after Tucholke and Embley (1984).*

circulation can be studied from the effects of deposition and erosion by bottom currents observed in seismic data. This paper focuses on the southern Atlantic, a region where water masses of Atlantic, Indian/Pacific and Antarctic origin meet. Sea-floor spreading and the opening of the South Atlantic Ocean started in the early Cretaceous (Ben-Avraham et al., 1993, 1997). The Agulhas Ridge has formed along the Falkland-Agulhas Fracture Zone (FAFZ), a transform fault between the African and South-American plates related to the breakup of West Gondwanaland (Ben-Avraham et al., 1997). The Agulhas Ridge represents a pronounced elevation of the sea-floor relative to the adjacent ocean basins, extending from approx. 41°S,13.5°E to 43°S,9°E (Fig. 5.1) south-west of the coast of South Africa. It separates the Cape Basin north of the ridge from the Agulhas Basin to the south and coincides with the north of the Meteor Rise at its south-western end. The north-eastern part of the Agulhas Ridge coincides with the location of a spreading centre of the mid-Atlantic ridge south of the FAFZ that was abandoned in the Late Cretaceous (LaBrecque and Hayes, 1979). The age of the Agulhas Ridge makes it a witness to a geological period in which continental drift led to the opening of gateways around the Antarctic and the closure of the Panamanian gateway (Droxler et al., 1998; Lawver and Gahagan, 1998). As a barrier for deep oceanic currents, the Agulhas Ridge had a strong impact on oceanic circulation which is recorded in the sediments near the Agulhas Ridge. Different regions where the sediments originate and the intensity of currents generate particles varying in grain size and fabric. Climatic variations affect relative amounts of calcareous and siliceous sediments through biogenic production influence on carbonate dissolution. The seismic image shows variations in reflectivity of sediments, whether by variation in physical or chemical properties of the sediments, as well as structural features such as drift systems. In this paper we study past ocean bottom currents from sequence stratigraphic analysis of seismic reflection data at the Agulhas Ridge to monitor changes in deep water flow in the South Atlantic Ocean during the Cenozoic. We correlate our seismic data with data from the Ocean Drilling Program (ODP) Leg 177 (Gersonde, Hodell, Blum et al., 1999) for calibration.

5.2 Oceanography

The present general circulation of oceanic currents around the Agulhas Ridge mainly constitutes the North Atlantic Deep Water (NADW), the Circumpolar Deep Water (CDW), and the Agulhas Current coming from the Indian Ocean (Lutjeharms, 1996; Reid, 1996). Near the southernmost tip of the African continent, the Agulhas current dissolves in a ring pattern and mixes with other water masses (Lutjeharms, 1996; De Ruijter et al., 1999). Cold AABW (Antarctic Bottom Water) mixes in the Antarctic Circumpolar Current (ACC) with water masses from the north to form the CDW (Orsi et al., 1999). Northward flowing branches of CDW are deflected in a mainly western direction near the Agulhas Ridge (Tucholke and Embley, 1984; Sykes et al., 1998). A branch enters the Cape Basin along the western coast of South Africa (Fig. 5.1), from where it flows in a southwestern direction along the ridge until it bends in a northward direction again at the southwestern part of the ridge. This water mass is significantly warmer in the Cape Basin than in other areas with comparable latitude due to mixing and the longer flow path (Tucholke and Embley, 1984). Part of the mixing comes from the NADW which is vertically located between upper and lower CDW (Reid, 1996). Cooling of the northern hemisphere since the late Pliocene increased the input of NADW at the expense of CDW in the South Atlantic ocean during glaciation cycles (Turneau and Ledbetter, 1989). The shallower Antarctic Intermediate Water originates from surface water around Antarctica. It flows northward into the South Atlantic, extending to depths of approximately 1000 m around 40°S (Turneau and Ledbetter, 1989). In the Cape Basin it follows an anti-cyclonic path (Shannon and Hunter, 1988) opposing the direction of underlying CDW. Historically, the onset of the AABW finds its origin in the Oligocene (Mackensen and Ehrmann, 1992; Zachos et al., 1994), during which the opening of the Drake Passage between South-America and Antarctica and the separation of Australia and Antarctica took place. This led to the formation of the ACC (Barker and Burrell, 1977; Kennett, 1977; Lawver and Gahagan, 1998) and is responsible for the thermal insulation of Antarctica.

5.3 Contourites

Sediment supply deep in the South Atlantic originates mainly from biogenic production and from deposition by bottom currents (e.g. Tucholke and Embley, 1984). Downslope turbidity currents and along-slope contour currents deposit and erode sediments in the oceanic basins (Faugères and Stow, 1993; Faugères et al., 1999). Contourites are defined as sediment bodies deposited or reworked by the sustained flow of thermo-haline driven geostrophic bottom currents (Heezen et al., 1966; Faugères and Stow, 1993) that are flowing parallel to bathymetric contours in deep sea basins. Such currents are also involved in the exchange of water masses between ocean basins, carrying mainly fine grained sediments due to the generally low current velocity. Deep-sea bottom currents are capable of redistributing sediment bodies over 1000 km in length (Faugères and Stow, 1993). On the other hand, high velocity bottom currents are also responsible for the creation of large erosional surfaces by scouring the sea-floor. Faugères and Stow (1993) classify contourite drifts in three main morphological types: (a) Giant elongate drifts, parallel to continental margins, or mid-ocean ridge flanks, (b) contourite sheets, sheet like, morphologically flat facies in more or less closed basins, and (c) channel related drifts. Giant elongate drifts have been found to originate in the Oligocene and early Miocene (Stow et al., 1998). Elongate mounded drifts in seismic sections appear mostly lenticular in shape with a convex geometry and a base that is usually a more or less flat major erosional surface (Faugères et al., 1999). In oceanic basins the contourite facies are often characterised by an asymmetric levee system due to enhanced deposition on one side and erosion on the other under the influence of the Coriolis force. On the Southern hemisphere this leads to preferential deposition on the left flank of the channel. This Coriolis effect, interaction between currents and morphology and variation in intensity and interaction with other currents also lead to a prograding lateral migration of the crest (Faugères et al., 1999). Sheet-like drift systems often have a discontinuous internal seismic structure, and tend to have low amplitude reflectors, mostly due to the fine and homogeneous sediments (Faugères and Stow, 1993). However, even a small change in supplied sediments, or a variation in current velocity can create erosional surfaces or beds with different seismic reflectivity properties, creating higher amplitude reflectors. Channel-confined drifts have an appearance similar to elongate mounded drifts, with moats along both margins (Faugères et al., 1999). These types of drifts are less commonly observed than the other types. It still is not clear how sea-level would influence the occurrence of contourites (Faugères et al., 1999). However, contourites are often observed from periods of climatic instability and sea-level change (Faugères and Stow, 1993). High sea-level enhances water mass exchange between the ocean basins, which leads to increased bottom current activity, but also tends to reduce turbidity current activity. On the other hand, bottom current activity is often masked by increased turbidity current activity during low-stands of the sea-level (Faugères and Stow, 1993). Antarctic glaciation had an impact on the composition of sediments through alteration in biogenic production rates, as well as variations of the source region and due to flow intensity variations also grain size of supplied terrigenous material. Whether a glaciation favours or diminishes bottom current activity depends on both time scale and origin of the water masses. Although contourite development and glaciation do not seem to be directly linked to each other, there still is an indirect link, as the opening or closing of gateways for ocean water exchange affect both.

5.4 Data and methods

5.4.1 Reflection seismic data

In this paper we present data from the seismic survey expedition with R/V Petr Kottsov during December 1997 and January 1998 carried out by the Alfred Wegener Institute for Polar and Marine Research (see Uenzelmann-Neben, 1998). Eight profiles of seismic data with a total length of approximately 2000 km were collected over the Agulhas Ridge extending into the Agulhas and Cape Basins (Fig. 5.1). An energy source of two GI-guns™, each with a volume of 45 cubic inch, operating at a pressure of 150 bar were used to obtain 96 channel records with 25 m spacing between the channels and a recorded length of 8 seconds, 1 millisecond sample-interval. The bandwidth of the data was around 150 Hz, with a maximum frequency of 75 Hz. Special care for noise reduction was necessary due to extreme weather conditions during acquisition. The data were sorted in CMPs with a distance of 25 m between the consecutive locations. Noisy traces have been removed and the data were filtered for noise reduction prior to velocity analysis. Stacked seismic sections were created after normal moveout correction and additional coherency filtering for further noise reduction. These sections were time-migrated to enhance the resolution of geological structures in the subsurface.

5.4.2 ODP Leg 177 data

The seismic profiles connect three ODP sites drilled during Leg 177 with R/V Joides Resolution between December 1997 and February 1998 (Gersonde, Hodell, Blum et al., 1999). Sites 1088 and 1090 were drilled at the Agulhas Ridge while Site 1089 is located in the adjacent Cape Basin (Fig. 5.1). middle Miocene to Holocene sediments have been recovered. The core samples were studied with respect to sedimentological, physical and chemical properties and preliminary age models have been established based on combined magneto- and biostratigraphic methods (Gersonde, Hodell, Blum et al., 1999).
Site 1088, at 2092 m depth on top of the Agulhas Ridge, consists mainly of calcareous sediments (Shipboard Scientific Party, 1999b), with carbonate percentages varying from 85 to 95 wt% (Fig. 5.2). In total, 233.7 m of Holocene to middle Miocene sediments were cored with the objective to recover a long Cenozoic carbonate sequence to study palaeoceanographic changes near the Sub-tropical Front (Shipboard Scientific Party, 1999b). Due to technical problems it was not possible to drill sediments of early Cenozoic age. Two hiatuses were found, in the middle Miocene and between Pliocene and Pleistocene.
At Site 1089, in the southernmost Cape Basin (Fig. 5.1), a sedimentary sequence of 264.9 m at a water depth of 4620 m was obtained, which documents the Holocene to the late Pliocene (2.4 Ma) (Fig. 5.2). The Pleistocene section has been deposited at high sedimentation rates (ca. 130-140 m/m.a.), while Pliocene sedimentation rates decline to

$\sim$ 40 m/m.a. (Zielinski and Gersonde, 2002). Core samples between 95 and 156 mcd (meters composite depth) (Shipboard Scientific Party, 1999c) show that the sediments are slightly slumped. However the sedimentary sequence remains stratigraphically continuous (Zielinski and Gersonde, 2002). This provides records of Pleistocene glaciation cycles with high temporal resolution. The sediments have a fluctuating carbonate content between 0 and 60 wt% due to variation in the amounts of terrigenous mud and changes in carbonate preservation. The Pliocene/Pleistocene boundary is well defined in Site 1089 and is located at ca. 230 mcd (Zielinski and Gersonde, 2002).
Site 1090, at the southern end of the Agulhas Ridge, was placed at a water depth of 3702 m. Due to one or two disconformities between 71.5 and 78.5 mcd, which separate lower Pliocene and probably uppermost Miocene sediments from lower Miocene sequences, drilling at Site 1090 reached the middle Eocene at 397 mbsf (meters below sea floor) (Shipboard Scientific Party, 1999d). While the study of planktic foraminifers by Galeotti et al. (2002) indicates two disconformities at 71.5 and 78.5 mcd, separating early Pliocene from late Miocene and late Miocene from early Miocene, respectively, shipboard stratigraphic data also including the geomagnetic inclination record reveal one disconformity at around 70 mcd which separates the early Pliocene from the early Miocene and spans ca. 14 m.a. (Shipboard Scientific Party, 1999d). Increased bottom-current velocity caused widespread hiatuses in oceanic sediments in many other areas as well (e.g. Ledbetter and Ciesielski, 1982; Keller, 1987). The study of planktic foraminifers also indicates strong reworking of late Cretaceous (Campanian-Maastrichtian to Miocene) planktic foraminifers at around 71.5 mcd (Galeotti et al., 2002). Three other short-ranging disconformities have been encountered in the Pleistocene (Venz and Hodell, 2002), two being close to the Plio-/Pleistocene boundary at around 40-43 mcd. Calcareous nannofossil investigations point to a hiatus at around 220 mcd, in the early Oligocene, which spans about 3 m.a. (Marino and Flores, 2002). Nannofossils, diatoms and mud comprise the major lithologic components of the sediments recovered at Site 1090. While the middle and early late Eocene consist of mud-bearing nannofossil ooze and chalk, the late Eocene to early Miocene is characterised by mud-bearing diatom ooze and diatom bearing nannofossil ooze and chalk. The Plio/Pleistocene sequences are characterised by alternations of nannofossil ooze and diatom-bearing nannofossil ooze. A chert layer has been encountered at 290 and 340 mbsf, respectively, in the Eocene section (Shipboard Scientific Party, 1999d). The disconformity at around 70 mcd is underlain by a tephra layer (Shipboard Scientific Party, 1999d).

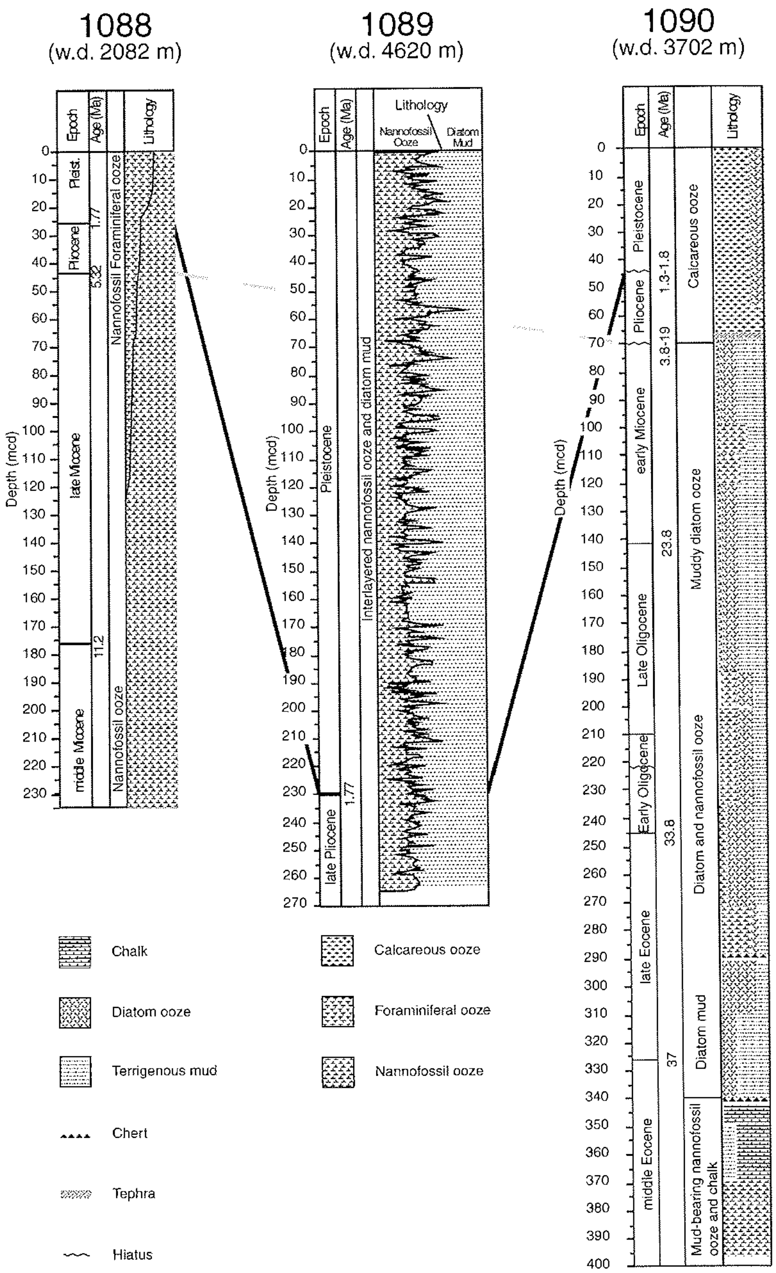

Fig. 5.2: *Summary of lithologies for ODP Leg 177 Sites 1088, 1089 and 1090 after Gersonde, Hodell, Blum et al. (1999); Shipboard Scientific Party (1999b,c,d). wd = water depth, mcd = meters composite depth*

5.4.3 Incorporation of geological and seismic data

The physical properties measured on the recovered sediments include density and seismic P-wave velocity (Gersonde, Hodell, Blum et al., 1999). From these data synthetic seismic data were constructed at the core locations, which can be compared with the recorded seismic data. In this way, age control of the seismic data is possible, as the synthetic data is based on the same core samples as is used for age dating by the analysis of fossils in the sediments. Erosional surfaces found in core samples, as well as changes in depositional conditions as inferred from core data, can be linked with reflection seismic horizons. Both chemical and physical properties of sediments have an impact on the density and P-wave velocity, and thus influence the reflectivity of seismic horizons.

Density and P-wave velocity are available for all three sites (Shipboard Scientific Party, 1999b,c,d). After removal of spurious data, correlation between various holes and interpolation to fill in depth ranges with missing data, it was possible to construct a series of seismic impedances, and with these, a reflectivity sequence. The P-wave velocities were used to convert the data from depth-domain into time-domain and after convolution with a 75 Hz Ricker wavelet synthetic seismograms were generated.

5.4.4 Results

On the basis of constructed synthetic seismograms, we identified the seismic reflectors on profile AWI-98008, at the location of Site 1088, corresponding with hiatuses like at the Pliocene-Pleistocene boundary (Shipboard Scientific Party, 1999b) and a hiatus at 209 mcd (Marino and Flores, 2002) in the middle Miocene. Also, increased sediment rates often accompany lithologic variations, creating reflectors, like at the Miocene-Pliocene boundary (denoted A in figure 5.3), where sedimentation increases from 7.5 m/m.a. to 17 m/m.a., and in the late Miocene (denoted B) where sedimentation increases from 17 m/m.a. to 30 m/m.a. (Shipboard Scientific Party, 1999b)

Figure 5.4 shows that the Miocene hiatus as cored at Site 1090 and the early Oligocene hiatus are related to distinct seismic reflectors as well. A comparison of the stratigraphic sequence in the seismic data at CDP 17000 of profile AWI-98001 (Fig. 5.4) and CDP 17700 near the location of Site 1090 shows that a sequence of approximately 80 m of sediments is missing at the early Oligocene hiatus at Site 1090. Considering a duration of 3 m.a. of the early Oligocene hiatus at Site 1090 (Marino and Flores, 2002) this would suggest sedimentation rates of 25-30 m/m.a. during the early Oligocene. These reflectors can be identified on several profiles in the Cape Basin, for instance profile AWI-98004 (Fig. 5.5) and profile AWI-98002 (Fig. 5.6), where the early Oligocene and the Miocene hiatus are denoted as reflectors O and M respectively. The sequence between O and M can be identified not only based on these strong reflectors and clear unconformities, like for the early Oligocene hiatus on profile AWI-98001, but also by the transparent seismic character of the sediments in between these reflectors. This is attributed to the moderate sedimentation rates of 10-20 m/m.a. without drastic change in the depositional facies (Diekmann et al., subm.) and a relatively high concentration of siliceous sediments

(Diekmann et al., subm.). Several hundred meters of sediment have accumulated in a buried drift where a mound has been built up in the CMP range 9450 - 9850 (Fig. 5.5). The strong reflector over this drift structure, just before a westward migration of the crest, can be related to the early Oligocene hiatus recovered at Site 1090 (Fig. 5.4).
The drilling at Site 1089 identified the location of the base of the Pleistocene, denoted as horizon P (Figs. 5.5, 5.6). During the Pliocene, of which sequences are located between reflectors M and P, an increase in well defined reflectors is observed. This holds even more for the Quaternary sediments, above reflector P. This increase in well defined seismic reflectors can be explained by the increase of the glaciation cycle frequency, responsible for sea-level variation and variations in sediment supply. This is clearly illustrated in Fig. 5.7, which shows that the density of the sediments correlates with seismic reflectors and that the seismic reflectors occur with a periodicity that correlates with marine isotope stages in Pleistocene times (Imbrie et al., 1984).

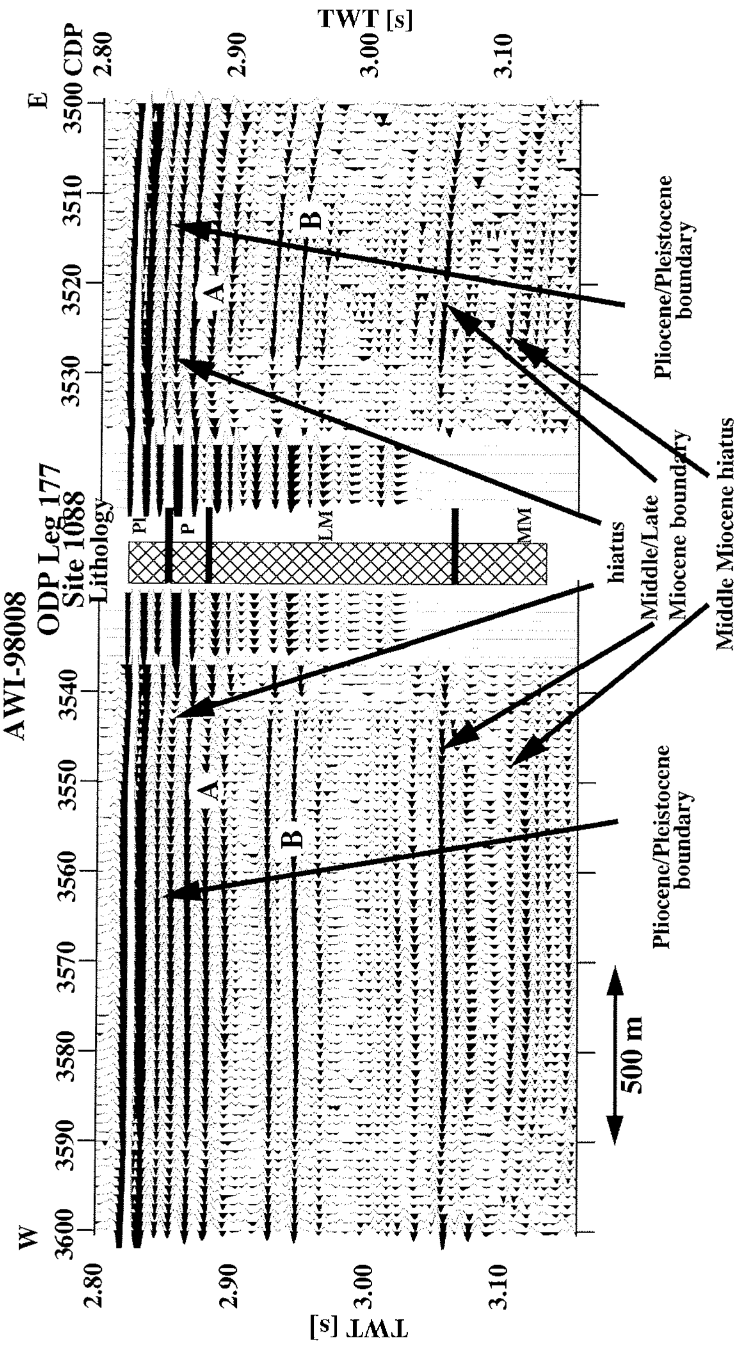

Fig. 5.3: *Lithology and synthetic seismograms derived from ODP Leg 177 Site 1088 core data (after: Shipboard Scientific Party, 1999b), on the northern segment of the Agulhas Ridge (see Fig. 5.1). The lithology is predominantly calcareous. Placement of lithologic boundaries are based on fossil analysis. The seismic reflectors of profile AWI-98008 show good correlation with these boundaries as well as with the synthetic data.*

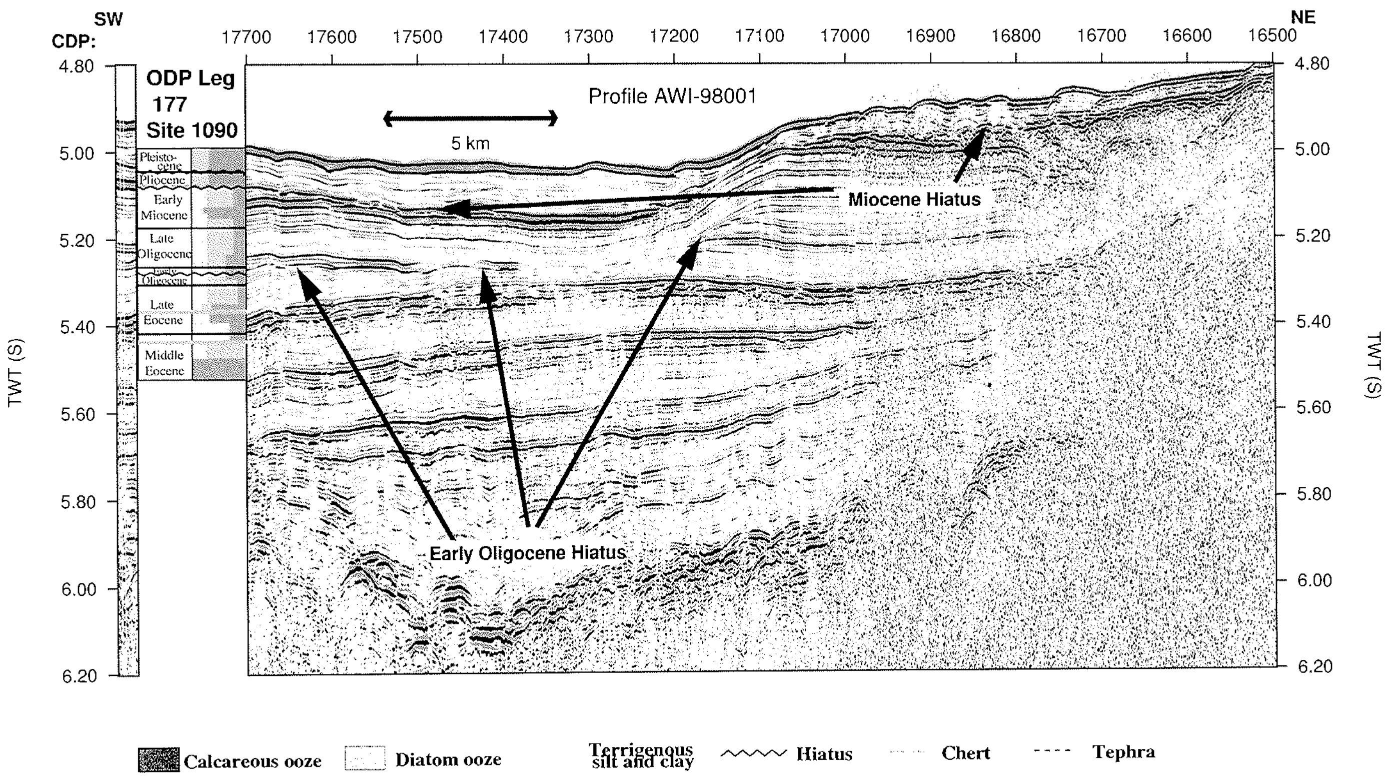

Fig. 5.4: *Lithology of ODP Leg 177 Site 1090 (Shipboard Scientific Party, 1999d) on the south-western side of the Agulhas Ridge correlated with seismic data. An early Oligocene hiatus can be traced in the Cape Basin as well, shown in Fig. 5.5 and 5.6 as reflector O. Reflector M in these figures corresponds to the Miocene hiatus found in Site 1090 cores.*

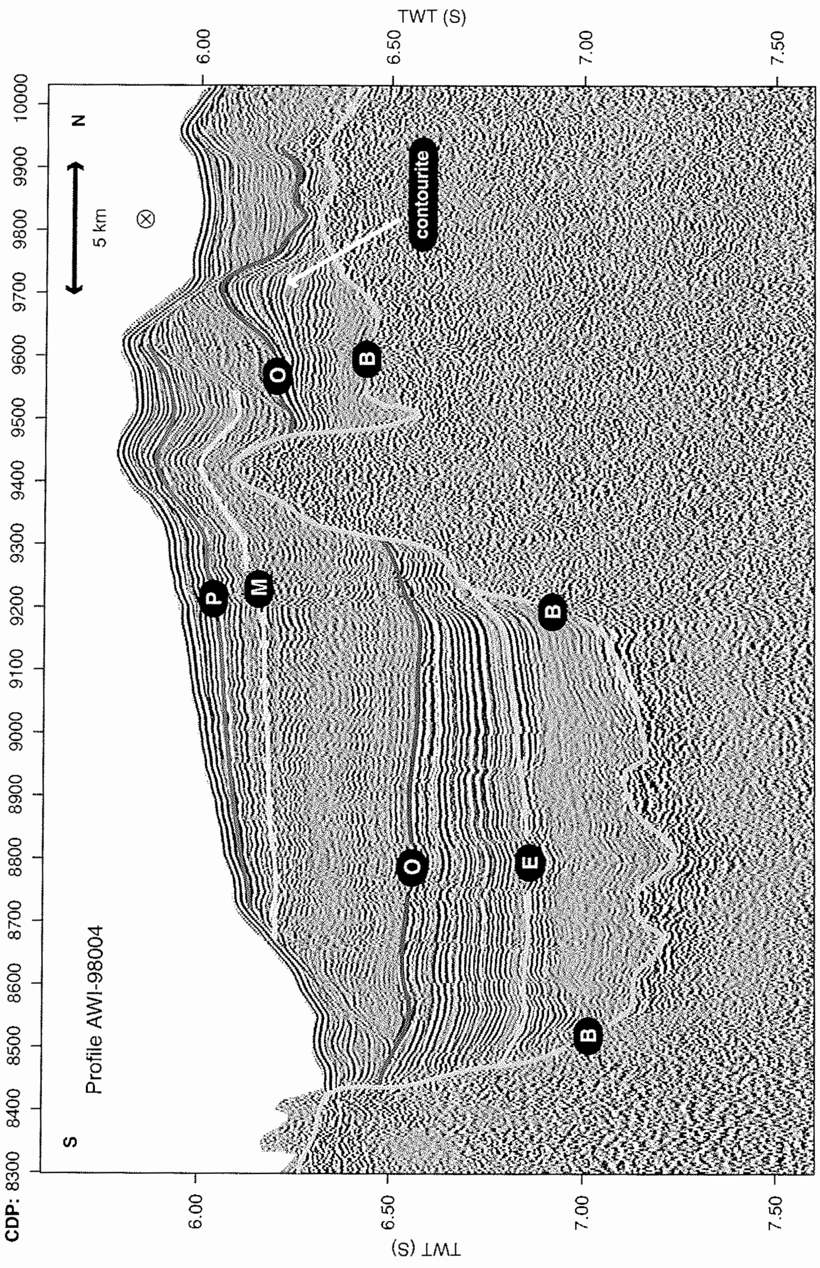

Fig. 5.5: Part of seismic profile AWI-98004 in the Cape Basin showing a contourite deposit. The ⊗ symbol denotes flow direction in westward direction of the palaeo bottom current, responsible for deposition of the contourite. Reflector E corresponds to the top of a pre-Oligocene sedimentary sequence, probably late Eocene, reflector O marks an early Oligocene erosional surface, reflector M corresponds to a Miocene hiatus, reflector P denotes base Pleistocene. B denotes top basement.

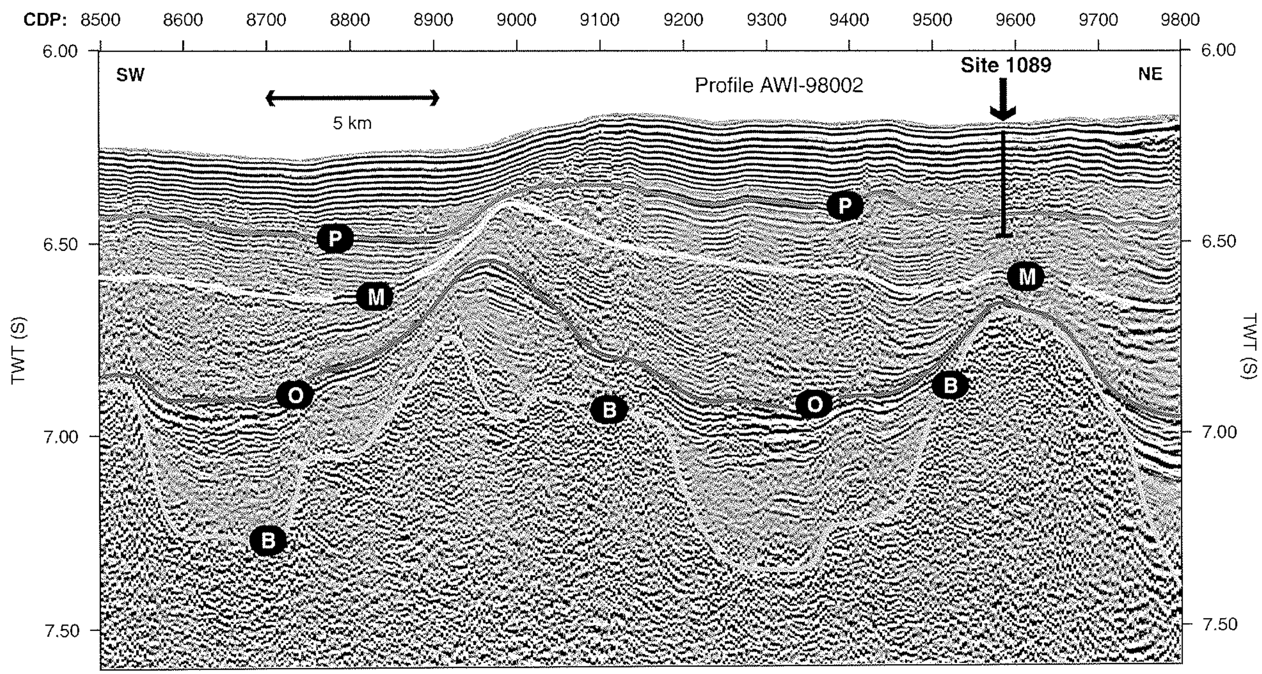

Fig. 5.6: *Part of seismic profile AWI-98002 with bottom current deposits. The reflector O denotes an early Oligocene erosional surface, reflector M corresponds to a Miocene hiatus and reflector P corresponds to base Pleistocene. B denotes top basement.*

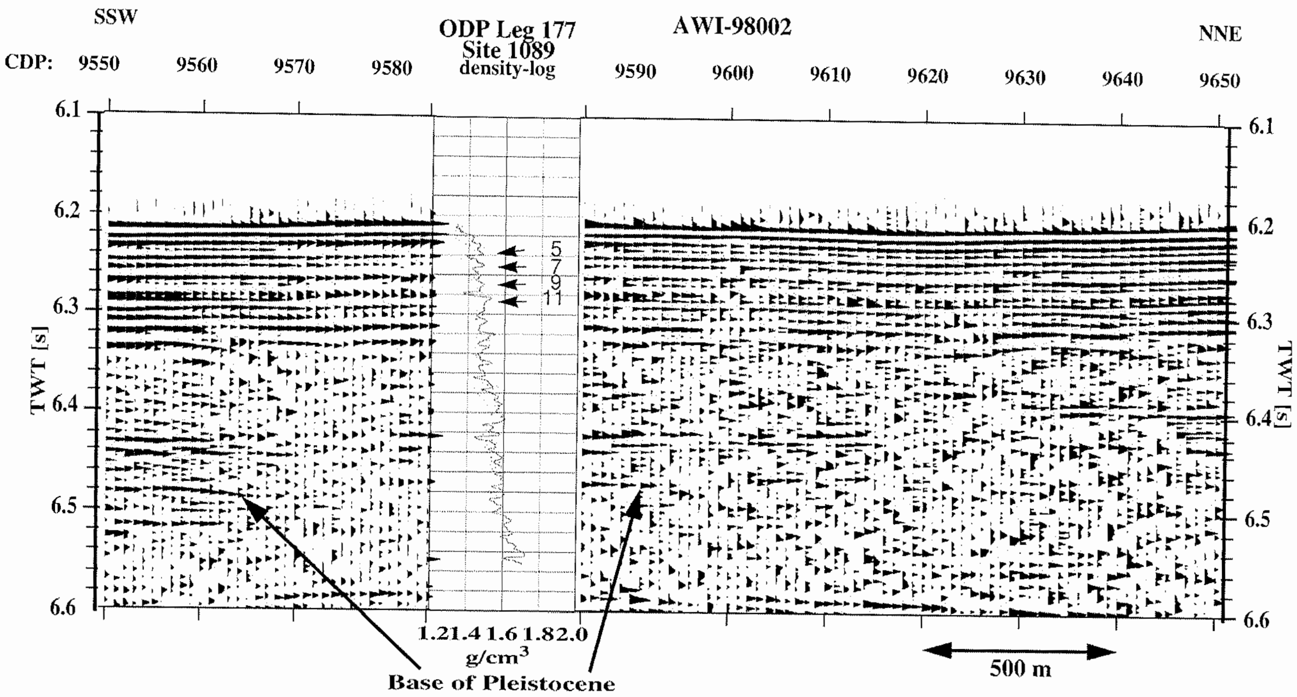

Fig. 5.7: *Densities derived from gamma ray porosity measurements (solid line) and direct measurements at selected core samples for ODP Leg 177 Site 1089, (Shipboard Scientific Party, 1999c) situated in the Cape Basin (see Fig. 5.1) correlated with seismic data. The base of the Pleistocene derived from fossil analysis is visible as a reflector in the seismic data (profile AWI-98002) and is denoted as reflector P in Fig. 5.5 and 5.6. The numbers indicate various oxygen marine isotope stages, age after Imbrie, Hays, Martinson, McIntyre, Mix, Morley, Pisias, Prell, and Shackleton (1984).*

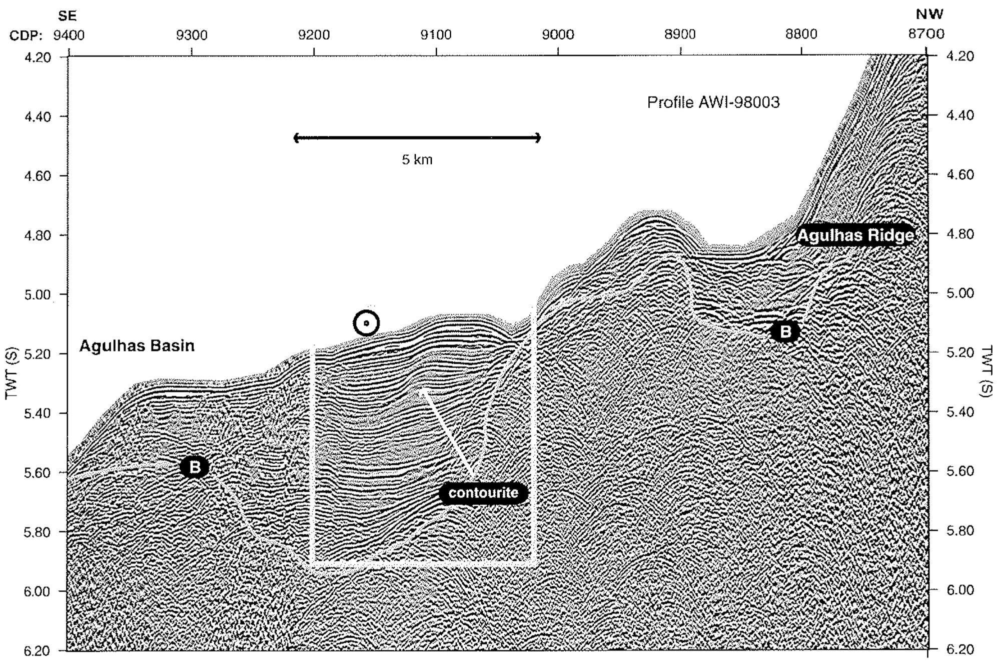

Fig. 5.8: *Profile AWI-98003 just south of the Agulhas Ridge. The outlined area shows a buried contourite drift, probably overlying a sequence of turbidites. The asymmetric appearance of the horizons suggests a current direction oblique to the profile in eastern direction (denoted by symbol ⊙). B denotes top basement.*

5.5 Discussion

The seismic profiles in the vicinity of the Agulhas Ridge show that the Agulhas Ridge has two ridge segments, separated by a 20 km wide moat, filled with sediments and a bathymetric relief of up to 3 km relative to the adjacent basins. The ridge itself is largely of magmatic origin (Hartnady and Le Roux, 1985; Kastens, 1987) and although near Site 1088 and 1090 there is a thick sedimentary sequence, it generally shows little sedimentary cover. By contrast, the Cape and Agulhas Basins show thick layers of sediments on top of the magmatic basement of the oceanic crust. The seismic data shows extensive occurrence of intrusions which affect Cenozoic sediments. This suggests that development of the Agulhas Ridge still continued after the spreading axis at its eastern boundary was abandoned in the Late Cretaceous (LaBrecque and Hayes, 1979). The thick sediment layers in the oceanic basins are interpreted as contourite sheets consisting of fine grained, bioturbated and homogeneous sediments. This is illustrated by the sediments in figures 5.5 and 5.6, between reflectors O, an early Oligocene hiatus and M, a hiatus between Miocene and Pliocene. Widespread discontinuities, marked by a continuous prominent reflector are a characteristic property of contourites (Faugères et al., 1999). Discontinuities in contourite facies are the result of a period of erosion or non-deposition due to intensified current activity or by a compositional change (Faugères et al., 1999). The sediments encountered on profiles AWI-98004 (Fig. 5.5) and AWI-98002 (Fig. 5.6) are seismically relatively transparent, ie. they show mainly low amplitude seismic reflections. This is indicative of a contouritic sheet that has been built up by a steady bottom current with little variations in sediment supply. Reflectors in intermittent reflective sequences are highly discontinuous, a result of bioturbation and differential compaction.

An expression of bottom currents forced to follow the Agulhas Ridge is observed in this sediment sequence at the northern end of profile AWI-98004 in the Cape Basin (Fig. 5.5). The transect of this drift is up to 7.5 km in a direction perpendicular to the Agulhas Ridge, with the crest migrating towards the Agulhas Ridge for younger sediments. The reflectors below the Oligocene hiatus within this elongate contourite drift (Fig. 5.5, CMP 9450 - 9850) are more pronounced than younger sediments. The explanation for this variation in reflectivity lies within changes in depositional environment, for instance relative changes in current velocities, as a higher velocity environment leads to coarser grain-sized sediments. Another possibility is a compositional change of the sediments, eg. by an increase or decrease of siliceous components. Indeed, the lithology of Site 1090 (Fig. 5.2) shows a change towards more terrigenous material in sediments younger than early Oligocene. An asymmetric signature of deposition and migration of the crest towards the left side of the current (on the southern hemisphere) is characteristic for elongate contouritic drifts due to the Coriolis effect and suggests a westward bottom current. This drift is also apparent on profile AWI-98008 as a very wide sequence of sediment layers as this profile is mostly parallel to the drift. The Agulhas Ridge has clearly acted as a barrier for sediment carrying ocean currents, forcing the current to flow parallel to the ridge. The present day bottom current in this part of the Cape Basin also follows a westward path (Tucholke and Embley, 1984; Faugères et al., 1993). From this observation we deduce that since the early Oligocene a bottom water current comparable to the present day bottom current sweeps the Cape Basin and follows the same trajectory. Previously, Johnson (Johnson, 1985) found a rapidly accumulating bottom current deposits beginning in the early Oligocene due to AABW flow in the western South Atlantic. This suggests that bottom current activity occurred already on a large scale in the Oligocene.

In the Agulhas Basin bottom current activity can be observed as well. Here, the bottom current direction is more ambiguous, as the main branch of ACC in the Agulhas Basin follows a westward path (Tucholke and Embley, 1984), but part of it is deflected in an eastward direction and flows counter-clockwise around the Agulhas Ridge. A result of this eastward branch is present in section AWI-98003, just south of the Agulhas Ridge (Fig. 5.8), where a small elongate contourite drift can be observed between CMP 9050 and 9150. The scale of this contourite is of much lesser extent than the drift on profile AWI-98004 in the Cape Basin (Fig. 5.5), due to the more pronounced basement topography in the Agulhas Basin which confines the drift on profile AWI-98003. The location of this drift limits its vertical scale since the location on the flank of the Agulhas Ridge prohibits the development of thick sediment packages and for this reason it is not possible to attach a known time scale from any of the ODP drill sites to the drift. The mound has a lateral extent of less than 2 km, overlain by sediments at 5.5 seconds TWT, probably originating at the top of the Agulhas Ridge and re-sedimented by downslope currents. Giant sheets of bottom current sediments are not observed in the Agulhas Basin as the topography is much rougher than it is in the Cape Basin. Material from the ridge, eroded by shallow currents, can be a source of the sediments in the form of turbidites, to be redeposited by bottom currents in the basins. Possible sources for erosion could be intermediate water masses or perhaps interaction with Agulhas Rings. As most recent ocean-floor spreading in the area of the Agulhas Ridge took place near the location of Site 1088, it is this part of the ridge which has the shallowest sea-floor. Closest to the African continent, this is also the location where possible interaction with rings shedded from the Agulhas Retroflection would be strongest. This effect should be one of supply of sediments, as in contrast to most of the Agulhas Ridge, Site 1088 shows a thick sediment cover for which core analysis shows that accumulation rates at Site 1088 are relatively high (Shipboard Scientific Party, 1999b). If this is the case, relatively high input of terrigenous particles from the African continent could be expected. The high carbonate content of 85 to 95 wt% (Shipboard Scientific Party, 1999b) suggests that deposition of sediments transported by Agulhas Rings does not play a big role on the Agulhas Ridge itself. Deeper in the Cape Basin where very high sedimentation rates are found, with a high content of terrigenous components the situation may be different.

5.6 Conclusions

Opening and closing of critical gateways for inter-ocean water exchange at the Eocene-Oligocene boundary contributed to the development of currents like the ACC and Circumpolar Deep Water, a mixture of AABW and water masses from the Atlantic, Indian and Pacific oceans. The effects of early bottom water currents can be found in the oceanic basins adjacent to the Agulhas Ridge, which already existed at the onset of AABW development. Our seismic data show bottom current activity, documented by contourite deposits, already in the Oligocene. A south-westward bottom current was inferred for the Cape Basin, along the northern slope of the Agulhas ridge. South of the Agulhas Ridge, a small contourite drift in the Agulhas Basin indicates an eastward flow of bottom water during deposition. It is not clear if this flow can be attributed to a branch of bottom water with an Antarctic origin, and neither can its age be determined, but like the Oligocene bottom current in the Cape Basin it has the same direction as the present day bottom current circulation as shown by Tucholke and Embley (1984). Widespread hiatuses formed in the early Oligocene and in the Miocene, related to periods of erosion or non-deposition, and rapidly increased sedimentation, near the Pliocene-Pleistocene boundary and in the Miocene, lead to abrupt lithologic variations. Such variations appear as outstanding reflectors in the otherwise low reflective seismic sequences as found throughout the Cape Basin. Variations in current activity, resulting in increased or decreased supply of sediments and intensity of current velocity are also responsible for the characteristics of the seismic reflections. Sediments of early Oligocene origin as well as Quaternary sediments show clear seismic reflectors, whereas sediments between the early Oligocene and the

Miocene hiatus are seismically transparent with few, discontinuous reflectors. This transparent package corresponds with an increase in the relative amount of terrigenous mud in the sediments, during a period in which deposition took place at moderate sedimentation rates. This indicates constant, low velocity, currents and hence small grain size sediments during late Oligocene and Miocene. For Pleistocene sequences, the climate instability resulted in rapid variation in sediment supply which leads to pronounced seismic reflectors.

Acknowledgements

We are grateful for the support of the captain and crew of R/V Petr Kottsov for their help during the expedition. We also want to thank Bernhard Diekmann for his comments and review of the draft paper. The expedition was funded by the German Bundesministerium für Bildung, Forschung und Technologie under contract No. 03G0532A. This research was funded by the Deutsche Forschungsgemeinschaft. We also want to thank the reviewers for their valuable comments. This is AWI contribution number AWI-N10080.

6. CENOZOIC BOTTOM CURRENT SEDIMENTATION IN THE CAPE BASIN, SOUTH ATLANTIC *

Etienne Wildeboer Schut[1], Gabriele Uenzelmann-Neben[1]
[1] Alfred-Wegener-Institut für Polar und Meeresforschung, Columbusstraße, 27580 Bremerhaven, Germany

SUMMARY

The Agulhas Ridge, which rises up to 2.5 km over the ocean floor of the adjacent Cape- and Agulhas Basins, located along the Falkland-Agulhas Fracture Zone, acts as a barrier for northward flowing deep water masses, deflecting them along the bathymetric contours of the Agulhas Ridge. Seismic data recorded over the Agulhas Ridge shows that the sediments transported by these deep water currents accumulate in contourite drifts. Several hundred metres of sediments have accumulated since the onset of intrusion of Antarctic Bottom Water (AABW) derived water masses into the basins of the South Atlantic. An erosional surface in early Oligocene sediments appears to mark a prominent change in the sedimentation pattern. Up to this event, strong and varying currents formed a rapidly accumulating sheet of sediments subdivided in units with significant seismic impedance contrasts, and thus strong reflections in the seismic image of these sediments. After the early

* Published in: Wildeboer Schut and Uenzelmann-Neben (2005), *Geophysical Journal International by the Royal Astronomical Society*, Vol. 161:325–333 (Blackwell Publishing Ltd); The definitive version is available at www.blackwell-synergy.com

Oligocene erosional event, a stable uni-directional bottom current established, with sedimentation of mainly muddy material, leading to the formation of a more than 200 km long, approx. 30 km wide *elongate contourite drift*. A period of non-deposition during middle Miocene is followed by an increase of well-defined seismostratigraphic units, most pronounced for sediments of Quaternary age. This suggests that build-up of the drift structure generally continued, with alternating episodes of erosion and sedimentation in response to glacial cycles.

Key words: South Atlantic, Agulhas Ridge, seismic reflection, contourites, bottom currents

6.1 Introduction

During the Cenozoic, starting at the end of the Eocene, a process of cooling started in the Southern Ocean (Berger and Wefer, 1996). A crucial step was the opening of several gateways between the worlds oceans as the continents which were formed after the Gondwana breakup drifted apart and established a ring of cold water around the Antarctic continent causing thermal insulation in the Oligocene (Lawver and Gahagan, 1998). This eventually led to the production of cold bottom water at high latitudes which subsequently was injected into the southern Atlantic Ocean. Northward flowing branches of Circumpolar Deep Water (CDW) enter the Agulhas Basin but further northward flow is blocked by the Agulhas Ridge, which separates the Agulhas Basin from the Cape Basin south-west of the coast of South Africa (Reid, 1989). Through the passage near the South African coast it enters the Cape Basin as a bottom current and follows a south-westward direction along the contours of the Agulhas Ridge (Tucholke and Embley, 1984). The northward extent and the intensity of water masses with Antarctic origin into the basins of the Atlantic Ocean shows variations over time, especially in response to Northern hemisphere glaciation cycles (Turneau and Ledbetter, 1989). Sediments transported by the CDW are deposited parallel to the Agulhas Ridge in the form of contourite drifts. The structure of these drifts in the Cape Basin can be used as an indicator for palaeo-current activity.

In order to reveal the internal structure of these drift deposits, and hence the evolution of the CDW in response to the climatic events of the Neogene, several multichannel seismic profiles were obtained across the northern flank of the Agulhas Ridge and southern part of the Cape Basin, and are interpreted here in terms of deep water geostrophic flow from the Southern Ocean. The acquisition of seismic data is required to reveal and classify large scale structures based on morphology and facies of deep-sea sediment bodies.

The interpretation of the seismic profiles opens the opportunity to trace drift structures over a wide area in an oceanic basin.

6.2 Regional setting

After the early Cretaceous breakup of Gondwana, the continents of Africa and South-America drifted apart, thereby opening the South Atlantic Ocean along the Falkland Agulhas Fracture Zone. Along this fracture zone, the Agulhas Ridge formed during the Late Cretaceous (Ben-Avraham et al., 1997). The Agulhas Ridge rises to 2 km below the sea surface, with the adjacent oceanic basins being over 5 km deep. It extends for more than 1100 km from the Agulhas Rift, a spreading centre abandoned 61.2 Ma ago (Marks and Stock, 2001), in the north-east at 40°S, 15°E (LaBrecque and Hayes, 1979) to the northern end of the Meteor Rise at 45°S, 4°E. The Agulhas Ridge separates the Cape Basin to the north from the Agulhas Basin to the south and, due to its topography blocks the exchange of water masses between these two basins.

After separation of Antarctica from its surrounding continents, a circumpolar current developed, which caused thermal insulation of the Antarctic continent (Barker and Burrell, 1977; Kennett, 1977; Lawver and Gahagan, 1998). This eventually led to Antarctic glaciation in the Oligocene and marked the beginning of the production of Antarctic bottom water (AABW) (Mackensen and Ehrmann, 1992; Zachos et al., 1994), originating mainly in the Weddell Sea area. In the present day situation, as AABW flows northward, it mixes with the warmer North Atlantic Deep Water (NADW) forming Circumpolar Water (CPW). In the Southern Ocean, the CPW splits in an upper and a lower branch, vertically separated by a tongue of NADW (Mantyla and Reid, 1983; Orsi et al., 1999). Circumpolar Deep Water (CDW), the lower branch, cannot cross the Agulhas Ridge, but enters the Cape Basin through a passage between the African coast and the north-eastern part of the Agulhas Ridge as a bottom current (Tucholke and Embley, 1984). Previous studies indicate that the Cape Basin was already swept by a proto-AABW bottom current during the Oligocene (Sykes et al., 1998; Tucholke and Embley, 1984).

6.3 Contourites

Contourites are defined as sediment bodies deposited or reworked by the sustained flow of thermo-haline driven, geostrophic, deep-water bottom currents (Heezen et al., 1966; Faugères and Stow, 1993). Due to morphological constraints, these currents often follow bathymetric contours in deep sea basins. Sediments are transported and redistributed over distances of thousands of kilometres (McCave, 1986). In this way sediments originating at the Antarctic can be transported into the basins of the Atlantic Ocean. Downslope turbidity currents form another important source of sediment input to bottom currents. Apart from being a major source of sediment influx in the oceanic basins, bottom currents can be strong enough to scour the sea-floor and create widespread erosional surfaces. The eroded particles add to the sediments already in suspension.

There are several types of contourite morphologies known to exist in ocean basins (Faugères et al., 1999, gives an overview and a classification). On the largest scale, there are contourite sheets, formed when bottom currents become trapped in a basin and sedimentation takes the form of building wide sheets, either abyssal sheets, distant from the basin boundaries, or slope sheets at a basin margin. The variation in geometry is very slight and the internal layers are often seismically transparent. A second frequent type of contourite deposit is the *elongate-mounded drift*, with length much greater than width and a distinctly mounded topography. These drifts are typically deposited parallel or sub-parallel to slopes. The base of such a drift is often an erosional surface developed after extensive previous erosion by bottom currents. Such erosional surfaces often appear on seismic sections as outstanding and discordant reflectors and then form the basis of new contourite drifts.

Seismostratigraphic units of contourite sediments often show an upward convex lenticular shape (Faugères et al., 1999). In some cases an asymmetry is observed in contourites. This is due to a preferential deposition of sediments on one side of the current under the influence of the Coriolis force (McCave and Tucholke, 1986; Faugères et al., 1999), leading to deflection of suspended material to the left hand side of the current on the southern hemisphere and to the right hand side on the northern hemisphere.

6.4 Obtaining an image from seismic data and sediment cores

Eight profiles of seismic data with a total length of approximately 2000 km were collected over the Agulhas Ridge, extending into the Agulhas and Cape Basins, during a seismic survey carried out by the Alfred Wegener Institute for Polar and Marine Research (Fig. 6.1; (Uenzelmann-Neben, 1998)). An energy source of two GI™ guns was used to record 8 seconds of data on a 96 channel streamer.

Physical properties data from ODP Leg 177 were used to establish the link between the image of sediment bodies obtained from the seismic data and the geological information obtained from recovered sediments during this drilling campaign in the Agulhas Ridge area. Drilling of Leg 177 took place at a total of seven locations, three of which (Sites 1088, 1089 and 1090) are in the vicinity of the Agulhas Ridge (Gersonde, Hodell, Blum et al., 1999). Core samples were dated based on their fossil contents and examined on several of their physical and chemical properties. Among the physical properties measured in core samples were density and seismic P-wave velocity. The density was measured with the Gamma Ray Porosity Evaluator (GRAPE) at a 2 or 4 cm sample interval and by Moisture and Density (MAD) measurements, usually once per core section (Shipboard Scientific Party, 1999a). GRAPE measurements exist over a length of 233 m for Site 1088, 265 m for Site 1089 and 397 m for Site 1090. The P-wave velocity was measured with a P-Wave Logger (PWL) at a 2 or 4 cm sample interval and with a P-wave Velocity Sensor 3 (PWS3) on selected core samples (Shipboard Scientific Party, 1999a). PWL measurements exist over a length of 162 m for Site 1088, 215 m for Site 1089 and 236 m for Site 1090, however these measurements yielded often poor results, especially for

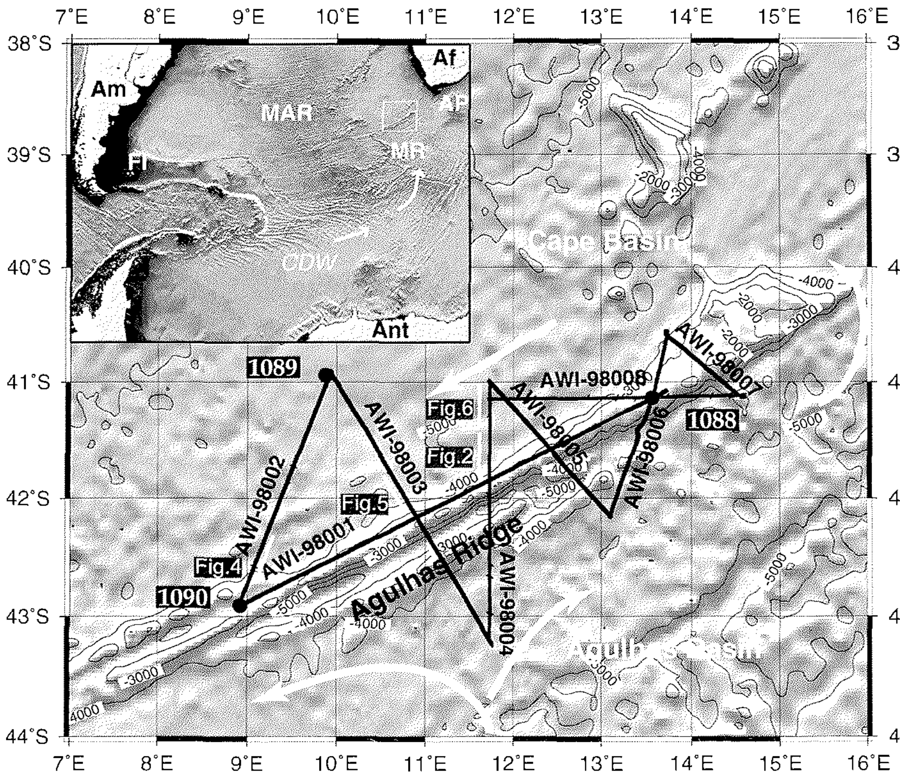

Fig. 6.1: *Bathymetry map of the Agulhas Ridge area (after Sandwell and Smith, 1997) with seismic profiles AWI-98001 through AWI-98008 and drilling locations of ODP Leg 177 Sites 1088, 1089 and 1090 (big dots); abbr.: AF: Africa, AM: South America, AP: Agulhas Plateau, ANT: Antarctica, FI: Falkland Islands, MAR: Mid Atlantic Ridge; arrows denote flow of the present day bottom water (after Tucholke and Embley, 1984).*

Site 1089, and were always close to 1500 m/s, the seismic velocity of water, largely irrespective of lithology. Density and P-wave measurements were filtered for spurious values and subsequently used to create a seismic impedance series, re-sampled to a uniform series of values along the cored sections. The reflectivity series calculated from the seismic impedances, yield synthetic seismograms after conversion from the depth-domain into time-domain and convolution with a seismic source signature. As the geological timescale and sediment type is known from the core samples, these synthetic seismograms serve as the link between core samples and seismic data, and can thus be used to calibrate the seismic records.

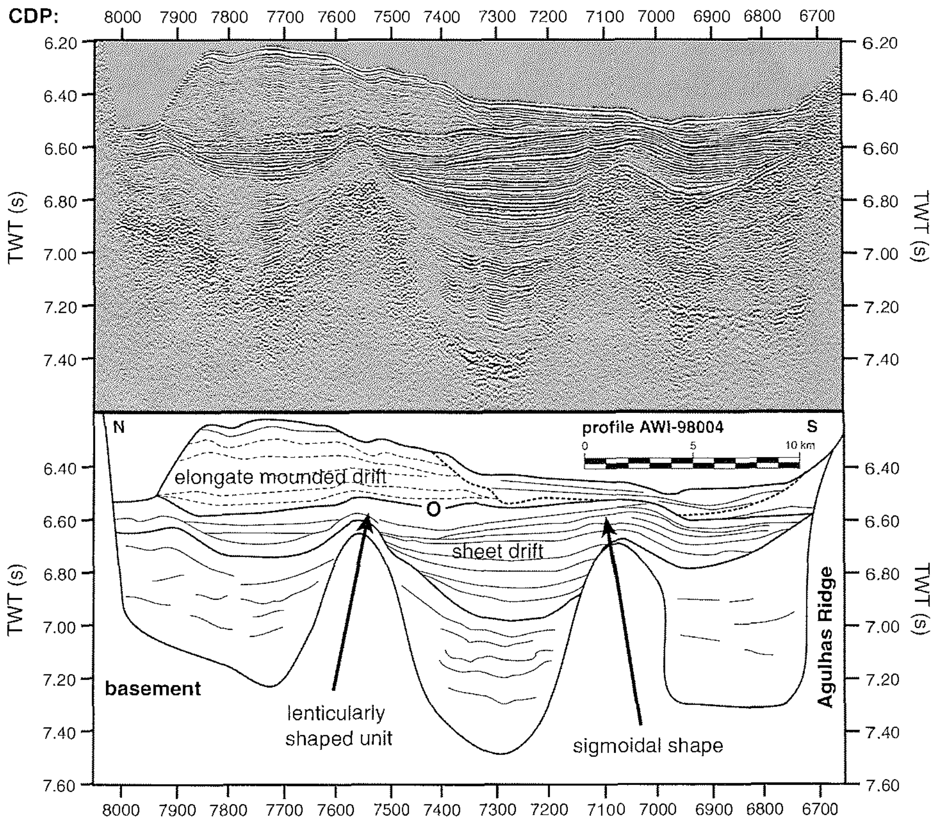

Fig. 6.2: *This section of profile AWI-98004 (position shown on Fig. 6.1) is located just south of the section shown in Fig. 6.6. The lenticular and sigmoidal shape of the seismic reflectors are indicative for sedimentation by bottom currents. The drift between CDP 7350 and 7950 above early Oligocene hiatus O shows a very low intensity, hummocky seismic reflectivity.*

6.5 Results

The lithology of the sediments at the three Leg 177 locations near the Agulhas Ridge show a mainly calcareous composition. Site 1088 (Fig. 6.1) shows a nearly continuous record up to middle Miocene (13 Ma) of nannofossil foraminifer ooze at the upper 20 m and decreasing foraminifer content in the underlying nannofossil ooze (Shipboard Scientific Party, 1999b). The sediments cored at Site 1089, located in the Cape Basin at an offset of approximately 140 km from the Agulhas Ridge (Fig. 6.1) are of Pliocene and Pleistocene age and contain reworked sediments, mainly of Pliocene age, but also some with lower Miocene and upper Eocene / Oligocene faunas (Shipboard Scientific Party, 1999c). The cores show that the amount of nannofossil ooze and diatom mud fluctuates, where the latter is somewhat more abundant. At the south-western part of the Agulhas Ridge, at Site 1090, where the oldest sediments, up to the middle Eocene were recovered (Shipboard Scientific Party, 1999c), also consist of a predominantly calcareous composition, although the carbonate content is lower than at Site 1088, also on top of the Agulhas Ridge, but further to the north east.

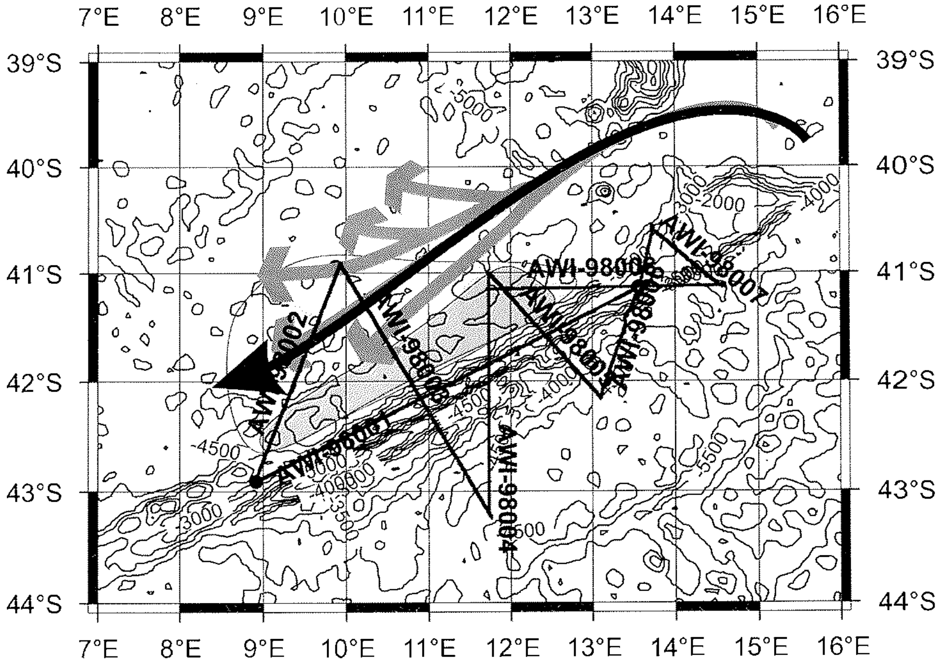

Fig. 6.3: *The light grey area shows the location of pre-early Oligocene sediments. The floor of the Cape Basin is plastered with parallel sheets of sediments of alternating composition, sedimented at a high rate by a strong current (grey arrows). An elongate mounded drift builds on top of this erosional surface (the darker grey area) by a proto-AABW type bottom current which follows the bathymetric contours of the Agulhas Ridge (black arrow).*

Seismic sections in the Cape Basin show two distinct series of reflections. The seismic image of the sediments below reflector O, at approx. 6600 ms e.g. in Figs. 6.2, 6.4 and 6.5, are more or less uniform without a distinctly mounded morphology over the seismic sections in the Cape Basin. The correlation between the seismic data and synthetic seismograms constructed from the physical properties measured on core samples at site 1088 shows that reflector O corresponds to a hiatus in the early Oligocene. In this set of Eocene / early Oligocene seismic units, structures can be found that are indicative of bottom current activity, as opposed to turbidity current deposits. Clearly present on profiles AWI-98002 (Fig. 6.4) and AWI-98004 (Fig. 6.2) are sediment packages shaped into lenticular units. The sediments above reflector O show different reflection characteristics in the form of separated drifts of a constrained width, and a considerable relief of several

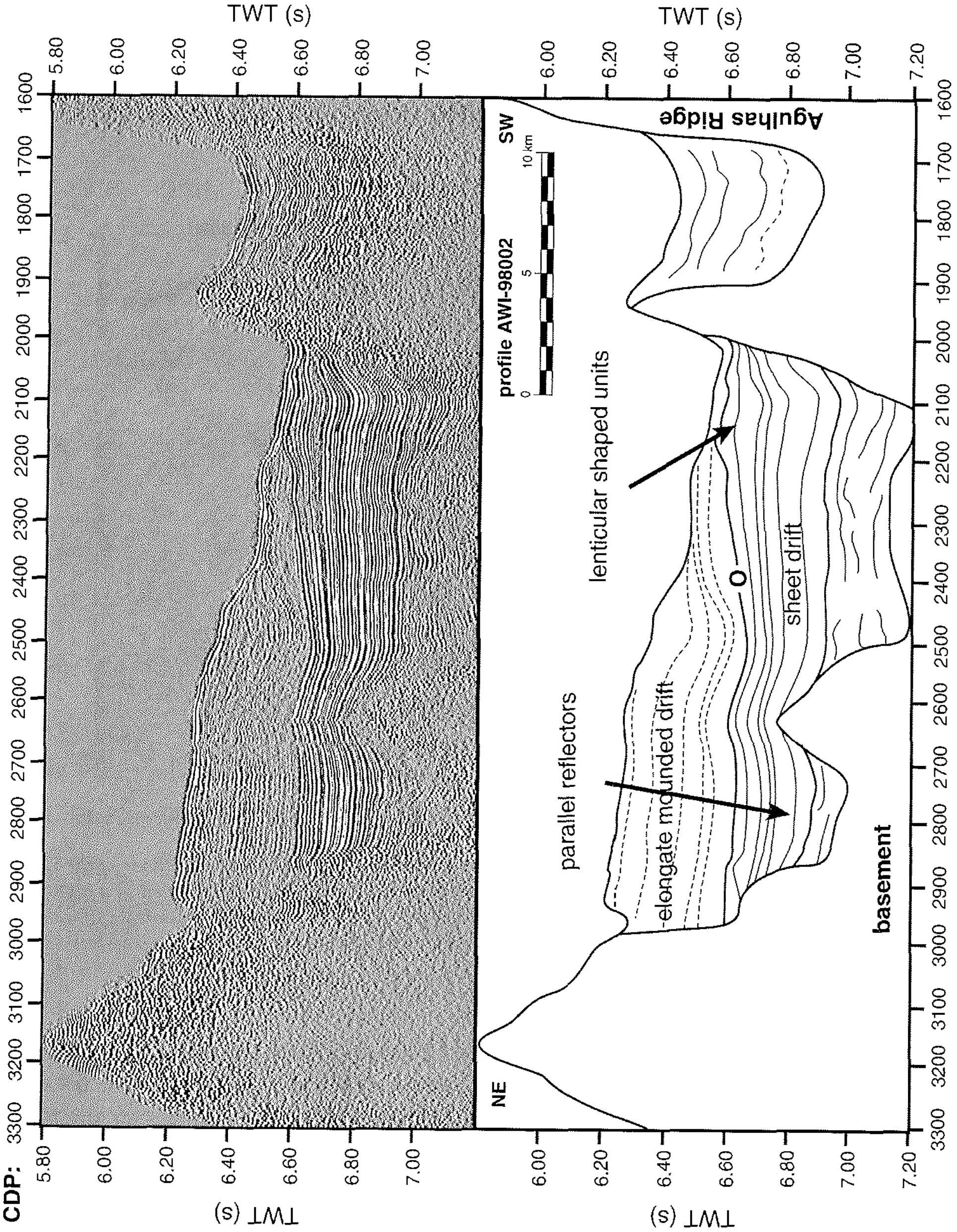

Fig. 6.4: *Shown is profile AWI-98002, just north of the Agulhas Ridge. Seismic reflector O marks the boundary between parallel to lenticular shaped, strongly reflective pre-early Oligocene units, and weakly reflective younger sediments.*

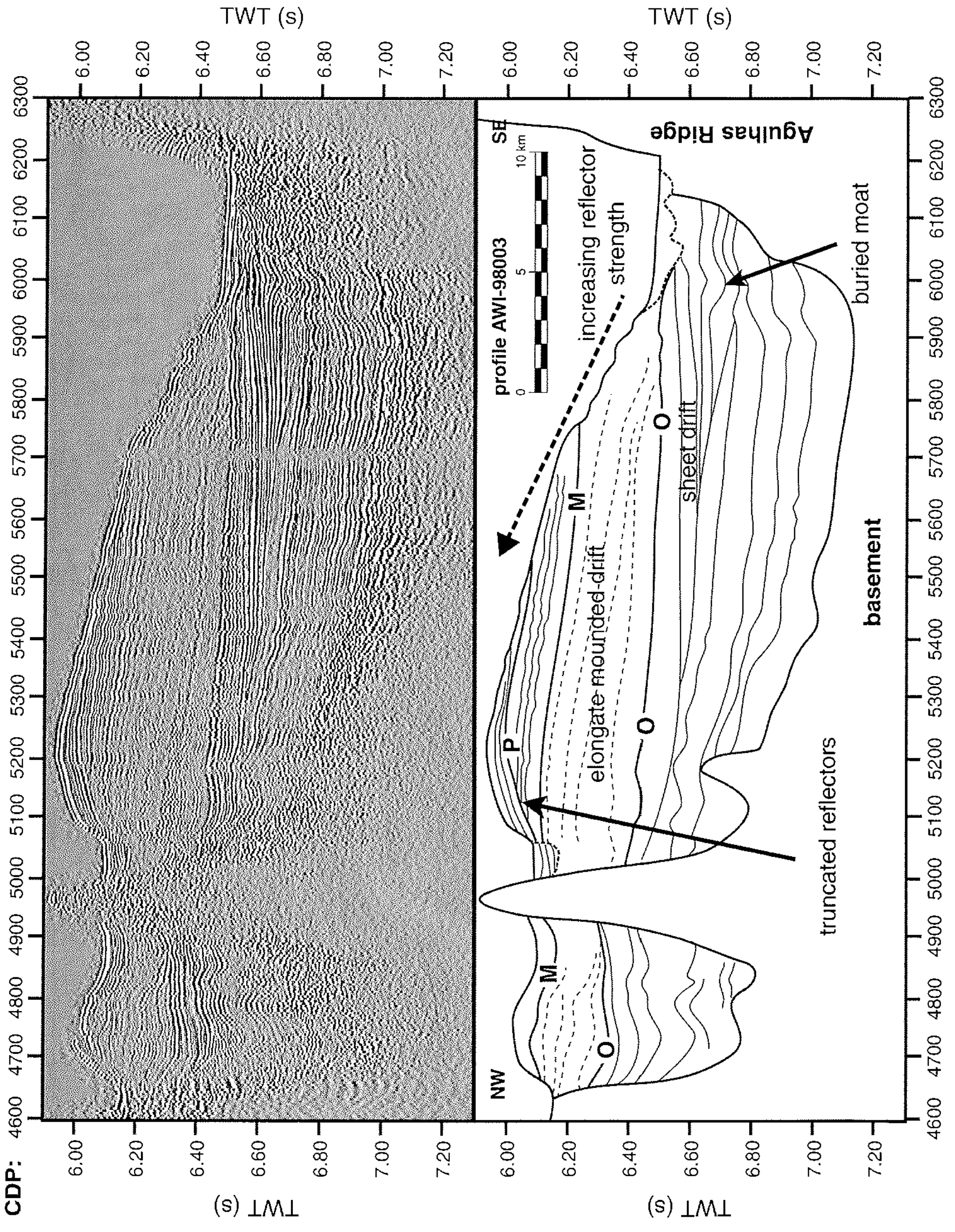

Fig. 6.5: *Profile AWI-98003 shows a stratigraphic sequence from Cretaceous basement to present. Reflector O is inferred to be early Oligocene in age and marks the top of a series of well defined seismic reflectors. Above middle Miocene reflector M, there is a progressively increase in reflectivity. An erosional surface (P) at the base of the Pleistocene truncates Miocene units near CDP 5100.*

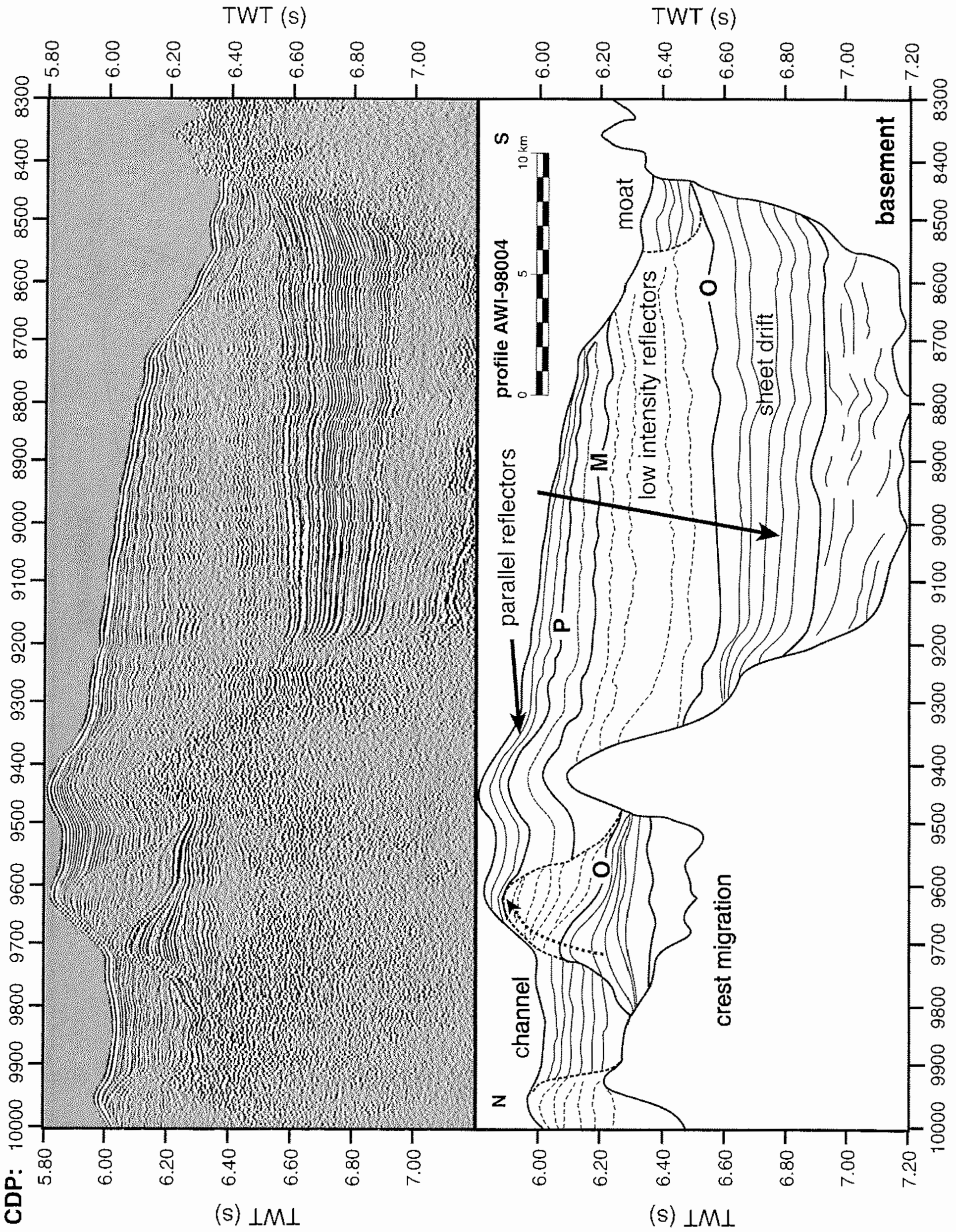

Fig. 6.6: *Seismic profile AWI-98004. A channel between CDP 9700 and 9900 has created a prograding sediment body, which shows southward migration over time. An abrupt change in the strength of seismic reflections is observed at reflector O (early Oligocene).*

hundreds of metres has been built up. In the Cape Basin, at about 50 km offset of the Agulhas Ridge, an elongate south-west trending sediment drift has developed parallel to the ridges northern flank, having a width of 30 to 40 km and a length of more than 200 km, on top of reflector O. This drift can be identified on several of the seismic profiles in the Cape Basin like in Fig. 6.5 for profile AWI-98003 between CDP 4600 and 6000, and in Fig. 6.2 for profile AWI-98004 between CDP 7350 and 7950. In contrast to the highly reflective older units, it shows a seismic image of sediments that are much more transparent.

Between the reflectors O and M (Fig. 6.5), the sediments accumulated in units with an hummocky appearance and mainly low intensity internal seismic reflections. Data from site 1090 shows that reflector M corresponds with an extensive hiatus dated as of middle Miocene age. The intensity of seismic reflectivity gradually become stronger and a division in well defined layers returns for units younger than reflector M (Figs. 6.5 and 6.6), though still less pronounced as for sediments below hiatus O. The youngest sediments, above reflector P (Fig. 6.5) sharp reflectors can again be observed. Still, these reflectors tend to be parallel to deeper reflectors, and sometimes even truncating the older units as in Fig. 6.5. Core-to-seismic correlation places this reflector at the base of the Pleistocene.

6.6 The influence of bottom current regime on sedimentation

The seismic image of sediments is an expression of the seismic impedance contrast between various units, which depends on the physical properties seismic velocity and density. Since the seismic velocity in water saturated sediments, relatively close to the ocean bottom, shows little variation for different lithologies, it is the density which has most impact on the seismic impedance. Especially large are the density contrasts at hiatuses, with different lithologies at either side of the interface.

Two distinct episodes of bottom current sedimentation are observed, the first plastering the ocean bottom (Fig. 6.3), starting probably in the Eocene and ending in the early Oligocene with a widespread hiatus associated with an erosional event (Wildeboer Schut et al., 2002). Following this event is a steady buildup of distinct drift structures.

The packages within the unit below reflector O are (sub-)parallel, sigmoidal (Fig. 6.2) or lenticular (Fig. 6.4) shaped. The strong seismic reflections in this unit indicate variations in current velocity, which determines the grain size of the deposited sediments, or even reversals in current direction. The shape of the structures indicate a contourite current type of sedimentation, as does the existence of a buried moat, on profile AWI-98003 (Fig. 6.5) near CDP 6000 just at the base of the Agulhas Ridge and parallel to it. Near CDP 9700 on profile AWI-98004 (Fig. 6.6), 75 km north of the Agulhas Ridge, a small-scale buried drift structure is found. A continuously southward migration of the crest has possibly prograded under the influence of the Coriolis force acting on a south-west setting bottom current. The top of this drift was initially associated with the erosional surface (reflector O), after approx. 100 m of sediments accumulated. Eventually it formed the basis of a continued build-up of the drift during Miocene and reaches a total thickness of approx. 200 m. The continued build-up of this buried drift suggests that the direction of the active bottom current remained the same during Oligocene and Miocene.

The low intensity, seismically almost transparent units of which a large part of the drift structure between the reflectors O and M is composed (Figs. 6.5 and 6.6), is an indication for a homogeneous, predominantly muddy composition. This is affirmed by the sediments of late Oligocene and Miocene age found in hole 1090 (Shipboard Scientific Party, 1999d).

Cores samples from drill site 1089, mainly of Pleistocene age, contain older fossils. This is an indication that re-sedimentation by a bottom current took place. Shallow-water diatoms throughout the entire sedimentary record demonstrates a steady input of sediments originating near the African coast (Shipboard Scientific Party, 1999c), which constrains the trajectory of the bottom current.

6.7 The history of Cenozoic bottom currents in the Cape Basin

Seismic images of contourite drifts often show mainly low intensity seismic reflections, due to a predominantly muddy composition. The intermediate to high amplitude reflectors encountered on seismic sections often reflect a change in the sediment accumulation rate or in the composition of the sediments. Variations of the seismic structure within contourites could therefore imply variations in the larger scale circulation pattern, whereby sediments from a different source region are brought in. A different type of original sediment input or variations in biogenic production leads to lithologies with a seismic velocity and density contrast which manifests itself as a seismic reflection. Another possibility is current velocity increase, reflected in a more sandy type of sediments.

The existence of contourite sheets shows that bottom current activity existed in the Cape Basin before timing of reflector O (early Oligocene), and transported a significant amount of sediments into the Cape Basin. Data from Site 1090 show that the Eocene/early Oligocene units correspond with high diatom abundances and high opal percentages and variability, and were deposited at high sedimentation rates (Shipboard Scientific Party, 1999d). This indicates the fluctuating paths of the oceanic currents at that time, picking up materials in varying source regions.

Increased current velocity can result in large erosional surfaces, which is one of the features that are characteristic of contourites (Faugères and Stow, 1993). This happened in the southern Cape Basin in the early Oligocene, after which the erosional surface became the base for large scale drift structures.

These type of large scale drifts were classified as giant elongate-mounded drifts by (Faugères and Stow, 1993), drifts much longer than wide along a continental margin, or along the flanks of Mid-Ocean Ridge systems.

Steady build-up of the drift structure with parallel to sub-parallel layers indicate that the current direction did not substantially change between early and late Oligocene.

The bottom current flow stabilised and a steady build-up of an elongate mounded drift commenced (schematically visualised in Fig. 6.3). During this period the current did not change significantly in speed or in the sediments it carried, as the seismic unit is highly transparent in contrast to the older units. Although current activity remained, and in the same direction as before, there were alternating periods of stronger and weaker bottom current flow. In the middle Miocene a hiatus is found, which is probably connected to a period of non-deposition when deeper waters could no longer reach the Cape Basin due to reduced production of the proto-AABW of that time (Sykes et al., 1998). When sedimentation continued, the seismic reflectors inside post middle-Miocene units become progressively more pronounced, although still weak compared to Eocene - early Oligocene reflectors.

Quaternary sediments have been exposed to alternating periods of stronger and weaker flow, to the point where erosion could take place. These episodes are probably connected with the Pleistocene glaciation cycles. Northern hemisphere cooling increased the input of NADW periodically which resulted in alternating diminished and increased CDW input into the South Atlantic ocean (Turneau and Ledbetter, 1989). Pleistocene hiatuses are not unique to the Cape Basin, and found on other locations of the South Atlantic ocean as well (Ledbetter and Ciesielski, 1982). Site 1089, with predominantly Quaternary sediments, shows stronger variation in the relative amount of siliceous and calcareous sediments than other Leg 177 Sites with mainly older sediments do. Bioturbation, prevalent in the Pleistocene sediments of Site 1089, the scarcity of dropstones and the presence of fossilised near coast species (Shipboard Scientific Party, 1999c) indicate that a bottom current is the primary source of sediments in the Cape Basin. Further, this evidences that the CDW enters the Cape Basin near the African coast and subsequently follows a south-westward trajectory along the Agulhas Ridge.

6.8 Conclusions

Drift deposition due to bottom current activity in the Cape Basin has probably been present at least since the end of the Eocene. The character of the sedimentation however changed drastically in the early Oligocene, after the glaciation of the Antarctic continent commenced and led to the production of Antarctic Bottom Water. Before the early Oligocene, a series of strong seismic reflectors, often parallel to sub-parallel, are present on all profiles in the Cape Basin in the form of a slope plastered sheet. This indicates rapid transitions in the velocity and/or chemistry of the accumulated sediments and possibly the path followed by the bottom current. With the introduction of a steady influx of water masses associated with a proto-AABW in the Cape Basin in a similar way as the present situation, large scale erosion took place. After settling down, the build-up of a large elongate mounded drift started parallel to the Agulhas Ridge.

Due to its pronounced elevation over the adjacent sea-floor the Agulhas Ridge prohibits the direct northward flow of circumpolar waters, forcing a path between the north-eastern end of the Agulhas Ridge and the African coast. Once in the Cape Basin, the bottom water flows parallel to the bathymetric contours of the Agulhas Ridge. The asymmetry of a buried contourite mound is probably due to Coriolis force deflection, and is an indicator for a current following a south-westward path, similar to present day CDW.

An elongate contourite drift of several hundred metres thickness accumulated while a steady sedimentation rate was maintained, until inflow temporarily halted in the middle Miocene. After a period of non-deposition, build-up of the drift continued. An increase in strong reflectors, and an increase in layers truncated by Pleistocene layers reveal increased current velocity for younger sediments, and probably a connection with glaciation cycles.

ACKNOWLEDGMENTS

We are grateful for the support of the captain and crew of R/V Petr Kottsov for their help during the expedition. The expedition was funded by the German Bundesministerium für Bildung, Forschung und Technologie under contract No. 03G0532A.
This research used data provided by the Ocean Drilling Program (ODP). The ODP is sponsored by the U.S. National Science Foundation (NSF) and participating countries under management of Joint Oceanographic Institutions (JOI), Inc. Funding for this research was provided by the Deutsche Forschungsgemeinschaft. This is AWI contribution AWI-N14969. Further, we would like to thank Keith Lewis for his constructive comments on the manuscript.

7. SUMMARY AND OUTLOOK

The Agulhas Ridge developed during the Cretaceous breakup of Gondwanaland. Since then, Antarctica has been separated from the surrounding continents and became thermally insulated. This led to the production of cold Antarctic Bottom Water in the polar region. Its low potential temperature makes it a heavy water mass which is confined by the topography of the ocean bottom around Antarctica. Mixing occurs with other water masses, and some of these newly formed water masses end up in the basins of the southern Atlantic ocean. The coldest and densest of the water masses which enters the Cape Basin is the Lower Circumpolar Deep Water (LCDW). As a bottom current, it sweeps the Cape Basin, and depending on the current strength, it is responsible for sedimentation and erosion in this basin. Erosion, or non-deposition cause prominent reflectors in the seismic data which can be traced back in the in the cores as hiatuses in the palaeontological sequence. A prominent hiatus occurs in the early Oligocene sequence. This hiatus marks a prominent change in sedimentation. The hiatus is ambiguous in the core data based on microfossil contents and the magnetic reversal record, but is clearly visible in the seismic data as an erosional surface. Other hiatuses as found in the cored sections, in the middle Miocene, around the Miocene/Pliocene boundary and in the early Pleistocene correspond to outstanding reflectors on the seismic sections. The Miocene hiatus corresponds to a well known middle Miocene global sea level low stand, at which time the CDW probably could not overcome topographic barriers to reach the Cape Basin. The sediments in the Miocene and Pliocene layers are contained inside thick packages, which show relatively low internal structure. The reason for this transparent nature lies in the high sedimentation rate, which is documented by the core record at site 1089 of ODP Leg 177.

Large amounts of sediments have been injected into the Cape Basin, where they formed thick packages, which show a large degree of transparency on a seismic image. These layers are interpreted as contourite sheets, deposited by a bottom current.

The shape of drift structures in the Cape Basin indicate that they were formed under the influence of contour currents, (sub-)parallel to the Agulhas Ridge. Preferential deposition on one side of a deep-sea channel parallel to the Agulhas Ridge is an indication for a sustained flow over a larger amount of time under coriolis force influence. It indicates that the direction of bottom current flow from the Oligocene onward follows a trajectory similar to the present day bottom current, by which northward flowing branches of the LCDW enter the Cape Basin through a passage between the north-eastern end of the Agulhas Ridge and the African continent and then follow a south-western path along the contours of the Agulhas Ridge. The implication of the of the existence of such a bottom current is that there must have been a southern source feeding it, from the Oligocene until present. Investigation of this source can contribute to our understanding the glaciation history of Antarctica.

The seismic image of the sediments deposited before the early Oligocene hiatus on the other hand show sharp and strong reflectors. This is an expression of the fundamentally different circulation regime which existed before a global conveyor belt was established, and large amounts of water mass exchange between the oceans did not yet occur.

Because geological data can be used to constrain the time scale of the image of sedimentological structures as provided by seismic data, and on the other hand seismic data can be used to extrapolate findings of core data over a wider area, is it desirable to make a connection between the core and seismic data. This can be done with physical properties measured on core data as an intermediate step. A major problem however is that of non-continuous measurements on core samples, due for instance to recovery problems. Wherever possible downhole measurements should be made instead, but these are not always available. Missing core data has to be interpolated and spurious data filtered, and when possible corrections should be made for different pressure and temperature conditions in the lab. After a continuous record of density and seismic P-wave velocity values is constructed, then a suitable wavelet should be chosen to match the seismic data.

One of the locations of Leg 177, Site 1090 was originally planned to be drilled in the Agulhas basin, but in absence of reliable bathymetric and seismic data it was instead located on the top Agulhas Ridge. Having seismic data available before starting drilling operations would allow for a much more precise planning of locations, as well as avoid drilling at locations where the sequences might be disturbed. The seismic data covered mainly the Agulhas Ridge and the Cape Basin whereas the data from the Agulhas Basin is rather sparse. Also, no drilling took place inside the Agulhas basin. Having data in the Agulhas Basin might have placed further constraints on the path along which sediments were transported.

It remains an open question whether the Agulhas Ridge remained tectonically active after the Cretaceous. The reflection seismic data indicates that this might be the case as there are volcanic intrusions inside the Cenozoic sediments and even recent sediments are affected by uplift. Also, regarded its age, it would be expected that the area would have been more affected by sea floor subsidence. To solve this problem information on the crustal structure and the age and composition of the volcanic material is needed.

Bibliography

Abreu, V. S. and Anderson, J. B., 1998. Glacial eustacy during the Cenozoic: Sequence stratigraphic implications. *AAPG Bulletin 82*, 1385–1400.

Adcock, S., 1993. In search of the well tie: What if I don't have a sonic log? *The Leading Edge 12*, 1161–1164.

Anisimov, M. V., Ivanov, Yu. A., and Subbotina, M. M., 2002. The global oceanic conveyor. *Oceanology 42*, 615–618.

Barker, P. F., 1979. The history of ridge-crest offset at the Falkland-Agulhas Fracture Zone from a small-circle geophysical profile. *Geophys. J. R. astr. soc. 59*, 131–145.

Barker, P. F., 2001. Scotia Sea regional tectonic evolution: implications for mantle flow and palaeocirculation. *Earth-Science reviews 55*, 1–39.

Barker, P. F. and Burrell, J., 1977. The opening of Drake Passage. *Marine Geology 25*, 15–34.

Ben-Avraham, Z., Hartnady, C. J. H., and Malan, J. A., 1993. Early tectonic extension between the Agulhas Bank and the Falkland Plateau due to the rotation of the lafonia microplate. *Earth Planet. Sci. Lett. 117*, 43–58.

Ben-Avraham, Z., Hartnady, C. J. H., and Kitchin, K. A., 1997. Structure and tectonics of the Agulhas-Falkland fracture zone. *Tectonophysics 282*, 83–98.

Berger, W. H. and Wefer, G., 1996. Expeditions into the past: Paleoceanographic studies in the South Atlantic. In: Wefer, G., Berger, W. H., Siedler, G., and Webb, D.J. eds., *The South Atlantic: present and past circulation.* Springer Verlag, Berlin, Heidelberg, pp. 363–410.

Blum, P., 1997. Physical properties handbook: a guide to the shipboard measurements of physical properties of deep-sea cores. In: *ODP tech. note*, vol. 26. Available from: Ocean Drilling Program, Texas A&M University, College Station, TX 77845-9547, U.S.A., available on the World Wide Web: `http://www-odp.tamu.edu/publications/tnotes/tn26/INDEX.HTM`.

Bonatti, E., 1978. Cenozoic evolution of Antarctic glaciation, the circum-Antarctic ocean, and their impact on global paleoceanography. *Earth Planet. Sci. Lett. 37*, 369–379.

Boyce, R.E., 1976. Sound velocity-density parameters of sediment and rock from DSDP drill Sites 315-318 on the Line Islands Chain, Manihiki Plateau, and Tuamotu Ridge in the Pacific Ocean. In: Schlanger, S.O., Jackson, E.D., et al. eds., *Init. Repts DSDP*, vol. 33. U.S. Govt printing office, Washington DC 20402, pp. 695–729.

Cande, S, LaBrecque, J., and Haxby, W., 1988. Plate kinematics of the South Atlantic: Chron C34 to present. *J. Geophys. Res. B 93*, 13 479–13 492.

Carter, R. M., 1985. The mid-Oligocene Marshall Paraconformity, New Zealand: coincidence with global eustatic sea-level fall or rise. *J. of Geology 93*, 359–371.

Carter, R. M. and Landis, C. A., 1972. Correlative Oligocene unconformities in southern Australasia. *Nature (Physical Science) 237*, 12–13.

Carter, R. M., McCave, I. N., Richter, C., Carter, L., et al., eds., 1999. *Proceedings of the Ocean Drilling Program, Initial Reports*, vol. 181 [CD-ROM]. Available from: Ocean Drilling Program, Texas A&M University, College Station, TX 77845-9547, U.S.A., available from World Wide Web: `http://www-odp.tamu.edu/publications/181_IR/181ir.htm`.

De Ruijter, W. P. M., Biastoch, A., Drijfhout, S., Lutjeharms, J. R. E., Matano, R. P., Pichevin, T., Van Leeuwen, P. J., and Weijer, W., 1999. Indian-Atlantic inter-ocean exchange: Dynamics, estimation and impact. *J. Geophys. Res. C 104*, 20 885–20 910.

Delius, H., Kaupp, A., Muller, A., and Wohlenberg, J., 2001. Stratigraphic correlation of Miocene to Plio-/Pleistocene sequences on the New Jersey shelf based on petrophysical measurements from ODP Leg 174A. *Marine Geology 175*, 149–165.

Diekmann, B., Kuhn, G., Gersonde, R., et al. Middle eocene to early Miocene sediment record of long-term climate change and environmental implications of a late Eocene opal event in the pelagic SE Atlantic sector of the Southern Ocean (ODP Site 1090), submitted.

Diekmann, B., Kuhn, G., Gersonde, R., and Mackensen, A., 2002. Middle Eocene to early Miocene climate development and reorganization of ocean circulation: evidence from biogenic and terrigenous depositional patterns in the Southern Ocean. *Earth Planet. Sci. Lett., submitted* Submitted.

Droxler, A. W., Burke, K. C., Cunningham, A. D., Hiner, A. C., Rosencrantz, E., Duncan, D. S., Hallock, P., and Robinson, E., 1998. Caribbian constraints on circulation beteen Atlantic and Pacific oceans over the past 40 million years. In: Crowley, T. J. and Burke, K. C. eds., *Tectonic boundary conditions for climate reconstructions*, vol. 39 of *Oxford monographs on geology and geophysics*. Oxford University Press, New York, Oxford, chap. 8, pp. 169–191.

du Plessis, A. and Simpson, E.W.S., 1974. Magnetic anomalies associated with the south-eastern continental margin of South Africa. *Mar. Geophys. Res. 2*, 99–110.

Edwards, R. A., 1998. Integration of seismic reflection, physical properties, and downhole logging data. In: Mascle, J., Lohmann, G. P., and Moullade, M. eds., *Proceedings of the Ocean Drilling Program, Scientific Results*, vol. 159. Available from: Ocean Drilling Program, Texas A&M University, College Station, TX 77845-9547, U.S.A., pp. 225–239, available on the World Wide Web: `http://www-odp.tamu.edu/publications/159_SR/CHAPTERS/CHAP_22.PDF`.

Exon, N. F., Kennett, J. P., Malone, M. J., et al., eds., 2001. *Proceedings of the Ocean Drilling Program, Initial Reports*, vol. 189 [CD-ROM]. Available from: Ocean Drilling Program, Texas A&M University, College Station, TX 77845-9547, U.S.A., available from World Wide Web: `http://www-odp.tamu.edu/publications/189_IR/189ir.htm`.

Faugères, JC. and Stow, D. A. V., 1993. Bottom-current-controlled sedimentation: a synthesis of the contourite problem. *Sediment. Geol. 82*, 287–297.

Faugères, JC., Mézerais, ML, and Stow, D. A. V., 1993. Contourite drift types and their distribution in the North and South Atlantic Ocean basins. *Sediment. Geol. 82*, 189–203.

Faugères, J. C., Imbert, P., Mézerais, M. L., and Cremer, M, 1998. Seismic patterns of a muddy contourite fan (Vema Channel, South Brazilian Basin) and a sandy deep-sea fan (Cap Ferret system Bay of Biscaye): a comparison. *Geology 115*, 81–110.

Faugères, J. C., Stow, D. A. V., Imbert, P., and Viana, A., 1999. Seismic features diagnostic of contourite drifts. *Mar. Geology 162*, 1–38.

Fulthorpe, C. S., Carter, R. M., Miller, K. G., and Wilson, J., 1996. Marshall Paraconformity: a mid-Oligocene record of inception of the Antarctic Circumpolar Current and coeval glacio-eustatic lowstand? *Marine and Petroleum Geology 13*, 61–77.

Galeotti, S., Coccioni, R., and Gersonde, R., 2002. Middle Eocene - early Pliocene Subantarctic planktic foraminiferal biostratigraphy of Site 1090, Agulhas Ridge. *Marine Micropaleontology 45*, 357–381.

Gardner, G.H.F., Gardner, L.W., and Gregory, A.R., 1974. Formation velocity and density - The diagnostic basics for stratigraphic traps. *Geophysics 39*, 770–780.

Gersonde, R., Hodell, D. A., Blum, P., et al., eds., 1999. *Proceedings of the Ocean Drilling Program, Initial Reports*, vol. 177 [CD-ROM]. Available from: Ocean Drilling Program, Texas A&M University, College Station, TX 77845-9547, U.S.A., available from World Wide Web: `http://www-odp.tamu.edu/publications/177_IR/177TOC.HTM`.

Gersonde, R., Hodell, D. A., and Blum, P., 2002. Leg 177 synthesis: insights into Southern Ocean paleoceanography on tectonic to millenial timescales. In: Gersonde, R., Hodell, D. A., and Blum, P. eds., *Proceedings of the Ocean Drilling Program, Scientific Results*, vol. 177. Available from: Ocean Drilling Program, Texas A&M University, College Station, TX 77845-9547, U.S.A., pp. 1–54, available on the World Wide Web: `http://www-odp.tamu.edu/publications/177_SR/VOLUME/SYNTH/SR177SYN.PDF`.

Gersonde, R., Hodell, D. A., Blum, P., et al., eds., 2003. *Proc. ODP, Sci. Results*, vol. 177 [CD-ROM]. Available from: Ocean Drilling Program, Texas A&M University, College Station, TX 77845-9547, U.S.A., available from World Wide Web: `http://www-odp.tamu.edu/publications/177_SR/177sr.htm`.

Hamilton, E. L., 1976. Variations of density and porosity with depth in deep-sea sediments. *J. Sediment. Petrol 46*, 280–300.

Haq, B. U., Hardenbol, J., and Vail, P. R., 1987. Chronology of fluctuating sea levels since the Triassic. *Science 235*, 1156–1167.

Hartnady, C. J. H. and Le Roux, A. P., 1985. Southern ocean hotspot tracks and the Cenozoic absolute motion of the African, Antarctic and South American plates. *Earth Planet. sci. lett. 75*, 245–257.

Heezen, B. C., Hollister, C. D., and Ruddiman, W. F., 1966. Shaping of the continental rise by deep geostrophic contour currents. *Science 152*, 502–508.

Imbrie, J., Hays, J. D., Martinson, D. G., McIntyre, A., Mix, A.C., Morley, J. J., Pisias, N. G., Prell, W. L., and Shackleton, N. J., 1984. The orbital theory of Pleistocene climate: support from a revised chronology of the marine $\delta^{18}o$ record. In: Berger, A., Imbrie, J., Hays, J., Kukla, G., and Saltzman, B. eds., *Milankovitch and climate*. D. Reidel, Dordrecht, Boston, Lancaster, pp. 269–305.

Johnson, D. A., 1985. Abyssal teleconnections ii. initiation of Antarctic Botttom Water flow in the southwestern Atlantic. In: Hsü, K. J. and Weissert, H. J. eds., *South Atlantic paleoceanography*. Cambridge University Press, Cambridge, chap. 14, pp. 243–281.

Kastens, K. A., 1987. A compendium of causes and effects of processes at transform faults and fracture zones. *Rev. Geophys. 25*, 1554–1562.

Keller, G., 1987. Paleodepth distribution of Neogene deep-sea hiatuses. *Paleoceanography 2*, 697–713.

Kennett, J. P., 1977. Cenozoic evolution of Antarctic glaciation, the circum-Antarctic ocean, and their impact on global paleoceanography. *J. Geophys. Res. 82*, 3843–3860.

Kennett, J. P. and Barker, P. F., 1990. Late Cretaceous to Cenozoic climate and oceanographic developments in the Weddell Sea, Antarctica: An ocean drilling perspective. In: Barker, P. F., Kennett, J. P., et al. eds., *Proceedings of the Ocean Drilling Program, Scientific Results*, vol. 113. Available from: Ocean Drilling Program, Texas A&M University, College Station, TX 77845-9547, U.S.A., pp. 937–960.

LaBrecque, J. L. and Hayes, D. E., 1979. Seafloor spreading history of the Agulhas Basin. *Earth Planet. Sci. Lett. 45*, 411–428.

Latimer, J. C. and Filipelli, G. M., 2002. Eocene to Miocene terrigenous inputs and export production: geochemical evidence from ODP Leg 177, Site 1090. *Palaeogeography, Palaeoclimatology, Palaeoecology 182*, 151–164.

Lawver, L. A. and Gahagan, L. M., 1998. Opening of Drake Passage and its impact on Cenozoic ocean circulation. In: Crowley, T. J. and Burke, K. C. eds., *Tectonic boundary conditions for climate reconstruction*, vol. 39 of *Oxford monographs on geology and geophysics*. Oxford University Press, New York, Oxford, chap. 10, pp. 212–223.

Lawver, L. A., Gahagan, L. M., and Coffin, M. F., 1992. The development of paleoseaways around Antarctica. In: Kennett, J. P. and Warnke, D. A. eds., *The Antarctic paleoenvironment: A perspective on global change*, vol. 56 of *Antarctic Research Series*. American Geophysical Union, pp. 7–30.

Ledbetter, M. T. and Ciesielski, P. F., 1982. Bottom-current erosion along a traverse in the south Atlantic sector of the Southern Ocean. *Marine Geology 46*, 329–341.

Livermore, R. A. and Woolet, R. W., 1993. Seafloor spreading in the Weddell Sea and southwest Atlantic since the late Cretaceous. *Earth Planet. sci. lett. 117*, 475–495.

Lutjeharms, J. R. E., 1985. Location of frontal systems between Africa and Antarctica: some preliminary results. *Deep-Sea Res. 32*, 1499–1509.

Lutjeharms, J. R. E., 1996. The exchange of water between the South Indian and the South Atlantic oceans. In: Wefer, G., Berger, W. H., Siedler, G., and Webb, D. J. eds., *The South Atlantic: Present and Past Circulation*. Springer-Verlag, Berlin, Heidelberg, pp. 125–162.

Lutjeharms, J. R. E. and Valentine, H. R., 1984. Southern Ocean thermal fronts south of Africa. *Deep-Sea Res. 31*, 1461–1475.

Mackensen, A. and Ehrmann, W. U., 1992. Middle Eocene through Early Oligocene climate history and palaeoceanography in the Southern Ocean: Stable oxygen and carbon isotopes from ODP sites on Maud Rise and Kerguelen Plateau. *Marine Geology 108*, 1–27.

Mantyla, A. W. and Reid, J. L., 1983. Abyssal characteristics of the World Ocean waters. *Deep-Sea Res. 30*, 805–833.

Marino, M. and Flores, J. A., 2002. Middle eocene to early Oligocene calcareous nannofossil stratigraphy at leg 177 site 1090.

Marks, K. M. and Stock, J. M., 2001. Evolution of the Malvinas plate south of Africa. *Mar. Geophys. Res. 22*, 289–302.

McCave, I. N., 1986. Local and global aspects of the bottom nepheloid layers in the world ocean. *Neth. J. Sea Res. 20*, 167–181.

McCave, I. N. and Tucholke, B. E., 1986. Deep current-controlled sedimentation in the western North Atlantic. In: Vogt, P. R. and Tucholke, B. E. eds., *The Geology of North America. The Western North Atlantic Region Volume M*. Geological Society of America, Boulder CO, pp. 451–468.

Melguen, M., 1978. Facies evolution, carbonate dissolution cycles in sediments from the eastern South Atlantic (DSDP Leg 40) since the Early Cretaceous. In: Bolli, H. M., Ryan, W. B. F., McKnight, B. K., Kagami, H., Melguen, M., Siesser, W. G., Longoria, J. F., Decima, F. P., Foresman, J. B., Hottman, W. E., and Natland, J. H. eds., *Init. Repts DSDP*, vol. 40. U.S. Govt printing office, Washington DC 20402, pp. 981–1024.

Meredith, M. P., Grose, K. E., McDonagh, E. L., and Heywood, K. J., 1999. Distribution of oxygen isotopes in the water masses of Drake Passage and the South Atlantic. *J. Geophys. Res C 104*, 20 949–20 962.

Mézerais, M. L., Faugères, J. C., Figueiredo, A., and Massé, L., 1993. Contour current accumulation off Vema Channel mouth, southern Brazil basin. *Şed. Geology 82*, 173–188.

Mikolajewicz, U., Maier-Reimer, E., Crowley, T. J., and Kim, K. Y., 1993. Effect of Drake and Panamanian gateways on the circulation of an ocean model. *Paleoceanography 8*, 409–426.

Orsi, A. H., Johnson, G. C., and Bullister, J. L., 1999. Circulation, mixing and production of Antarctic Bottom Water. *Progress in Oceanography 43*, 55–109.

Reid, J. L., 1989. On the total geostrophic circulation of the South Atlantic Ocean: flow patterns, tracers and transports. *Progr. in Oceanography 23*, 129–244.

Reid, J. R., 1996. On the circulation of the South Atlantic Ocean. In: Wefer, G., Berger, W.H., Siedler, G., and Webb, D.J. eds., *The South Atlantic: Present and Past Circulation*. Springer-Verlag, Berlin, Heidelberg, pp. 13–44.

Ricker, N. H., 1953. The form and laws of propagation of seismic wavelets. *Geophysics 18*, 10–40.

Rind, D., Russell, G., Schmidt, G., Sheth, S., Collins, D., deMenocal, P., and Teller, J., 2001. Effects of glacial meltwater in GISS coupled atmosphere-ocean model; 2. a bipolar seesaw in Atlantic Deep Water production. *J. Geophys. Res. D 106*, 27 355–27 365.

Rintoul, S. R., 1991. South Atlantic interbasin exchange. *J. Geophys. Res 96*, 2675–2692.

Sandwell, D., 1984. Thermomechanical evolution of oceanic fracture zones. *J. Geophys. Res. B 89*, 11 401–11 413.

Sandwell, D. T. and Smith, W. H. F., 1997. Marine gravity anomaly from Geosat and ERS-1 satellite altimetry. *J. Geophys. Res. B 102*, 10 039–10 054.

Shannon, L. V. and Hunter, D., 1988. Antarctic Intermediate Water around South Africa. *S. Afr. J. mar. Sci. 6*, 107–117.

Shipboard Scientific Party, 1999a. Explanatory notes. In: Gersonde, R., Hodell, D. A., Blum, P., et al. eds., *Proc. ODP, Init. Repts.*, vol. 177. Available from: Ocean Drilling Program, Texas A&M University, College Station, TX 77845-9547, U.S.A., pp. 1–57 [CD–ROM], available from World Wide Web: `http://www-odp.tamu.edu/publications/177_IR/CHAP_02/Output/chap_02.htm`.

Shipboard Scientific Party, 1999b. Site 1088. In: Gersonde, R., Hodell, D. A., Blum, P., et al. eds., *Proc. ODP, Init. Repts.*, vol. 177. Available from: Ocean Drilling Program, Texas A&M University, College Station, TX 77845-9547, U.S.A., pp. 1–66 [CD–ROM], available from World Wide Web: `http://www-odp.tamu.edu/publications/177_IR/CHAP_03/Output/chap_03.htm`.

Shipboard Scientific Party, 1999c. Site 1089. In: Gersonde, R., Hodell, D. A., Blum, P., et al. eds., *Proc. ODP, Init. Repts.*, vol. 177. Available from: Ocean Drilling Program, Texas A&M University, College Station, TX 77845-9547, U.S.A., pp. 1–97 [CD–ROM], available from World Wide Web: `http://www-odp.tamu.edu/publications/177_IR/CHAP_04/Output/chap_04.htm`.

Shipboard Scientific Party, 1999d. Site 1090. In: Gersonde, R., Hodell, D. A., Blum, P., et al. eds., *Proc. ODP, Init. Repts.*, vol. 177. Available from: Ocean Drilling Program, Texas A&M University, College Station, TX 77845-9547, U.S.A., pp. 1–101 [CD–ROM], available from World Wide Web: `http://www-odp.tamu.edu/publications/177_IR/CHAP_05/Output/chap_05.htm`.

Shipley, T. H., 1983. Physical properties, synthetic seismograms, and seismic reflections; correlations at Deep Sea Drilling Project Site 534, Blake-Bahama Basin. In: Sheridan, R. E., Gradstein, F. M., et al. eds., *Init. Repts DSDP, Norfolk, Virginia to Fort Lauderdale, Florida, October-December, 1980*, vol. 76. U.S. Govt printing office, Washington DC 20402, pp. 653–666.

Stow, D. A. V., Faugères, JC., Viana, A., and Gonthier, E., 1998. Fossil contourites: a critical review. *Sediment. Geol. 115*, 3–31.

Sun, Y. F., 2000. Core-log-seismic integration in hemipelagic marine sediments on the eastern flank of the Juan de Fuca Ridge. In: Fisher, A., Davis, E.E., and Escutia, C. eds., *Proceedings of the Ocean Drilling Program, Scientific Results*, vol. 168. Available from: Ocean Drilling Program, Texas A&M University, College Station, TX 77845-9547, U.S.A., pp. 21–35, available on the World Wide Web: `http://www-odp.tamu.edu/publications/168_SR/chap_03/chap_03.htm`.

Sykes, T. J. S., Ramsay, A. T. S., and Kidd, R. B., 1998. Southern hemisphere Miocene bottom-water circulation: a palaeobathymetric analysis. In: Cramp, A., MacLeod, C. J., Lee, S. V., and Jones, E. J. W. eds., *Geological Evolution of Ocean Basins: Results from the Ocean Drilling Program.*, vol. 131 of *Special Publications*. Geological Society, London, chap. 10, pp. 43–54.

Tucholke, B. E. and Embley, R. W., 1984. Cenozoic regional erosion of the abyssal sea floor off South Africa. In: Schlee, J. S. eds., *Interregional Unconformities and Hydrocarbon Accumulation*, vol. 36 of *AAPG Memoir*. pp. 653–666.

Turneau, R. and Ledbetter, M. T., 1989. Deep circulation changes in the South Atlantic ocean: response to initiation of northern hemisphere glaciation. *Paleoceanography 4*, 565–583.

Uenzelmann-Neben, G., ed., 1998. *Sedimentation and tectonics of Agulhas Ridge and Agulhas Plateau*, vol. 273 of *Reports on Polar Research*. Alfred Wegener Institute for Polar and Marine Research, D-27568 Bremerhaven, Federal Republic of Germany.

Venz, K. A. and Hodell, D. A., 2002. New evidence for changes in plio-pleistocene deep water circulation from Southern Ocean ODP Leg 177 Site 1090. *Palaeogeography, Palaeoclimatology, Palaeoecology 182*, 197–220.

Wildeboer Schut, E. C. C. and Uenzelmann-Neben, G., 2003. The challenge of tieing seismic data to geologic information: An example from odp leg 177, sites 1088-1090. *Mar. and petrol. geol.* Submitted.

Wildeboer Schut, E. C. C. and Uenzelmann-Neben, G., 2005. Cenozoic bottom current sedimentation in the cape basin, south atlantic. *Geophys. J. Int. 161*, 325–333.

Wildeboer Schut, E. C. C., Uenzelmann-Neben, G., and Gersonde, R., 2002. Seismic evidence for bottom current activity at the Agulhas Ridge. *Global and Planetary Change 34*, 45–58.

You, Y., Lutjeharms, J. R. E., Boebel, O., and De Ruijter, W. P. M., 2003. Quantification of the interocean exchange of intermediate water masses around southern africa. *Deep-sea Res. Part II 50*, 197–228.

Zachos, J., Pagani, M., Sloan, L., Thomas, E., and Billups, K., 2001. Trends, rhythms, and aberations in global climate 65 ma to present. *Science 292*, 686–693.

Zachos, J. C., Stott, L. D., and Lohmann, K. C., 1994. Evolution of early Cenozoic marine temperatures. *Paleoceanography 9*, 353–387.

Zielinski, U. and Gersonde, R., 2002. Plio-Pleistocene diatom biostratigraphy from ODP Leg 177, Atlantic sector of the Southern Ocean.

Zühlsdorff, L. and Spiess, V., 2001. Modeling seismic reflection patterns from Ocean Drilling Program Leg 168 core density logs: Insight into lateral variations inn physical properties and sediment input at the eastern flank of the Juan de Fuca Ridge. *J. Geophys. Res B 106*, 16 119–16 133.

ABBREVIATIONS

AABW:	Antarctic Bottom Water
ACC:	Antarctic Circumpolar Current
cdp:	common depth point
ccd:	carbonate compensation depth
CDW:	Circumpolar Deep Water
cmp:	common mid point
DSDP:	Deep Sea Drilling Project
FAFZ:	Falkland-Agulhas Fracture Zone
mbsf:	meters below sea floor
mcd:	meters composite depth
ms:	milli seconds
NADW:	North Atlantic Deep Water
nmo:	normal moveout
ODP:	Ocean Drilling Program
PF:	Polar Front
SAF:	Subantarctic Front
STF:	Subtropical Front
Sv:	Sverdrup ($= 10^6 m^3 s^{-1}$)
twt:	two way traveltime

ACKNOWLEDGEMENTS

I would like to thank all persons that helped and supported me during my research. In the first place these are Prof. Dr. H. Miller and Dr. Gabriele Uenzelmann-Neben for enabling me to carry out this research and for counselling and support. Thanks also to Prof. Dr. U. Bleil (Bremen University) for co-reviewing my work. A special thanks goes to Axel Ehrhard (presently at Hamburg University) who demultiplexed the seismic data and helped me getting familiar with the processing software. Dr. Johannes Rogenhagen (Fielax GmbH) helped me out on numerous occasions. This ranges from GMT through OpenWorks™ to his expertise on awk (and xfig). I should also thank him, and Mechita, Carsten, Anette and Matthias for the many scientific and not-so-scientific discussions in D1460. Dr. Rainer Gersonde helped in the preparation of my first paper, with helpful comments and bringing a lot of literature on micro-palaeontology and palaeo-oceanography to my attention. To my colleagues of geophysical department, friends and family: thank you for your support. I am grateful to the Deutsche Forschungsgemeinschaft and the Alfred-Wegener-Institute for their financial support.